12-2007

Development and Evaluation of Brain Tumor Targeted Liposome Delivery System for Paclitaxel

Murali Krishna Divi
University of Tennessee Health Science Center

Development and Evaluation of Brain Tumor Targeted Liposome Delivery System for Paclitaxel

DOI
10.21007/etd.cghs.2007.0073

Development and Evaluation of Brain Tumor Targeted Liposome Delivery System for Paclitaxel

A Dissertation
Presented for
The Graduate Studies Council
The University of Tennessee
Health Science Center

In Partial Fulfillment
Of the Requirements for the Degree
Doctor of Philosophy
From The University of Tennessee

By
Murali Krishna Divi
December 2007

Acknowledgements

My overwhelming thanks goes to my advisor and committee chair, Dr. George C. Wood, who has in every way been available as a resource be it emotionally, socially, scholarly, or administratively. I cannot overstate the importance of his involvement in my graduate career. I would like to gratefully acknowledge the enthusiastic technical support of Dr. M. Waleed Gaber for the scientific discussions on optical imaging. I would also like to thank all of my committee members, Dr. M Waleed Gaber, Dr. Atul J. Shukla, Dr. Ram Mahato and Dr. James R. Johnson for their help, critical comments and relevant discussions.

I must also thank Dr. Laura A. Thoma, Director, UT Parenteral Medications Laboratories (PML), for her encouragement and financial support for this study. I am grateful to Dr. M Waleed Gaber and his group, especially Bharathi, Janice, and Christy, for helping me with imaging experiments. I would also like to acknowledge the timely support of all of my friends in PML, Hari Desu, Vinayagam Kannan, Frank Horton, Barry Braganza, Himanshu, Gwen Stornes, and Jennifer Hart.

Finally, I am forever indebted to my parents and my wife for their understanding, endless patience and encouragement when it was most required.

Abstract

Background: Primary brain tumors are a relatively common cause of cancer-related deaths. High-grade gliomas are the most common type of primary brain cancer, and the affected patients have a median survival of less than 1 year. Almost all malignant gliomas are incurable with the present standards of healthcare. Currently accepted therapeutic adjuvants to surgery, such as radiotherapy and chemotherapy, provide only a minor improvement in the disease course and life expectancy for patients diagnosed with malignant gliomas. Often, chemotherapy has failed to make any significant impact on the prognosis of disease because of significant local and systemic toxicity, problems with transport of the drug across the blood brain barrier (BBB), and a high degree of chemoresistance demonstrated by tumor cells. Newer targeted delivery systems with more specificity for gliomas, improved safety profiles, and an enhanced ability to permeate through the BBB are actively under development as the next generation glioma therapies.

Blood brain barrier and vascular endothelial cells in and around glioma brain tumors highly express certain receptors such as transferrin for iron transport into brain tumors respectively. To explore the potential of this tumor induced expression of transferrin receptors for targeting drug carriers, in this study, I have developed and characterized liposome carriers containing paclitaxel, for targeted delivery to the glioma brain tumors.

Methods: A liposome drug delivery system specifically aimed at glioma tumors was designed in this study. Liposomes composed of egg phosphotidylchole (EPC), hydrogenated soybean phosphatidylcholine (HSPC), cholesterol, distearoyl phosphoethanolamine-PEG-2000 conjugate (DSPE-PEG) and DSPE-PEG-maleimide were prepared by the lipid film hydration and extrusion process. Transferrin (Tf) with affinity for transferrin receptors over-expressed on blood brain barrier and glioma tumor vasculature were coupled to the distal end of poly ethylene glycol coated long circulating liposomes. The liposome delivery system was characterized in terms of size, lamellarity, ligand density, and drug loading properties. The effect of lipid concentration and type in the formulation on paclitaxel loading in the liposomes was studied. Functional properties of the delivery system were evaluated for, i) *in vivo* blood circulation time using blood sampling method and also using a novel intravital microscopic method, ii) Selective tumor localization in both flank and intracranial glioma models, and iii) anti-tumor efficacy in mouse flank and intracranial glioma tumors. Further, in order to improve physical and chemical stability of the delivery system and hence enhance its shelf life, a lyophilized formulation and process were developed.

Results: Light scattering and electron microscopic observations of the formulations revealed presence of small unilamellar liposomes of about 133 nm in diameter. High performance gel filtration chromatography determinations of ligand coupling to the liposome surface indicated that about 72% of the transferrins were conjugated with biotin groups on the liposome surface. Optimized liposome formulation with 100 mM lipid concentration, 1:33 drug-to-lipid ratio, 5 mol% cholesterol, 5 mol% DSPE-PEG, and 0.01 mol% DSPE-PEG-biotin content yielded 1.3 ± 0.2 mg/mL

liposomal paclitaxel with 97.2 ± 3% of the drug being entrapped in the liposomes. These liposomes released no significant amount of the encapsulated drug over 72 Tf-LCL at 37°C. Targeted liposomes showed significantly higher rate and extent of tumor accumulation in glioma flank tumors *in vivo* compared to non-targeted liposomes. Targeted liposomes also possessed long circulating properties with a $T_{1/2}$ of about 9 Tf-LCL in mice. This increased circulation longevity, attributed to steric stabilization effects of PEG, enhanced target accumulation. Near infrared fluorescence imaging demonstrated that these liposomes accumulated selectively in flank tumors with tumor targeting index of 10.59 ± 1.08. Paclitaxel incorporated into the targeted liposomes delayed tumor growth by 7.7 days in 5 doses of 2 mg/Kg body weight. However, no significant tumor growth retardation was observed when paclitaxel was administered in free form (Cremophor EL solubilized form) at similar dose. A process and formulation were developed for freeze-drying the targeted liposome delivery system. Liposome formulations stabilized with 15% sucrose outside the liposomes were able to maintain particle size distribution and drug loading close to initial upon freeze-drying and rehydration.

Conclusion: A stable and effective targeted liposome delivery system was developed for paclitaxel to take this drug selectively to glioma brain tumors. This targeted delivery system could potentially improve therapeutic benefits of anticancer drugs with and increase safety when compared to existing solution dosage forms.

Table of Contents

List of Figures

List of Abbreviations

BBB	Blood brain barrier
CCD	Charge coupled device
CED	Convection enhaced delivery
DSPC	1, 2-Distearoyl-sn-glycero-3-phosphocholine
DSPE-PEG	1,2-Distearoyl –sn-glycero-3-phosphoethanolamine-N-[PEG(2000)] conjugate
Egg PC	Egg phosphatidylcholine
GFP	Green fluorescent protein
HPGFC	High performance gel filtration chromatography
HPLC	High performance liquid chromatography
Tf-LCL	Hour
HSPC	Hydrogenated soybean phosphatidylcholine
Kd	Kilo Dalton
LCL	Long-circulating liposomes (Non-targeted liposomes)
LUVs	Large unilamellar vesicles
MAb	Monoclonal antibody
MLVs	Multilamellar vesicles
MPS	Mononuclear phagocytic system
MWCO	Molecular weight cutoff
PBS	Phosphate buffered saline
PDI	Polydispersity index
PEG	Polyethylene glycol
PL	Phospholipid
PSD	Particle size distribution
RES	Reticular endothelial system
SD	Standard deviation
SSTL	Sterically stabilized targeted liposomes
SUVs	Small unilamellar vesicles
$T_{1/2}$	Circulation half-life
Tf-LCL	Transferrin coupled long-circulating liposomes (Targeted liposomes)
T_g	Glass transition temperature
T_m	Phase transition temperature

Chapter 1: Literature Review

1.1 Introduction

Each year more than 200,000 people in the United States are diagnosed with primary or metastatic brain tumors. Brain tumors are the leading cause of solid tumor cancer death in children under the age of 20. Adults with newly diagnosed brain tumors like astrocytomas have a median survival of less than one year (Curran Jr., Scott et al. 1993; DeAngelis, Burger et al. 1998; Surawicz, Davis et al. 1998). Despite dramatic improvements in neuroimaging and neurological techniques, the prognosis in patients with brain tumors has not improved significantly during the past 40 years (DeAngelis, Burger et al. 1998). The main stay of treatment in patients with high grade brain tumors is resection followed by radiation. Chemotherapy has been used occasionally, but has proven to be of limited impact on the survival of these patients (Curran Jr., Scott et al. 1993; DeAngelis, Burger et al. 1998; Surawicz, Davis et al. 1998; Jemal, Thomas et al. 2002). Almost all malignant gliomas are incurable with the present standards of healthcare. Currently accepted therapeutic adjuvants to surgery, such as radiotherapy and chemotherapy, provide only a minor improvement in the disease course and life expectancy for patients diagnosed with malignant gliomas. Often, chemotherapy has failed to make any significant impact on the prognosis of disease because of significant local and systemic toxicity, problems with transport of the drug across the blood brain barrier (BBB), and a high degree of chemoresistance demonstrated by tumor cells (Green, Byar et al. 1983; Grant, Liang et al. 1995; Fine, Wen et al. 2003).

Thus, there is a desperate need for targeted delivery systems that can enhance the efficacy by altering the pharmacokinetics of anticancer drugs in such a way that therapeutic concentrations of drug reaches the target site. Targeted drug delivery systems can also minimize toxic side effects of current anti cancer drugs (Allen 2004).

1.2 Challenges in Brain Tumor Therapy

The treatment of brain tumors is complicated by many factors. The primary factor is the protective or shielding function of monolayer of polarized brain endothelial cells in the form of blood brain barrier (BBB) (Begley 1996; Pardridge 1999; Begley 2003). These endothelial cells are connected by complex tight junctions, where by they show a very high trans-endothelial electrical resistance of about 2000 Ωcm^2 results in reduced para-cellular diffusion (Lo, Singhal et al. 2001). The BBB is dynamically regulated by ependymal cells like astrocytes, neurons and pericytes (Edwards 2001; Scherrmann 2002). Basal lamina separates the endothelial cells from ependymal cells. This structural complexity results in a permeability barrier between blood within brain capillaries and the extracellular fluid in brain tissue. Only lipophilic solutes that can freely diffuse through the capillary endothelial membrane may passively cross the BBB. The passive diffusion of drug molecules across the BBB depends on their blood brain concentration gradient and lipid solubility. The passive diffusion is inversely related to the degree of ionization and molecular weight of the drug molecules. About 98% of small molecule drugs and 100% of large molecules drugs do not cross the blood brain barrier due to these factors (Pardridge 1999; Pardridge 1999; Pardridge 2003). As a consequence the

therapeutic value of many potent anticancer drugs is diminished. Compared with the normal brain vasculature of healthy tissues, blood vessels in brain tumors are often highly abnormal, with distended capillaries with leaky walls, leading to inconsistent drug delivery. Accumulation of interstitial fluid leads to an increase in the intratumoral interstitial pressure, thus limiting the penetration of drugs into brain tumors (Jain 1994; Brown and Giaccia 1998; Jain 1998; Jain 1999). Localized hypoxia which can lead to tumor resistance as a result of irregular blood flow. Drug metabolizing enzymes are located in the cerebral microvasculature primarily serve a protective role against exogenously administered molecules. Efflux transport systems like P-glycoprotein (P-gp) and multidrug resistance associated protein (MRP) further restrict drug accumulation in the brain (Fricker and Miller 2004).

The second challenge in the brain tumor therapy is the lack of specificity of anticancer agents to the pathological site. An optimal delivery system should be able to direct drugs exclusively to their desired sites of action, with minimal toxic exposure to sensitive non- target tissues. Lack of specificity towards brain tumors leads to a third challenge, the systemic toxicity associated with the drug. For achieving therapeutic concentrations in the brain, drugs need to be administered at high concentrations which are very toxic to normal vital tissues. High peak concentrations of antineoplastic agents may cause severe toxic effects. Drugs with short distribution half-lives can lead to sub-therapeutic levels of chemotherapy and may result in a minimal probability of circulating the drug through the tumor vascular bed (Medina, Zhu et al. 2004).

Myelosuppression and cardiotoxicity are considered dose limiting factor in conventional cancer therapy with free doxorubicin (Drummond, Meyer et al. 1999). For

an anthracycline anticancer agent, drug-induced congestive heart failure is the most significant concern due to its very poor prognosis. In addition to myelosuppression and cardiotoxicity, alopecia, mucositis, nausea, and vomiting are common at all doses with the anthracycline antineoplastic drugs. Other important factors include the apparent resistance of brain tumors to conventional treatments, the susceptibility of adjacent normal brain to adverse effects of therapy, and the limited capacity of brain tissue for repair (Grossman, Fisher et al. 1998; Huynh, Deen et al. 2006). Together these factors are responsible for complexity of drug delivery to brain.

1.3 Current Brain Tumor Therapy Approaches

The common treatment techniques for brain tumors are surgery, radiotherapy, chemotherapy, usually as a last resort. The intensity, combination, and sequence of these treatments depend on the subtype, size, location, and patient age, health status, and medical history (Green, Byar et al. 1983; Grant, Liang et al. 1995; DeAngelis, Burger et al. 1998; Fine, Wen et al. 2003). The standard surgical procedure is called a craniotomy, in which the surgeons remove a piece of the skull bone, and then remove the tumor from the brain tissue. However, in certain cases including when the patients does not want surgery, a gamma knife may be used where beams of gamma irradiation are focused on a single, specific target in the brain. This can be very effective if the circumstances are right. These factors include tumor size, stage, location, and type of tumor. Radiation treatment has an essential role in the treatment of brain tumors. If a tumor is removed surgically, radiation is generally given to kill any remaining tumor cells that may be in

the surrounding brain tissue. In some cases, the entire tumor can not be removed surgically; however a portion of it might be, in this situation, radiation is given to reduce, or halt the tumor progression. In cases where surgery is not an option, radiation is given in an attempt to control the tumor as much as possible. On occasion, patients with high-grade tumors are given radiotherapy in conjunction with chemotherapy in an attempt to control the tumor (Grossman, Fisher et al. 1998).

Chemotherapy is a common treatment method for some tumor types; however it is not for brain tumors. Chemotherapy involves using cytotoxic drugs to kill cancer cells, and in the brain there is the blood-brain barrier which the standard chemotherapy drugs cannot penetrate. However, certain genetic characteristics in some types of brain tumors that makes them more susceptible to the effects of chemotherapy. Currently, chemotherapy is generally only administered as a salvage therapy, for recurrent or slow-progressing tumors. There are a variety of investigative treatments available for brain tumors; however they are generally used when the common treatments have failed. Some examples of investigative treatments include immunotherapy, angiogenesis inhibitors, and transplant procedures and high-dose chemotherapy (Grossman, Fisher et al. 1998).

In immunotherapy, the goal is to boost the patients own immune system so it can destroy the tumor cells within the body. Angiogenesis inhibitors try to interfere with the growth of blood vessels to the tumor in an attempt to starve the tumor of nutrients and oxygen. Transplant procedures and high dose chemotherapy takes advantage of the fact that chemotherapy destroys all cells, not just cancer cells. By performing a bone marrow transplant after a high-dose of chemotherapy, the bone marrow will produce new healthy

cells while the cancer cells should not regenerate (Batchelor and Byrne 2006; Koo, Reddy et al. 2006; Richards, Khuntia et al. 2007).

1.3.1 Convection enhaced drug delivery (CED)

Convection enhanced drug delivery is a novel approach designed to circumvent the blood brain barrier issue by the direct administration of drugs into the solid tumor tissue. This method enhances the delivery of drugs directly into brain tumors. CED uses a pressure gradient established at the tip of an infusion catheter to create bulk flow that forces the drug through the interstitial space. CED can distribute large therapeutic molecules over considerable distances. Several studies have documented the use of CED in conjunction with small molecule drugs, proteins and viral vectors (Hall and Sherr 2006; Lopez, Waziri et al. 2006; Raghavan, Brady et al. 2006).

1.3.2 Implantable wafers

Implanted polymers are currently in use for the treatment of brain tumors. This delivery system provides sustained release of drug to the tumor using a matrix that also protects unreleased drug from degradation. Gliadel® carmustine -impregnated biodegradable polymeric wafer system, is the first new therapeutic to be approved by the FDA in 23 years for patients with gliomas. Multiple clinical trials have demonstrated safety and efficacy of Gliadel® wafers. There are several research groups are now working on the intracranial delivery of polymers impregnated with various drugs such as taxol , adriamycin, 5-fluorouracil, mitomycin, nimustine hydrochloride, mitoxantrone, and camptothecin in experimental animals. Potential disadvantages of the technique are

risk of local neurotoxicity and drug release cannot be controlled once the device has been implanted without physically removing it (Dimeco, Li et al. 2002; Tae, Hui et al. 2002; Ewend, Elbabaa et al. 2005).

1.3.3 Osmotic blood brain barrier disruption (OBBBD)

According to this method, the blood brain barrier will be transiently disrupted using a concentrated sugar solution. The high osmotic pressure created by the sugar solution results in shrinkage of the endothelial cells, thus opening the tight junctions between them for a period of a few hours. Permeability of small molecules across the blood brain barrier can be enhanced using this method. Hypertonic solutions of mannitol are most commonly used for blood brain barrier disruption in therapeutic trials in patients with brain tumors. OBBBD will be followed by administration of intra-arterial chemotherapy. Animal studies suggest that this method is able to increase concentrations of chemotherapeutic agents in the brain parenchyma up to 90 fold. OBBBD has been used to treat hundreds of patients and is currently employed in several phase I/II clinical trials. Toxicity is a major concern with BBBD. The normal brain is vulnerable to cytotoxic agents, thus this factor was outweigh the benefits of barrier opening (Kroll and Neuwelt 1998; Fortin 2003).

1.3.4 Biochemical blood brain barrier disruption (BBBBD)

Several chemical and biological agents are under investigation for selectively increasing the permeability of the capillaries of the tumor. This method is more reliable technique to disrupt the BBB, and gives a more precise time-window for brain drug

delivery when compared to osmotic blood brain barrier disruption. Potassium channel agonists like minoxidil was used to activate potassium channels to selectively increase the permeability of the capillaries of the tumor to give drugs a greater access to the tumor cells (Ningaraj, Rao et al. 2002; Ningaraj, Rao et al. 2003). This strategy is based on the finding that tumor capillaries express higher levels of potassium channels compared to those in normal brain. Leukotrienes, histamine and vasoactive peptides, have been reported to cause blood brain barrier disruption and temporarily increase the permeability of blood vessels (Black, King et al. 1990; Chio, Baba et al. 1992). Bradykinin, and its synthetic analog RMP- 7 can also increase the tight junction permeability by activating B2 receptors of the endothelial cells (Bartus, Elliott et al. 1996). However, these strategies are also shown unacceptable toxicity during clinical trials, thus limiting the scope of this treatment strategy (Packer, Krailo et al. 2005).

1.3.5 Carrier mediated drug delivery

The carrier mediated drug delivery approach makes use of endogenous transport systems that are present in brain endothelial cells. A number of carrier transport systems at the BBB are responsible for brain uptake of nutrients from the systemic circulation. Thus, transport systems exist for glucose, amino acids, choline, vitamins, low density lipoprotein (LDL), and nucleosides. Among these transporter systems large neutral amino acid transport system (LAT) has the maximum transport rate and is less specific for its substrates. The LAT is capable of transporting numerous endogenous as well as exogenous amino acids. L-dopa, alpha-methyldopa and baclofen have been shown to be taken into brain by LAT mediated transport.(Terasaki and Tsuji 1994). The glucose

transporter was explored to facilitate the penetration of glucose prodrugs of chlorambucil into the brain (Terasaki and Tsuji 1994; Tsuji and Tamai 1999).

1.3.6 Receptor mediated drug delivery

The brain capillary endothelium expresses specific transcytosis systems for circulating nutrients and signaling molecules which cannot diffuse through the blood brain barrier. These include systems for the transport of insulin, insulin-like growth factors, transferrin, and leptin. The brain uptake of drugs can be improved by conjugation of endogenous compounds, which uses receptor mediated transcytosis. Endogenous peptides such as insulin, transferrin, and receptor specific monoclonal antibodies (MAb) that undergo transcytosis through the BBB *via* the endogenous receptor system have been used as drug transport vectors in literature (Terasaki and Tsuji 1994; Huwyler, Wu et al. 1996; Huwyler, Yang et al. 1997; Wu 1997; Pardridge 1999; Partridge 1999; Allen 2002; Pardridge 2002; Qian 2002; Pardridge 2003; Schnyder and Huwyler 2005; Soni, Kohli et al. 2005; Jain, Chourasia et al. 2006; Koziara, Lockman et al. 2006; Newton 2006; Wu, Barth et al. 2006; Soni, Kohli et al. 2007). Several coupling methods were reported for conjugation of a drug to this transport vector, these include chemical linkers, avidin-biotin technology, and polyethylene glycol linkers (Temsamani, Rees et al. 2001).

Brain delivery of non-transportable peptides and small molecules by this approach has been extensively explored by Pardridge et al (Pardridge 1998; Pardridge 1999; Pardridge 1999; Partridge 1999; Pardridge 2002; Pardridge 2002; Pardridge 2003). Receptor mediated transport process involves binding of the receptor and peptide at one side of the BBB (i.e. the luminal membrane), translocation of the receptor–peptide

complex through the cytoplasm, and dissociation of the peptide from the receptor on the external surface of abluminal membrane. One of the most extensively explored vectors for receptor mediated transcytosis has been the anti-rat transferrin-receptor antibody OX26, which recognizes an external epitope of the transferrin receptor (Huwyler, Wu et al. 1996; Huwyler, Yang et al. 1997; Pardridge 1999; Pardridge 1999; Partridge 1999; Pardridge 2002). Transferrin as brain drug delivery vector was evaluated and is found to be as effective in transporting biotinylated therapeutics as OX26, without antigenicity (Liao, Li et al. 2001; Li and Qian 2002).

1.4 Liposomal Approaches for Brain Tumor Targeting

Liposomes have been investigated over decades as systemic drug delivery vehicles for the delivery and targeting of drugs to targeting sites in the body (Torchilin 2005). Liposomes have gained increased attention, because of their structural versatility in terms of size, composition, surface charge, ability to incorporate most of the drugs regardless of solubility. The key features of liposomes include controlled retention of entrapped drugs in the presence of biological fluids, prolonged vesicle residence in circulation and enhanced vesicle uptake by target cells. However, the *in vivo* use of classical liposomes is hampered by the very rapid clearance of liposomes from the circulation by the reticuloendothelial system. Liposomes coated with biocompatible polymers PEG or ganglioside are widely used in the market and are known as “stealth” liposomes. These biocompatible polymer coatings are believed to prevent recognition of liposomes by macrophages due to reduced binding of plasma proteins (Silvander 2002;

Cattel, Ceruti et al. 2003; Moghimi and Szebeni 2003). These modifications can enhance the circulation time half-life of liposomes considerably.

Conventional liposomes larger than 100 nm are not delivered to brain *in vivo* (Schackert, Fan et al. 1989; Gennuso, Spigelman et al. 1993), because these agents are not transported through the brain capillary endothelial wall (BBB) *in vivo.* However, rapid advances have been made in the fields of receptor biochemistry, and monoclonal antibodies. The application of these technologies for ligand-mediated BBB targeting is a logical outgrowth of these advances.

Targeted liposome that permeate through blood brain barrier and act to concentrate the drug molecules at their target site would provide a variety of advantages over agents lacking this specificity. Targeting potential of liposomal delivery systems has been enhanced by attaching site-specific ligands to these systems (Allen 1997; Noble, Kirpotin et al. 2004; Soni, Jain et al. 2005). These types of delivery systems are critical for in vivo transport and delivery of macromolecules as well as small molecules for brain tumors. For example, since a greater portion of the administered dose of a drug is sequestered at a particular locus in the brain, the delivery system should be highly efficacious and the drug dose could be reduced. In addition, nontarget site toxicities are attenuated since lower concentrations of the drug are present. A significant improvement in the therapeutic index can be achieved by lowering of the effective dose.

In recent years, several studies have demonstrated that the use of the transferrin uptake pathway is highly effective for treating cancer in animal models and in humans. As an example, the conjugation of transferrin with anticancer drugs such as doxorubicin has

shown the potential to circumvent the cardiotoxicity and development of drug resistance (Lai, Fu et al. 2005; Soni, Jain et al. 2005; Soni, Kohli et al. 2007).

One of the most extensively explored vectors for receptor-mediated transcytosis has been the anti-rat transferrin-receptor antibody OX26, which recognizes an external epitope of the transferrin receptor. Transferrin, as brain drug delivery vector, was evaluated and was found to be as effective in transporting biotinylated therapeutics as OX26, without any significant antigenicity (Liao, Li et al. 2001; Soni, Kohli et al. 2005; Soni, Kohli et al. 2007).

Huwyler et al. (Huwyler, Wu et al. 1996; Wu 1997) have demonstrated that 85 nm liposomes can be sterically stabilized with DSPE-PEG2000 which contains a lipid at one end and maleimide at the distal end to the liposome. Monoclonal antibodies can be coupled with a sulfide linkage to the maleimide moiety of these stealth liposomes to form immunoliposomes. The OX26 monoclonal antibody is linked to stealth liposomes because this antibody binds to BBB transferrin receptor, and it has been successfully used as a vector in delivery of small and large molecules to the brain (Shi and Pardridge 2000; Pardridge 2002; Pardridge 2002; Qian 2002). As an example, the brain volume of distribution of daunomycin in OX26 MAb conjugated PEGylated immunoliposomes was increased with time following intravenous administration (Huwyler, Yang et al. 1997; Schnyder, Krahenbuhl et al. 2005).

Human gliomas and a variety of solid tumors highly express epidermal growth factor receptor (EGFR), and clinical trials indicate that this antigen has important roles in cancer etiology and progression. Epidermal growth factor receptor (EGFR)–targeted immunoliposomes showed significant antitumor activity against flank U87 tumor

xenografts in nude mice (Mamot, Drummond et al. 2003; Mamot, Drummond et al. 2004; Mamot, Drummond et al. 2005; Mamot, Ritschard et al. 2006).

Cancer cells that over express the IL-13 receptor α2 protein have been targeted using human interleukin-13 as a targeting ligand. Anti-tumor efficacy of doxorubicin sterically stable human interleukin-13 (IL-13)-conjugated liposomes were found to be superior to non targeted liposomes in a subcutaneous glioma tumor mouse model (Madhankumar, Slagle-Webb et al. 2006). Lactyl stearate coupled liposomes for targeting monocarboxylic acid transport system of the brain were reported by Jain et al. (Jain, Chourasia et al. 2006). Brain concentrations of rifampin delivered in lactyl stearate-coupled liposomes were 6 – 8 times higher when compared to non targeted liposomes. Monoclonal antibody (mAb) 2C5 conjugated immunoliposomes were studied against brain tumors. 2C5-immunoliposomes had shown significantly better accumulation in the subcutaneously grown brain tumor than non-specific control IgG-immunoliposomes (Gupta, Levchenko et al. 2005).

1.5 Targeted Liposomal Delivery System Design Considerations

Development of an effective targeted drug delivery system requires considerations of many design and scientific aspects. Several recent reviews address these considerations. (Allen 2002; Scherrmann 2002; Allen 2004; Schnyder and Huwyler 2005; Torchilin 2005). In general, critical design characteristics include: 1) choice of target organ for selection of passive or active targeting method; 2) selection of a targeting antigen or receptor that has homogeneous over expression and has a vital role in tumor

progression with minimal expression in normal tissue; 3) selection of a stable, specific, and non-immunogenic targeting ligand that can undergo endocytosis efficiently; 4) a stable liposome formulation with small (< 100 nm) size, and zeta potential ~ 20 mV, 5) minimal leakage of drug, 6) long *in vivo* circulating properties, 7) minimal interaction with blood components, 8) selective extravasation into tumors along with high tumor localization capability; 9) a stable and rapid conjugation method with high conjugation efficiency; and 10) a highly potent anticancer drug with a possibility for high liposome encapsulation. Each of the design considerations as well as their interactions has a critical role in determining the success of a targeted liposome delivery system.

1.5.1 Target organ

Based on the target organ, the liposomal targeting method can be selected. By regulating the liposome properties like size, charge and composition, liposomes can be designed to deliver their contents to specific sites such as liver, spleen, and permeable vasculature of some solid tumors by passive targeting. However, active targeting may be a logical option to target pathological sites like brain tumors which have limited accessibility.

1.5.2 Target receptor or antigen

For efficient targeting, the targeted receptor or antigen should have homogeneous, high expression on the surface of the target cells. The antigen or receptor should not be down regulated. Circulating shed antigen will compete with the target cells for binding of the targeted therapeutics, and any complexes that form would be rapidly cleared from the

circulation. The receptors or antigens which undergo endocytosis of antibodies increases efficacy of drug delivery, presumably by inducing tumor cells to endocytose immunoliposomes (Allen 2002).

1.5.3 Target ligand or antibody

Several factors determine the selection of a target ligand. Non-antibody ligands are relatively stable, inexpensive to manufacture and are readily available. However they can bind to some non-target tissues. Endogenous ligands like folic acid and transferrin found in significant levels in body fluids and the free ligands will compete for binding with the targeted therapy (Allen 2002). For a high degree of selectivity towards target tissues, monoclonal antibodies or antibody fragments can be selected. Cost, stability and potential immunogenicity are major disadvantages with antibodies. Along with the choice of a ligand, the ligand density can have a potential impact on targeting efficiency of a targeted liposome. High ligand densities are preferable for enhancing the binding to target cells. However, high ligand density can lead to rapid clearance from the circulation. Additionally, achieving high ligand density is expensive and difficult to produce (Pardridge 1999).

1.5.4 Liposome formulation

1.5.4.1 Composition

An ideal liposome formulation for targeted drug delivery should be stable with small (< 100 nm) size, zeta potential ~ 20 mV, minimal leakage of drug, long *in vivo*

circulating properties, minimal interaction with blood components, selective extravasation into tumors along with high tumor localization capability (Torchilin 2005). Liposomes made up of saturated phospholipids like HSPC, DSPC or SPC along with optimum levels of cholesterol can produce stable liposomes with minimal leakage (Allen 2002). The fluidity of liposome bilayers can be altered by using phospholipids with different T_m, which in turn can vary depending upon the length and nature (saturated or unsaturated) of the fatty acid chains. Liposomes containing high phase transition temperature lipids (T_m >37 °C) are rigid at the physiological temperature and are less leaky. In contrast, liposomes composed of low T_m lipids (T_m < 37 °C) are more susceptible to leakage of drugs encapsulated in aqueous phase at physiological temperatures. The fluidity of bilayers also influences interaction of liposomes with plasma components and cell membranes. Liposomes composed of high T_m lipids were reported to have lower extent of uptake by RES, compared to those containing low T_m lipids (Drummond, Meyer et al. 1999). Incorporation of cholesterol into the lipid bilayer increases membrane rigidity thereby affecting their stability both *in vitro* and *in vivo* (Kirby, Clarke et al. 1980). For hydrophobic drugs, unsaturated lipids like egg phosphatidylcholine or egg sphingomyelin can enhance drug loading into liposomes (Straubinger, Sharma et al. 1993; Sharma and Straubinger 1994). Anti-oxidants like α-tocopherol in the formulation were shown to reduce auto-oxidation of lipid components and prolong the shelf lives of liposomes (Hunt and Tsang 1981).

1.5.4.2 Liposome size

The in vivo circulation half life and tumor accumulation of liposome is mainly depends on its size. Small unilamellar liposomes (≤ 100 nm) are opsonized less rapidly and to a lower extent than large liposomes (> 300 nm) and therefore the rate liposome uptake by the reticular endothelial system (RES) increases with size of the vesicle (Harashima, Sakata et al. 1994; Papisov 1998). Inclusion of PEG-lipids in the liposome composition was shown to result in clearance rates that are relatively insensitive to size in the range of 80 to 250 nm (Lasic, Martin et al. 1991; Woodle and Lasic 1992; Lasic 1994; Ceh, Winterhalter et al. 1997; Lasic 1997).

Optimal liposome size depends on the tumor target. The macromolecular size of liposomes prevents them from passing through the 2 nm pores found in the endothelium of blood vessels in most healthy tissues or even the 6 nm pores found in post capillary venules (Seymour 1992). In tumor tissue, the vasculature is discontinuous, and pore sizes vary from 100 to 780 nm enables accumulation of liposomes in these areas (Yuan, Dellian et al. 1995). Negatively charged liposomes were believed to be more rapidly removed from circulation than neutral or positively charged liposomes (Gabizon and Papahadjopoulos 1992).

1.5.4.3 Liposome surface charge

Surface charge properties of liposomal colloidal systems are critical in determining their drug carrier potential, since they will control their interactions with plasma proteins. Lipid composition can influence the liposomal surface charge. Lack of surface charge can reduce physical stability of small unilamellar liposomes by increasing

their aggregation (Kaye 1981; Sharma and Sharma 1997). However, negatively charged liposomes were believed to be more rapidly removed from circulation than neutral or positively charged liposomes (Gabizon and Papahadjopoulos 1992). It is reported that the negatively charged liposomes are predominantly taken up by cells through coated-pit endocytosis, while cationic liposomes deliver contents to cells either by fusion with cell membranes or through coated pit endocytosis (Sharma and Sharma 1997).

1.5.4.4 Steric stabilization

Colloidal stability of liposomes can be enhanced by addition of hydrophilic polymers or glycolipids like PEG conjugated lipids, ganglioside-GM1 or phosphatidylinositol into liposomes. Sterically stabilized liposomes showed prolonged lifetimes in the circulation as compared with nonstabilized liposomes. Sterically stabilized liposomes are less reactive toward serum proteins and less susceptible to RES uptake than nonstabilized liposomes (Allen and Chonn 1987). The mechanism by which PEG induces dehydration of the head group region of lipids is related to the fact that PEG, chemically attached to the lipid head group, undergoes steric exclusion from the liposome surface in a similar way to free PEG (Tirosh, Barenholz et al. 1998). This results in greater density of the grafted PEG further from the surface. Thus, the local concentration gradient of PEG chains from the liposome surface leads to an osmotic imbalance, changes in thermodynamic properties and hydration of the lipids. At higher concentrations (> 10 mol%) PEG chains will be in highly overlapped brush configuration. Due to repulsion of PEG chains, at these high concentrations of PEG lipids, weakening of the bilayer packing was observed. Although sterically stabilized

liposomes prolong circulation time and decrease liposomal uptake by the RES, they do not actively target the liposome to the tumor (Tirosh, Barenholz et al. 1998).

1.5.4.5 Conjugation method

There are several approaches available for conjugation of ligands on liposomes for achieving targeted delivery. These conjugation methods are selected based on delivery system requirements like time required for conjugation, stability of conjugate, conjugation efficiency. An ideal conjugation method should occur rapidly with stable bond formation. The conjugation efficiency should be more than 70%. This linker should not affect the reactivity of the ligand or stability of the liposomal drug.

A variety of functionalized lipids are available for attaching ligands with covalent or non covalent bonds (Pardridge 1999; Allen 2004). The chemical-based linkers employ activating reagents such as maleimidobenzoyl N-hydroxysuccinimide ester (MBS) or 2-iminothiolane (Traut's reagent), which activate primary amino groups on surface lysine (Lys) residues of the ligand. This results in the formation of a stable thioether linkage which is comprised of only a single sulfur atom and will not be subjected to cleavability. The resulting thio-ether bond is stable under physiological conditions. Cleavable bonds like ester and disulfide bond between ligand and liposome have been shown to be suboptimal for targeted drug delivery to tumors (Martin, Hubbell et al. 1981). The major disadvantage with chemical coupling methods is a low yield in the coupling efficiency. Non covalent coupling methods like avidin-biotin conjugation are more rapid (Loughrey, Bally et al. 1987), stable and higher coupling efficiency can be achieved (Hansen, Kao et al. 1995; Sakahara and Saga 1999). The type and length of the polymer spacer was also

found to influence target recognition and binding in liposomes that already contained PEG-derivatized lipids (Gabizon et al. 1999).

A novel and relatively simple post insertion technique was reported by several groups for preparation of targeted liposomes (Ishida, Iden et al. 1999; Allen, Sapra et al. 2002). According to this method, micellar conjugates of the ligand needs to be co-incubated with preformed liposomes which can form targeted liposomes. However, this post-insertion technique is usually performed at elevated temperatures (55 to 60 °C) to accommodate lipid bilayers with higher melting temperatures. Therefore, the denaturation of protein ligands under these conditions is a concern.

1.5.4.6 Choice of drug

For optimal targeted liposomal delivery, the drug must be compatible with the liposome structure and should show efficient loading into the liposomes. The drug leakage rate from liposomes might limit the choice of drugs that are available for liposomal targeted delivery. Highly lipophilic drugs tend to associate mainly with the bilayer compartment of the liposome. This can result in lower entrapment stability due to faster redistribution of the drug to plasma components (Sharma and Sharma 1997). Even though amphipathic drugs are reported to be suitable for liposomal carriers, targeted liposomal system should be optimized for each drug (Drummond, Meyer et al. 1999).

1.6 Transferrin Receptor Mediated Brain Tumor Targeting

Transferrin receptor mediated endocytosis is one of the best-characterized and well documented processes in tumor targeted drug delivery (Shi and Pardridge 2000; Pardridge 2002; Qian 2002; Soni, Jain et al. 2005; Soni, Kohli et al. 2005). Transferrin receptors are reportedly present on the surface of diverse classes of cell types and mediate the internalization of iron-saturated transferrin through receptor-mediated endocytosis (Qian 2002). Transferrin holds promise as a drug targeting ligand because of the high expression of transferrin receptors on the surface of tumor cells. The density of transferrin receptor is correlated with the extent of cell growth and division. Tumor cells ordinarily divide faster than normal cells and consequently express more transferrin receptors (Prior, Reifenberger et al. 1990; Ishida, Maruyama et al. 2001; Widera, Norouziyan et al. 2003).

Many exciting studies have been carried out recently using transferrin or the transferrin receptor (TfR) as a targeting ligand to deliver a wide range of therapeutic agents into malignant sites that overexpress transferrin receptors (Pardridge 1999; Qian 2002; Lai, Fu et al. 2005; Soni, Kohli et al. 2005; Soni, Kohli et al. 2007).

1.6.1 Transferrin and transferrin receptor mediated endocytosis

The transferrins are a family of iron-binding proteins that transport iron among its sites of absorption, storage and utilization. A major pathway for cellular iron uptake is by internalization of the complex of iron-bound transferrin and the transferrin receptor (TfR). Diferric-transferrin binds to the TfR on the cell surface and the transferrin–transferrin receptor complexes are routed into the endosomal compartment after

endocytosis via clathrin-coated pits. Upon maturation and loss of the clathrin coat, the endosome is acidified, and iron is released from transferrin and then transported to the cytosol by a divalent metal transporter (Qian 2002). The apo-transferrin–transferrin receptor complex is then recycled through exocytic vesicles back to the cell surface and apo-transferrin is released into the circulation and re-used (Qian 2002).

1.6.2 Transferrin receptor in brain drug delivery

Brain capillary endothelial cells do possess specific receptor-mediated transport mechanisms that potentially can be exploited as a means to deliver therapeutics to the brain (Wu 1997; Pardridge 1998; Pardridge 1999; Pardridge 1999; Partridge 1999; Pardridge 2002; Pardridge 2002; Qian 2002; Pardridge 2003; Widera, Norouziyan et al. 2003; Soni, Jain et al. 2005).

The extent of transferrin receptor expression in glioma brain tumors has been shown to be significantly greater than in normal brain tissue, with expression linked to the severity of the tumor (Kurpad, Zhao et al. 1995). In the literature, several targeted liposomal approaches have been explored as a promising tool for the brain delivery of therapeutic and diagnostic agents (Pardridge 1999; Pardridge 1999; Pardridge 2002; Pardridge 2003; Schnyder, Krahenbuhl et al. 2005; Soni, Jain et al. 2005; Soni, Kohli et al. 2005; Soni, Kohli et al. 2007). Brain delivery of non-transportable peptides and small molecules by vector mediated approach has been extensively explored by Pardridge et al. According to Pardridge et. al., receptor-mediated transport of ligand mediated immunoliposomes at the BBB involved binding of the receptor and peptide at one side of the BBB (i.e. the luminal membrane), translocation of the receptor–peptide complex

through the cytoplasm, and dissociation of the peptide from receptor on the external surface of abluminal membrane. One of the most extensively explored vectors for receptor mediated transcytosis has been the anti-rat transferrin-receptor antibody OX26, which recognizes an external epitope of the transferrin receptor (Pardridge 1999; Pardridge 1999).

In a recent study, OX26 immunoliposomes directed against the rat transferrin receptor revealed brain accumulation of daunomycin in OX26-immunoliposomes to higher levels as compared to brain uptake of free daunomycin, or daunomycin incorporated within pegylated liposomes or within unspecific IgG2a isotype control immunoliposomes (Schnyder, Krahenbuhl et al. 2005). In another study, daunomycin encapsulated, 80 nm long circulating targeted liposomes with 30 OX26 antibodies per liposome resulted in optimal brain delivery (Huwyler, Wu et al. 1996). Targeted liposome delivery system has the ability to enhance the brain drug delivery as a single liposome may carry up to 10,000 drug molecules. The OX26 monoclonal antibody has been successfully used as a vector in delivery of small and large molecules to the brain (Huwyler, Wu et al. 1996; Huwyler, Yang et al. 1997; Pardridge 1998; Pardridge 1999; Pardridge 2002; Pardridge 2003; Soni, Jain et al. 2005). These reports on novel vector based liposomes revealed a potential for both brain drug delivery and brain gene delivery.

Transferrin as a brain drug delivery vector was evaluated and was found to be as effective in transporting biotinylated therapeutics as OX26, without antigenicity (Liao, Li et al. 2001). In another study transferrin coupled liposomes showed 10 fold higher brain uptake of doxorubicin when compared a solution formulation (Soni, Kohli et al. 2007). Transferrin receptor mediated drug targeting is found to be a promising tool for

enhancing the brain delivery of the drugs to treat brain tumors (Li and Qian 2002; Soni, Jain et al. 2005).

1.7 Avidin Biotin Conjugation Method for Attaching Transferrin on Liposomes

The major drawback of covalent chemical coupling strategies is the difficulty in obtaining reproducible and high coupling efficiencies (Schnyder, Krahenbuhl et al. 2004). In contrast to chemical conjugation methods, avidin/biotin conjugation method is a non covalent coupling method. But the avidin-biotin conjugation is extremely strong with a dissociation constant (*Kd*) in the order of 10^{-15} M and dissociation half-life of about 89 days (Sakahara and Saga 1999). Stability of the avidin/ biotin bond is very high in blood circulation; however it is labile in tissues (Pardridge 1999). Avidin, an egg white protein, is a 64-kDa homotetramer`that has four biotin binding sites per molecule(Green 1964; Green and Joynson 1970; Green 1990). The use of avidin/biotin technology applied to brain drug delivery involves the incorporation of biotinylated lipids in the liposome, and the construction of a conjugate of the OX26 and an avidin, streptavidin (SA) or neutral light avidin (Kang and Pardridge 1994). Owing to its cationic nature, avidin is rapidly removed from the plasma compartment following administration *in vivo* (Green 1990; Qian 2002). This rapid plasma clearance results in a reduced plasma area under the concentration curve (AUC) and sub-optimal bioavailability and pharmacokinetics of the drug–vector complex. However, neutral forms of avidin such as streptavidin or neutral light avidin are not rapidly removed *in vivo* (Qian 2002), and do not degrade the pharmacokinetic properties of the conjugate.

A relatively new coupling procedure for the preparation of pegylated immunoliposomes was reported by Snyder et. al., (Schnyder, Krahenbuhl et al. 2004). In this new technique, OX26 mAb was attached to sterically stabilized liposomes using a non-covalent biotin–streptavidin method. Streptavidin-conjugated OX26 mAb was used, since streptavidin has a much lower isoelectric point (pI 5–6) as compared with the highly basic pI of 10 for avidin. In addition, streptavidin is not a glycoprotein, which reduces its potential for binding to carbohydrate receptors (Schnyder, Krahenbuhl et al. 2004). Both factors reduced the amount of non-specific binding, and thereby the systemic clearance *in vivo* (Green 1990). The biotin at the end of the PEG terminus allows optimal target recognition of the bound mAb. Coupling of a streptavidin-conjugated antibody was reported to be simple, rapid and highly reproducible (Schnyder, Krahenbuhl et al. 2004). The multivalency of avidin binding of biotin causes the formation of high-molecular-mass aggregates when the drug or liposome is multibiotinylated and these high-molecular mass aggregates are rapidly cleared by the reticulo-endothelial system *in vivo* (Loughrey, Bally et al. 1987; Qian 2002). This conjugation method has been used in the conjugation of OX26 with the brain-derived neurotrophic factor (BDNF) and a neuropeptide, vocative intestinal peptide analog (VIPa) (Pardridge 1999).

1.8 Problems Associated with Targeted Liposome Delivery Systems

Delivery of drugs to brain tumors using targeted liposomes involves numerous complications. Major problems associated with targeted delivery systems are rapid clearance from the circulation and minimal interaction of targeted delivery system with

target cells after reaching the target site (Allen 2002; Allen 2004). Tumor targeted liposomes must at the very least exhibit accumulation properties comparable to nontargeted liposomes. Several physical factors play key roles in inhibiting liposome targeting following extravasation. Factors such liposome composition, size, charge and nature of the vascular barrier, tumor structure and binding site can affect the efficacy of targeted liposome (Harding, Engbers et al. 1997; Barenholz 2001).

Beyond the targeting strategy, several formulation issues need to be addressed for development of stable targeted liposomal delivery systems. The production of liposomes, with attached targeting ligands, requires an extensive number of modification steps. The feasibility of manufacturing a one-step antibody-targeted liposome formulation under Good-Manufacturing-Practices (GMP) regulations of sterility and quality control is, difficult. Manufacturing and quality factors like batch-to-batch reproducibility, entrapment efficiency, particle size control and scale up are the major problems limiting the manufacturing and development of commercially viable targeted liposomal dosage forms (Sharma and Sharma 1997).

1.9 Lyophilization of Targeted Liposomes

The therapeutic applications of targeted liposomes are dependent on the physical integrity and stability of the lipid bilayer structure. In the liquid state, liposome formulations are subject to both physical and chemical instability (Sharma and Sharma 1997). These stability parameters are critical to the *in vivo* behavior of liposomal drug delivery systems. Liposomal size distribution is a critical parameter with respect to the

pharmacokinetic and pharmacodynamic behavior of drugs that are site-specifically targeted *in vivo* (Van Bommel and Crommelin 1984; Van Winden, Zhang et al. 1997). One of the practical difficulties with liposomes for delivery of drugs to target cells is that liposomes are relatively unstable during storage.

Lyophilization is the method of choice for enhancement of long-term stability of liposomes (Ausborn and Nuhn 1990; Ausborn, Nuhn et al. 1992). In the process, most of the water molecules are excluded from the specimen and the aqueous suspension becomes a powder that can be stored at selected, even at ambient, temperatures. Prior to use, reconstitution of the particulate system is achieved by rehydration of the dry powder (Liu 2006). Additionally, removal of water by lyophilization prevents hydrolysis of phospholipids. Other chemical and physical degradation processes are also retarded by low molecular mobility in the solid phase. Further, freeze-drying of liposome formulations, if performed successfully, results in a pharmaceutically elegant dry cake which can be reconstituted within seconds to obtain the original dispersion (Jonkman-de Vries, Talsma et al. 1994; Wang 2000; Tang and Pikal 2004).

Lyophilization of targeted liposomes is more complex when compared to large multilamellar conventional liposomes (Van Winden, Zhang et al. 1997; Zhang, Van Winden et al. 1997). Liposome bilayer membranes may be damaged during the lyophilization cycle mainly by mechanical stress caused by high pressures vesicle membranes are exposed to during ice crystal formation and chemically from increased concentrations of solute during freezing and dehydration. This can lead to massive aggregation and fusion of the vesicles as well as leakage of the entrapped compounds upon reconstitution of the lyophilized cake. In the absence of cryoprotectants, small

targeted liposomes will be converted in to large multilamellar liposomes, upon lyophilization and reconstitution (Peer, Florentin et al. 2003). This change in size of the liposomes is detrimental for targeted drug delivery. Cryoprotectants have been shown to decrease vesicle fusion and leakage caused by both freeze-thaw and the freeze-drying process (Sun, Leopold et al. 1996; Crowe, Oliver et al. 1997; Crowe, Carpenter et al. 1998; Van Winden and Crommelin 1999). Sugars like trehalose, sucrose, mannose or glucose were used as cryoprotectants at high concentrations (~ 30%) in the original liposome preparations. Among these sugars, trehalose is particularly effective in preserving the liposomes. Crowe et al. have carried out extensive investigations on possible mechanisms by which sugars protect biological membranes during freeze-drying (Crowe, Oliver et al. 1997; Crowe, Carpenter et al. 1998). Cryoprotectants are noneutectic in nature forming an amorphous frozen matrix upon cooling. The freeze process generally occurs very quickly in the presence of cryoprotectants upon cooling to the freezing point depression. The role attributed to these cryoprotectants is replacement of structure- stabilizing water-based hydrogen bonds at the liposomal surface, which are lost in the process of drying (Van Winden and Crommelin 1999).

Several factors can affect the stability of the liposomes in the dry state (Crowe and Crowe 1988). These factors include size and charge of liposomes, type and concentration of stabilizing sugar, and the dry mass ratio between the stabilizing sugar and lipid. Small (< 60 nm) and large (> 1000 nm) lyophilized liposomes are found to be unstable even in extremely high concentrations of sugars (Crowe and Crowe 1988). The stability of lyophilized liposomes can be significantly increased by the addition of small amount of negatively charged lipid in the bilayer. The efficacy of sugar depends on the

size of liposomes and dry mass ratio between the stabilizing sugar and lipid (Crowe and Crowe 1988). Cryoprotection of liposomes is greatest when formulating with these sugars at high concentrations (5% to 20%)(Jovanovic, Bouchard et al. 2006). Vesicle fusion can be decreased at lower concentrations than are needed to minimize leakage. Prevention of leakage requires the sugar be present both inside and outside the liposome (Crowe and Crowe 1988). Advantages of formulating liposomes with trehalose include being less reactive than reducing sugars, higher *Tg'* than sucrose, a high melting temperature (100°C at 2% moisture), low hygroscopicity, and FDA approval as an injectable ingredient (Crowe, Crowe et al. 1987; Crowe 2007).

Peer et al. have reported lyophilization of targeted unilamellar liposomes without added sugars. Hyaluronan, the surface bound ligand in the targeted bioadhesive liposomes also protected liposomes during freeze-drying process. They proposed that hyaluronan, like sugars, protects liposomes by providing substitute structure-stabilizing hydrogen bonds (Peer, Florentin et al. 2003). Ugwu et al. have reported lyophilization of liposome formulations of mitoxantrone using sucrose as a cryoprotectant (Ugwu, Zhang et al. 2005). Sucrose was found to be more effective in minimizing drug leakage from the lyophilized liposomes. Long-term stability studies showed that lyophilized formulation was stable for up to 13 months when stored at refrigerated condition. 5-fluorouracil lyophilized liposomes with saccharose as a cryoprotectant were reported by Glavas Dodov et. al. Saccharose cryoprotection yielded a stable and less permeable 5-fluorouracil lyophilized liposome formulation (Glavas-Dodov, Fredro-Kumbaradzi et al. 2005).

Cui et al., have reported a novel lyophilized liposome system with tertiary butyl alcohol /water co-solvent system. This process gave a stable free flowing lyophilized powder with sucrose as a cryoprotectant (Cui, Li et al. 2006).

1.10 Non Invasive Optical Fluorescence Imaging in Drug Development

Non invasive imaging techniques are particularly attractive for early proof of principle trials in animals and humans. These non-invasive imaging techniques makes possible the tracking of biological activity non-invasively in real-time, at the molecular level. These methods can be used to assess anti-cancer therapies over the course of treatment *in vivo*. Current animal models of human disease require a large number of target cells, and these models use the therapeutic endpoints of gross tumor growth or death of the animal. Non-invasive, imaging of tumor growth and metastasis allows longitudinal evaluation of tumor development before, during and after treatment, offers an excellent preclinical strategy to assess tumor response and recurrence. These methods are rapid, easy to perform and amenable to high throughput (Abbott, Chugani et al. 1999; Edinger, Sweeney et al. 1999). Non invasive imaging methods can reduce the statistical variability, as the same animal is imaged at multiple time points. Each experimental animal will acts as its own statistical control which can further improve the statistical quality of the data (Jacobs, Dittmar et al. 2002; Shah and Weissleder 2005).
Several non-invasive imaging technologies have been explored to monitor the therapy using PET, SPECT, MRI, and optical imaging (Contag 2002). Reporter genes with optical signatures (eg, fluorescence and bioluminescence) are low-cost alternatives for

real-time analysis of gene expression in small animal models. Optical imaging is a safe and reliable imaging method as visible light has no safety issues for using in biological systems also visible light can penetrate relatively deeply into certain tissues.

Optical imaging can be divided into two forms: those modalities in which external light is required, and bioluminescent imaging in which internal light from luciferase enzymes is used for functional measurements. The useful wavelengths of optical imaging technologies range from 580 nm 800 nm. Blue-green light (400–590 nm) is strongly attenuated by tissue, whereas red to near infrared (NIR) light (590–800 nm) is less affected (Contag 2002).

Non invasive monitoring of tumor growth and response to therapeutic interventions at early stages of tumor growth in animal models is critical for the development of effective strategies for the tumor therapy (Edinger, Sweeney et al. 1999). Fluorescence imaging is the most sensitive approach, and it has gained great interest with the development of genetically encoded highly efficient fluorescent probes based on green fluorescence protein (GFP).

Conventional methods for measuring tumors in mice rely on physical caliper measurements that are not externally detectable early in the time course of the tumor progression. By contrast, optical fluorescence imaging offers quantitative data from time zero in the disease course. Mice with immunodeficiency like severe combined immunodeficient mice (SCID) or nude mice have been useful for studying tumor xenografts (Edinger, Sweeney et al. 1999; Sweeney, Mailander et al. 1999; Contag 2002). Recently, Sweeney et. al., reported a novel noninvasive, direct, and sensitive quantification method of tumor burden *in vivo*. This method is based on bioluminescence

imaging. Several groups reported the method of non invasive imaging of tumor growth and effect of therapy on tumor regression using bioluminescence (Sweeney, Mailander et al. 1999). Bioluminescence imaging of tumor growth can be accomplished by introducing a constitutively expressed bioluminescent reporter gene encoding the photoprotein firefly luciferase into the chromosomes of a tumor-cell line. Implantation of these genetically modified tumor cells in to immunodeficient mice results bioluminescent tumors. Distribution and growth of these cells can be monitored real time by using the light produced by the transformed cells and transmitted through the anesthetized animal tissues. The use bioluminescence imaging for the study of infection and gene expression in living animals has been demonstrated effectively in several studies (Schmidt-Wolf, Negrin et al. 1991; Contag, Contag et al. 1995; Contag, Spilman et al. 1997). Bouvet et. al, reported a whole-body optical imaging method of genetically fluorescent pancreatic tumors growing and metastasizing to multiple sites in live mice The GFP-expressing pancreatic tumor cell lines were used in this study for generating pancreatic tumors. Whole-body imaging was carried out with a fluorescence light box, with a thermoelectrically cooled color CCD camera. In this study, strong GFP fluorescence allowed detailed simultaneous quantitative imaging of tumor growth and multiple metastasis formation of pancreatic cancer (Bouvet, Wang et al. 2002).

Whenever tissue absorbs light, there is a chance that fluorescent light will be emitted. In addition to absorption, tissue 'autofluorescence' can severely limit signal to background ration (SBR). Use of a NIR filter set essentially eliminates autofluorescence. There are several dyes that are fluorescent in the NIR range that can be conjugated to biomolecules and developed as imaging reagents (Frangioni 2003; Ballou, Ernst et al.

2005; El-Deiry, Sigman et al. 2006). Because there is little NIR fluorescence contrast generated by most tissues, most *in vivo* studies administer exogenous contrast agents. Heptamethine cyanines are fluorophores commonly used as contrast agents in fluorescence imaging. Among these the indocyanines are the most widely used as they do not have the aggregation problems associated with the other subclasses. Peak excitation of this class is at 760–800 nm, and peak emission at 790–830 nm (Bremer, Ntziachristos et al. 2001; Frangioni 2003; Rao, Dragulescu-Andrasi et al. 2007). Indocyanine green (ICG) is the first FDA approved and least toxic contrast agent which can be used in humans (Desmettre, Devoisselle et al. 2000). Recently, a noninvasive imaging of integrin expression in brain tumor xenografts was reported by Chen et. al. Arginine-glycine-aspartic acid (RGD)-Cy5.5 conjugate was used for NIR imaging in subcutaneous U87MG glioblastoma xenografts. The RGD-Cy5.5 conjugate elevated cell-associated fluorescence on integrin-expressing tumors (Chen, Conti et al. 2004).

A new NIR dye, 1, 1'-dioctadecyl- 3, 3, 3', 3'-tetramethylindotricarbocyanine iodide (DIR) was recently reported by Kalchenko et. al. DiR has absorption and fluorescence maxima at 750 and 782 nm, respectively. This lipophilic dye was used to directly label the membranes of human leukemic cell lines, primary murine lymphocytes and erythrocytes. Noninvasive whole-body imaging of DiR-labeled cell homing in intact animals was reported using a CCD camera (Kalchenko, Shivtiel et al. 2006).

1.11 Paclitaxel

Paclitaxel is a diterpenoid pseudoalkaloid isolated from *Taxus brevifolia*, discovered at Research Triangle Institute (RTI) in 1967. Paclitaxel is approved by the FDA for the treatment of ovarian and breast cancers. Paclitaxel was the first of a new class of microtubule stabilizing agents and is considered as one of the most significant advances in chemotherapy of the past 15–20 years. Paclitaxel promotes the polymerization of tubulin. Specifically, paclitaxel binds to the β subunit of tubulin. Tubulin is the "building block" of microtubules, and the binding of paclitaxel locks these building blocks in place.The tubulin/paclitaxel complex is extraordinarily stable and does not disassemble. This causes the cell death by disrupting the normal tubule dynamics required for cell division (Sharma and Straubinger 1994; Hennenfent and Govindan 2006; Slavin, Chhabra et al. 2007). Paclitaxel is also known to induce programmed cell death (apoptosis) in cancer cells by binding to an apoptosis stopping protein called Bcl-2 (B-cell leukemia 2) and thus arresting its function (Henley, Isbill et al. 2007). Normal cells are also affected adversely, but cancer cells are far more susceptible to paclitaxel treatment.

Paclitaxel has anti-neoplastic activity particularly against primary epithelial ovarian carcinoma, breast cancer, colon, head, non-small cell lung cancer, and AIDS related Kaposi's sarcoma (Rowinsky and Donehower 1993; Rowinsky, Wright et al. 1993; Markman, Francis et al. 1994; Rowinsky, Wright et al. 1994). Paclitaxel is also used for the prevention of restenosis of coronary stents (Sun and Eikelboom 2007). Tseg et. al., reported the potential use of paclitaxel efficacy against malignant brain tumors (Tseng, Bobola et al. 1999).

The paclitaxel molecular weight is 853 Da. Paclitaxel is white to off-white crystalline powder. It is highly lipophilic, insoluble in water with a melting point of 216–217 °C. Paclitaxel has a biphasic plasma clearance. The generally accepted dose is 200–250 mg m^{-2} and is given as 3 and 24 Tf-LCL infusion. Terminal half-life was found to be in the range of 1.3–8.6 Tf-LCL (mean 5 Tf-LCL) (Rowinsky and Donehower 1993; Rowinsky, Wright et al. 1994). The drug undergoes an extensive P-450 mediated hepatic metabolism and less than 10% drug in the unchanged form is excreted in the urine. Most of the drug is eliminated in feces. More than 90% of the drug binds rapidly and extensively to plasma proteins (Rowinsky, Wright et al. 1993).

Paclitaxel is poorly soluble in an aqueous medium, but can be dissolved in organic solvents. Numbers of reports have been published on the solubility of paclitaxel and acceptable value of aqueous solubility is 0.6 mM (Tarr and Yalkowsky, 1987; Swindell and Krauss, 1991). Solubility of paclitaxel can't be affected by change in pH due to lack of functional groups that are ionisable in a pharmaceutically acceptable pH range (Tarr and Yalkowsky 1987).

Paclitaxel is currently formulated in a vehicle composed of 1:1 blend of cremophor EL and ethanol which is diluted with 5–20-fold in normal saline or dextrose solution (5%) for administration. This formulation is stable in unopened vials for 5 years at 4 °C. However, several hypersensitivity reactions were reported with cremophor formulation (Sparreboom, van Zuylen et al. 1999). Several approaches have been explored towards the development of aqueous based formulations for paclitaxel, including co-solvency, micellar solubilization, emulsification, cyclodextrins, nanoparticle and liposome formations, that do not require solubilisation by Cremophor. Among all

these drug carrier systems, liposomes represent a mature technology with a considerable potential for encapsulation of lipophilic molecules like paclitaxel and have been used to formulate a variety of hydrophobic, poorly soluble drugs (Straubinger, Sharma et al. 1993; Sharma and Straubinger 1994; Torchilin 2005). Sharma et. al., developed a liposome-based formulation composed of phosphatidylcholine and phosphatidylglycerol for paclitaxel. The in *vitro* growth-inhibitory activity of liposomal paclitaxel against a variety of tumor cell lines was found to be similar to that of the free drug (Sharma and Straubinger 1994).

Polilactofate microsphere (Paclimer) formulation of paclitaxel was evaluated for release of drug *in vivo* for malignant brain tumors therapy (Dang, Dordunoo et al. 1999; Pradilla, Wang et al. 2006). Koziara et al., reported paclitaxel nanoparticles for potential treatment of brain tumors. Paclitaxel nanoparticles showed a significant increase in the drug brain uptake and its toxicity toward p-glycoprotein expressing tumor cells (Koziara, Lockman et al. 2004).

Paclitaxel encapsulated in cationic liposomes (LipPac) was evaluated for vascular targeting. Remarkable retardation of tumor growth was observed with paclitaxel encapsulated cationic liposomes when compared to control formulations, in a subcutaneous tumor model (Schmitt-Sody, Strieth et al. 2003). A novel lyophilized liposome-based paclitaxel (LEP-ETU) formulation was reported by Zhang et. al. This formulation is reported to be physically and chemically stable for at least 12 months at 2–8 and 25 8 ºC (Zhang, Anyarambhatla et al. 2005). Paclitaxel loaded tumor-specific 2C5 immunomicelles were evaluated by Torchillin et al. These targeted immunomicelles resulted in an increased accumulation of paclitaxel in the Lewis lung carcinoma tumor

compared with free paclitaxel or paclitaxel in nontargeted micelles and showed enhanced tumor growth inhibition (Torchilin, Lukyanov et al. 2003; Torchilin 2004). A folate receptor targeted liposomal formulation of paclitaxel was reported by Wu et. al. The folate targeted liposomes were made to selective targeting of the folate receptors, which are frequently over expressed on epithelial cancer cells. A 3.8-fold greater cytotoxicity was observed with folate receptor targeted liposomes containing paclitaxel, compared to non-targeted control liposomes in KB cells (Wu, Liu et al. 2006).

Chapter 2: Statement of Problem

2.1 Limitations of Conventional Brain Tumor Chemotherapy

Each year more than 200,000 people in the United States are diagnosed with primary or metastatic brain tumors. Brain tumors are the leading cause of solid tumor cancer death in children under the age of 20. Adults with newly diagnosed brain tumors like astrocytomas have a median survival of less than one year (Curran Jr., Scott et al. 1993). Despite dramatic improvements in neuroimaging and neurological techniques, the prognosis in patients with brain tumors has not improved significantly during the past 40 years (Grossman, Fisher et al. 1998; Jemal, Thomas et al. 2002; Ewend, Elbabaa et al. 2005; Newton 2006). The main stay of treatment in patients with high grade brain tumors is resection followed by radiation. Chemotherapy has been used occasionally, but has proven to be of limited impact on the survival of these patients (Richards, Khuntia et al. 2007).

Almost all malignant gliomas are incurable with the present standards of healthcare. Currently accepted therapeutic adjuvants to surgery, such as radiotherapy and chemotherapy, provide only a minor improvement in the disease course and life expectancy for patients diagnosed with malignant gliomas. Often, chemotherapy has failed to make any significant impact on the prognosis of disease because of significant local and systemic toxicity, problems with transport of the drug across the blood brain barrier (BBB), and a high degree of chemoresistance demonstrated by tumor cells (Green, Byar et al. 1983; Grant, Liang et al. 1995; DeAngelis, Burger et al. 1998; Surawicz,

Davis et al. 1998; Fine, Wen et al. 2003). Effectiveness of chemotherapy in brain tumors depends on adequate delivery of the drugs to cancer cells. Now a variety of very potent anticancer drugs are available. However, there are many issues in delivering them effectively to kill these tumors. Before a blood borne chemotherapeutic agent can begin to attack malignant cells of a brain tumor, it must accomplish three critical tasks. First, it must stay in the systemic circulation, find and reach the target tumor site. Then, it must extravasate into the tumor interstitium. And finally, it should migrate through the tumor matrix to distribute throughout the tumor and kill all of the malignant cells.

Unfortunately, brain tumors develop in such a way to hinder most of these steps (Jain 1990; Jain 1994; Jain 1998). As a result, brain tumors remain incurable despite the development of several potent anticancer drugs. This is mainly due to inaccessibility of brain tumor cells and to the poor penetration of drugs through blood brain barrier. An elevated interstitial pressure further limits drug diffusion into tumor cells. These barriers virtually restrict our ability to kill the brain tumor cells per se with the available anticancer drugs and with conventional delivery methods; therefore, there is a desperate need for targeted delivery systems.

2.2 Basis for the Transferrin Receptor Mediated Tumor Targeting

Transferrin receptor (TfR) currently shows promise as a site for receptor-mediated targeting of glioma. The density of TfR is correlated with the extent of cell growth and division. Neoplastic cells ordinarily divide faster than normal cells and consequently express more TfR than their surroundings. This discrepancy is even more appreciable in

the stable environment of the brain. The extent and diffuseness of TfR expression in glioma has been shown to be significantly greater than in normal brain tissue, with expression linked to the severity of tumor. The relative over expression of these transferrin receptors offers the potential for favorable targeting of brain tumors over its surrounding normal tissue. Transferrin has also be widely applied as a targeting ligand in the active targeting of anticancer agents, proteins, and genes to primary proliferating malignant cells that overexpress transferrin receptors.

2.3 Primary Objective

The primary objective of the study was to develop and evaluate liposomal targeted delivery systems of conventional or novel anti-cancer agents for malignant glioma therapy.

In this project, a liposomal targeted delivery system for the paclitaxel was developed to selectively transport this drug to the brain tumor vasculature for malignant glioma therapy.

The overall hypothesis of this project was that by attaching brain targeting and/or tumor specific ligands on the surface of liposomes, therapeutic concentrations of anti-cancer agents can be delivered to gliomas with minimal peripheral side effects via over expressed receptors.

2.4 Specific Aims

The specific aims of this study were to:

1. Design a brain tumor targeted liposomal delivery system for paclitaxel.
2. Develop a process for the preparation of the targeted liposomal delivery system.
3. Characterize the prepared delivery system.
4. Evaluate functional properties of the targeted delivery system *in vivo.*
5. Use whole body optical imaging for characterization of tumor growth and liposomal tumor localization.
6. Evaluate antitumor efficacy of paclitaxel liposomal delivery systems in flank and intracranial glioma tumors.
7. Develop a lyophilized formulation for the targeted liposome delivery system to enhance its storage stability.

Chapter 3: Preparation and *In Vivo* Evaluation of Fluorescent Labeled Targeted Liposome Delivery Systems

3.1 Introduction

Liposomes are versatile carriers for targeted drug delivery by the intravenous route. Various types of liposomal formulations have been extensively used as carriers for increasing the therapeutic index of cytotoxic drugs (Lasic, Martin et al. 1991; Lasic 1994; Allen 1997; Lasic 1997; Torchilin 2004; Torchilin 2005; Torchilin 2005). The major concern associated with the use of liposomes for targeting tumor cells in extravascular sites is the rapid clearance from the systemic circulation. These liposomal carriers are subjected to rapid clearance by circulating phagocytes and by macrophages of liver and spleen (Harasym, Bally et al. 1998; Torchilin 2005). Short circulation life time decreases passive accumulation of targeted liposomes in the tumor tissue. Long circulation lifetimes are required in order to maintain target site accumulation of liposomal drugs, an essential requirement for target cell access and increased circulation half-life can result in increased accumulation within a target site.

One of the strategies to circumvent this problem is to design long circulating liposomes with steric stabilization (Lasic 1994; Lasic 1997). Surface modification of liposomes with hydrophilic polymers such as polyethylene glycol (PEG) resulted in decreased recognition and subsequent phagocytosis by cells of the mononuclear phagocytic system (MPS). The concentration of PEG lipid in the liposomes and size of liposomes are two critical parameters which can be optimized for increasing the

circulation times of liposomes for achieving anticipated increase in localization within the target tumor site (Lasic, Martin et al. 1991; Papahadjopoulos, Allen et al. 1991; Lasic 1994; Lasic 1997; Moghimi and Szebeni 2003; Torchilin 2005). An understanding of the liposome targeting to tumor, its blood circulation, and distribution to various organs can be achieved by labeling with fluorescent dyes (Torchilin 2005; Kalchenko, Shivtiel et al. 2006).

In this study, we report the preparation and characterization of fluorescent labeled conventional, sterically stabilized and targeted liposomes. The blood circulation half-life in rats for fluorescent labeled formulations was determined. The sterically stabilized liposomes prepared using 5% PEG and about 100 nm in size showed a pronounced increase in the blood residence time (17 Tf-LCL) with a significant decrease in uptake by RES when compared with conventional liposomes. We also report the localization of the fluorescent liposomes in a flank C6 glioma xenograft bearing nude mice using non-invasive near infrared fluorescence imaging. We also provide evidence of selective tumor localization of targeted liposomal formulations in comparison to non targeted liposomes and solution formulation as controls.

3.2 Materials and Methods

3.2.1 Materials

Hydrogenated soybean phosphatidylcholine (HSPC), 1,2-distearoyl -glycero-3-phosphoethanolamine-N-[PEG(2000)] conjugate (DSPE-PEG), and DSPE-PEG-

maleimide were from Northern Lipids Inc., Vancouver, Canada. Cholesterol, and biotinylated Transferrin were obtained from Sigma, St. Louis, MO. DIR and DII were purchased from Invitrogen, Carlsbad, CA. These chemicals were used as received. All other chemicals and solvents were of analytical grade.

3.2.2 Liposome preparation

Liposomes were produced by lipid hydration method followed by extrusion method using hydrogenated soy phosphatidylcholine (HSPC), cholesterol (95: 5 molar ratios). The DII or DIR dyes were encapsulated in the lipid bilayers due to its lipophilic nature. For preparation of long circulating liposomes (LCL), poly ethylene glycol-2000 grafted distearoyl phosphatidyl ethanolamine (DSPE–PEG2000) was incorporated. For preparation of transferrin conjugated liposomes (Tf-LCL), a portion of DSPE-PEG2000 (0.01 mol%) was replaced with DSPE-PEG2000-biotin. Transferrin (Tf) was non-covalently conjugated at the distal end of DSPE-PEG2000-biotin via a streptavidin-biotin bond. The dye loading was quantified via spectrofluorometry. A centrifugal ultrafiltration device (Centricon 100, MWCO 100 KD, Millipore, Bedford, MA) was used to separate the free dye from the dye encapsulated in the liposomes. Free and total dye concentration in the liposomes was determined using a FLx800 fluorometric plate reader (BioTek Instruments, Inc, Winooski, VT) after 70% isopropanol extraction. The percent dye encapsulated in the liposomes was calculated from the free and total dye in the liposomes.

3.2.3 Liposome size, morphology and zeta potential

The size analysis of liposomes was performed by the dynamic light scattering technique using a Malvern zeta-sizer nano particle size analyzer (Malvern Instruments, Malvern, UK). A 25 µL of this sample was diluted to 1 mL with water for injection for particle size determination. The diluted aqueous sample (1 mL) was added to a 2 mL cuvette and the particle size analysis was performed in triplicate. The average particle size was calculated form the results. The transmission electron microscopic (TEM) studies were carried out using 3 mm Forman coated copper grid (400 mesh) at 60 KV using negative staining by 2% uranyl acetate at 200,000 X magnifications on a JEOL 1200EX TEM.

3.2.4 Quantification of transferrin conjugation

A sensitive gel filtration chromatographic method was developed and validated to quantitate transferrin. The gel filtration chromatographic system consisted of a Waters 600 controller, Waters 717 plus auto sampler and a Waters 2996 photodiode array detector. Data were acquired and processed with Waters Millennium 32 software (version 4.0). Gel filtration chromatographic separation was achieved on a TSK Gel G3000 SWXL (30 cm X 7.8 mm, 5 micron) column from Tosoh bioscience (South San Francisco, CA). The isocratic mobile phase consisting of 0.5 N phosphate buffered saline (pH 7.2) was pumped at a flow rate of 0.5 mL/min with an injection volume of 30 µL. Transferrin (retention time, 4.8 min) was monitored at 220 nm with a photodiode array detector. All analyses were performed in triplicate, and the mean peak area was used to determine the concentration of transferrin in the samples. Free Tf was separated from the

liposome encapsulated part using a Centricon centrifugal filter device (Centricon 100, MWCO 100 KD, Millipore, Bedford, MA). An aliquot of the liposome dispersion (100 μL) was diluted to 1 mL with hydration buffer (phosphate buffered saline pH 7.2), and this sample was transferred to the centrifugal filter device. The sample was centrifuged at 5000 rpm for 30 minutes in a fixed-angle centrifuge. Free transferrin in the filtrate was then determined using high performance gel filtration chromatography (HPGFC). Subtraction of free transferrin from the total amount added gave the amount of liposome-conjugated Tf. Tf estimations were done in triplicate, and the values were reported as mean ± SD.

3.2.5 Determination of blood circulation time of formulations

Fluorescent liposome formulations or fluorochrome in solution formulations were administered systemically to Sprague Dawley rats via tail vein. At predetermined time points, blood samples were withdrawn. The serum was separated and treated with ice cold 70% isopropyl alcohol followed by centrifugation at 12,000 x g for 5 min for extraction of dye. Fluorescence intensity in the clear supernatant was determined using a FLX800 fluorometric plate reader (BioTek Instruments, Inc, Winooski, VT) (Excitation 555 / Emmission: 575 nm).

3.2.6 Cranial window preparation for intravital fluorescence imaging (IVM) of blood circulation time of liposomes in rats

Cranial window preparation was made according to published method (Gaber, Yuan et al. 2004). Briefly, a glass cranial window (0.8 × 0.8 mm), extending from the

bregma to lambda sutures and centered on the sagittal suture, was placed and fixed over the surgically exposed cerebral cortex. Before surgery, the animals were anesthetized with an i.m. injection (1 mL/Kg) of ketamine/xylazine solution (87 mg ketamine/mL + 13 mg Xylazine/mL). Animals were placed in a stereotaxic frame (Kopf Instruments, Tujunga, CA), and their body temperature was maintained at approximately 37°C using a heating pad. One dose of the chloromycetin (50 mg/kg body weight) was given before surgery. The scalp and underlying soft tissue over the parietal cortex were removed. A rectangular cranial window was made using a low-speed dental drill (0-8000 rpm, Densply Midwest) along with artificial cerebral-spinal fluid irrigation. The dura mater was cleared using iris microscissors. A glass plate was fixed to the bone using cyanoacrylate glue. After one week of recovery from the surgery, animals were ready for data collection. Fluorescent liposome formulation containing 40 µg of DII was administered systemically to rats via tail vein and subjected to fluorescence excitation. The emitted light through the cranial window was detected by a CoolSNAP® monochrome camera attached to a fluorescence intravital microscope at 0, 1, 4, 24 and 48 Tf-LCL time points. Images acquired were processed with Metamorph® software (version 6.2). The fluorescence produced from the liposomes was observed through this glass window using an intravital microscope (model MM-11, Nikon, Melville, NY, USA) with a DII filter (Excitation 555 / Emmission: 575 nm).

3.2.7 C6 GFP flank glioma tumor model and NIRF imaging of liposomal tumor localization

C6-GFP cells in exponential growth were harvested with 0.25% trypsin with EDTA for 5 min at 37°C. The cells were centrifuged for 5 min at 1,000 RPM. The pellets were resuspended in sterile phosphate buffered saline (PBS), at a concentration of 100,000,000/mL and placed on ice. Adult female CD1 nu/nu mice (25-30g) were used for all studies and handled in accordance with protocols approved by the Animal Care and Use Committee at the University of Tennessee Health Science Center. Mice were anesthetized with intraperitoneal injection of ketamine/xylazine at a dosage of 8.7/1.3 mg/100 g body weight. To create flank glioma tumors, 4,000,000 C6-GFP glioma cells in 200 µL of phosphate buffered saline were injected subcutaneously into the flank using a 27 ½ G needle. Tumor growth was measured on every 3rd day with a vernier caliper, and tumor volume was measured using the formula W^2 X L / 0.52. W refers to width and L is the length of the tumor. Near infrared whole body optical images of mice were taken with a CCD camera (Princeton Instruments Inc., Trenton, NJ) using GFP filter (excitation: 475 nm and emission: 510 nm). Acquired images were processed for measuring the pixel intensity of the GFP fluorescence from the tumors using the Metamorph® software (version 6.2) for determining the C6 GFP tumor area.

After 18 days of tumor cell inoculation, animals were injected retroorbitally with DIR labeled (5 µg of DIR in 50 uL) formulations. (n = 3 per group). The area and pixel intensity of the dye in the tumor was compared with the background intensity in the surrounding normal tissue using non-invasive optical imaging with a CCD camera (Princeton Instruments Inc. Trenton, NJ) with a DIR filter (excitation: 750 nm and

emission: 782 nm) (Omega optical, Brattleboro, VT) at 0, 1, 4, 6, 8, 24 and 48 Tf-LCL after injection. Acquired images were processed for measuring the pixel intensity of the DIR fluorescence from the tumors using the Metamorph® software (version 6.2) for determining the C6 GFP tumor area. Tumor to muscle accumulation ratio of DIR dye labeled formulations was determined to calculate the tumor targeting index. After 48 Tf-LCL of injection, animals were anesthetized and subjected to transcardiac perfusion, first with 20 ml of normal saline, and then with the same amount of 4% paraformaldehyde to fix the tissues. Optical images of isolated organs (tumor, brain, liver, and spleen) were taken with a CCD camera using white light, GFP (excitation: 475 nm and emission: 510 nm) and DIR (excitation: 750 nm and emission: 782 nm) filters for visualization of tumor area and DIR dye localization in tissue. Acquired images were then processed for measuring the pixel intensity of the GFP and DIR fluorescence from the tumors using the Metamorph® software (version 6.2) for determining the C6 GFP tumor area and DIR localization respectively.

3.3 Results and Discussion

3.3.1 Preparation and characterization of fluorescent labeled liposomes

Fluorescent labeled liposomal formulations were prepared by Bangham method followed by polycarbonate membrane extrusion. To attach the transferrin ligand to the liposomes, the streptavidin-biotin conjugation method was used (Loughrey, Bally et al. 1987). Dye incorporation efficiency was determined by subtracting the free dye fraction

from the total dye and was found to be 95.0 ± 3%. The non conjugated liposome formulation showed average vesicle sizes of 81 ± 7 nm with a unimodal distribution. The covalent coupling of Tf to the liposome surface led to a slight increase in diameter to about 115 ± 11 nm. This slight increase in size was most probably due to the attachment of Tf to the liposome surface, which somewhat increased the hydrodynamic diameter of liposomes. The TEM images (Figures 3-1, 3-2) revealed that the long circulating liposomes are round and spherical in shape. The zeta potential of Tf conjugated and non conjugated long circulating liposomes was -18.0 ± 1.2 mV. The Tf conjugation of LCL resulted in slight increase in the zeta potential of liposomes to -25.5 ± 1.5 mV. The transferrin conjugation was studied using TEM. The surface of non conjugated liposomes was relatively smooth (Figure 3-2). However, the surface of Tf conjugated liposomes was more granular (Figure 3-1). The total amount of the liposome attached transferrin in the formulations was determined by using the high performance gel filtration chromatography (HPGFC). Based on free Tf concentration from a typical formulation, about 72% of Tf was coupled to the liposomes. It was found by this method that about 4 µg of the Tf was bound to 1µM of the total lipid; this corresponds to approximately 5 Tf molecules per 100 nm liposome.

3.3.2 Determination of blood circulation time

The blood circulation time of fluorescent labeled formulations was determined using blood sampling method. In this experiment, fluorescent labeled formulations were injected into Sprague Dawley rats via tail vein injection. The fluorescence in clear serum

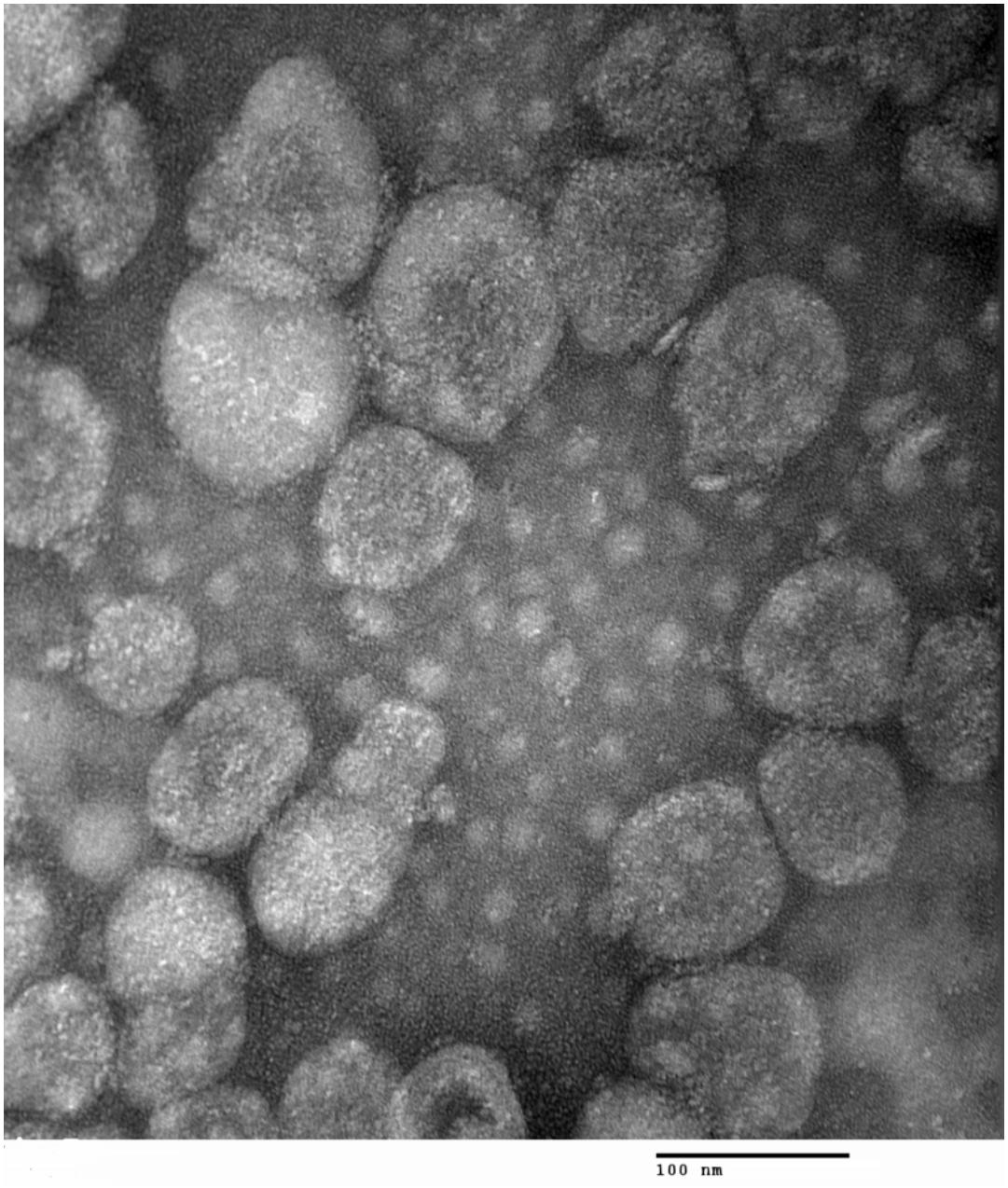

Figure 3-1. Transmission electron micrograph of the transferrin conjugated long circulating liposomes. (Magnification ×250,000).

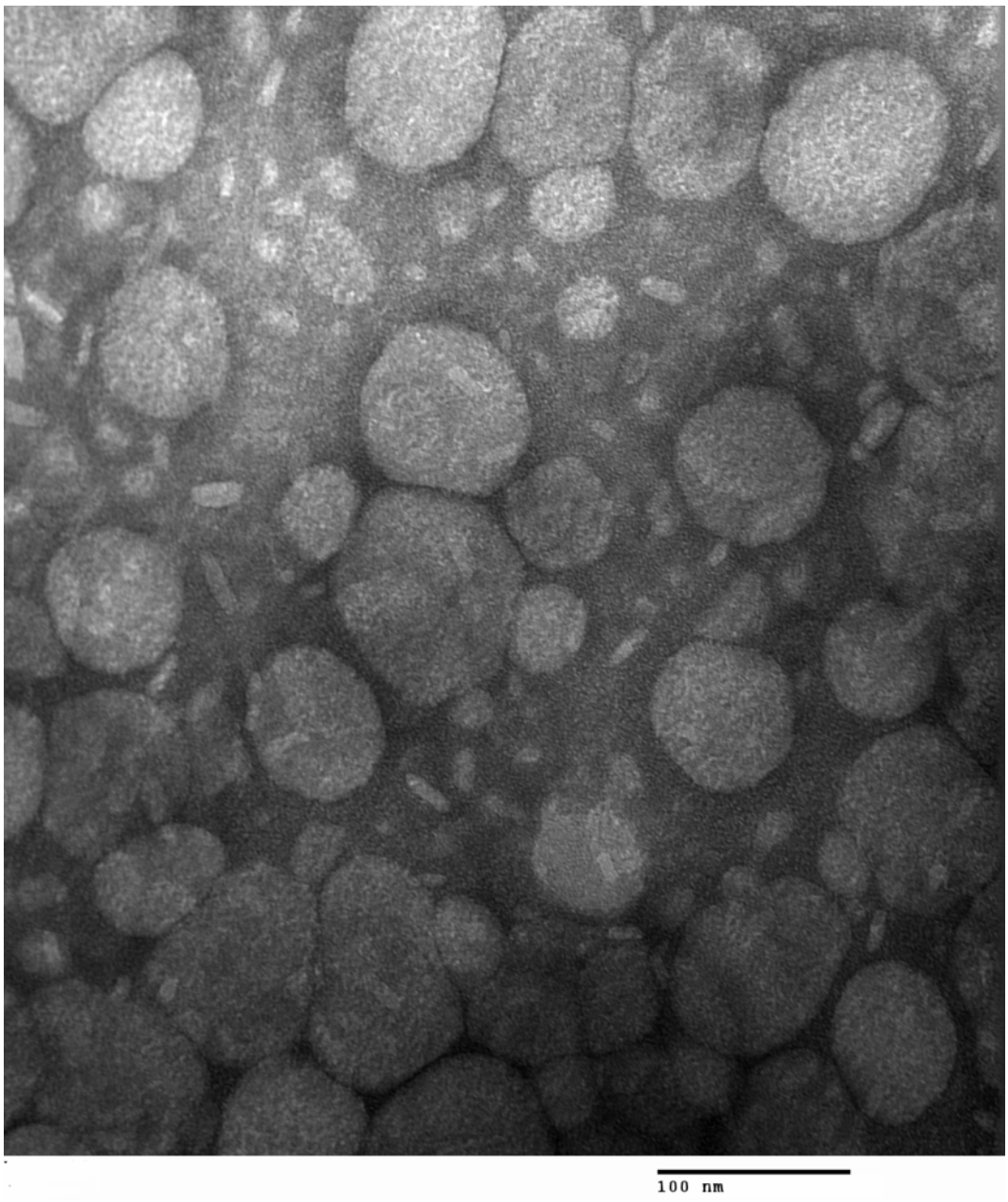

Figure 3-2. Transmission electron micrograph of the non conjugated long circulating liposomes. (Magnification ×250,000).

samples were measured with a spectrofluorimetric plate reader. As shown in the Figure 3-3, blood circulation half life of long circulating liposomes (with 1% DSPE-PEG2000) in the brain microvasculature was about 12 Tf-LCL, whereas the DII solution formulation (DII in water containg 3% cremophor EL) was cleared within 1 Tf-LCL after administration. An increase in DSPE-PEG2000 concentration in the liposomes prolonged the *in vivo* circulation, and maximum *in vivo* circulation half-life of about 17 Tf-LCL was achieved with a formulation containing 5% of DSPE-PEG2000 in total lipids (Figure 3-4). Liposomes larger than 300 nm showed a significant reduction in blood circulation time when compared to 100 nm liposomes (Figure 3-5). The conjugation of Tf on the distal end of PEG chains led to a reduction in blood circulation half-life (~ 9 Tf-LCL) as compared to LCL (~17 Tf-LCL) (Figure 3-6). Blood circulation time of transferrin conjugated liposomes was also determined by real-time monitoring of circulating fluorescent labeled liposomes in rat brain pial vessels using intravital microscopy. Blood circulation half-life of transferrin conjugated liposomes with novel intravital microscopic technique was comparable with blood sampling method. Intravital microscopic imaging of transferrin conjugated liposomes also revealed their probable interaction with the brain microvasculature after 24 Tf-LCL time point (Figure 3-7). However, these liposomes appeared to clear from the vasculature into the surrounding brain tissue by the 48 Tf-LCL time point.

3.3.3 NIRF imaging of liposomal tumor localization

We adopted an optical whole-body imaging technique for monitoring tumor localization of liposomes in mice. DIR has absorption and fluorescence maxima at 750 and

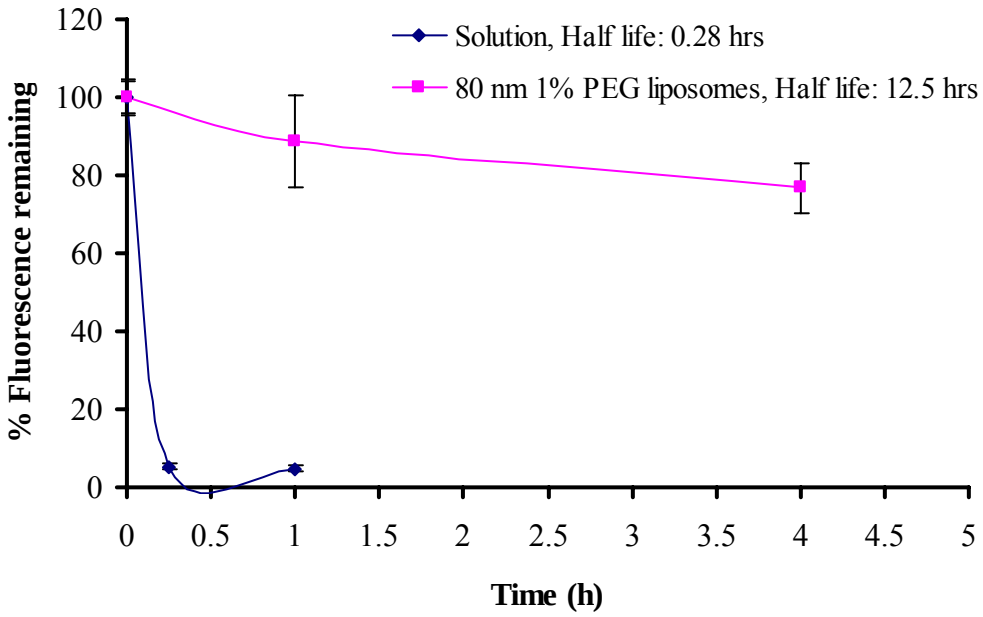

Figure 3-3. Blood clearance of solution and 1% PEG liposomes. The Sprague Dawley rats received fluorescent labeled formulations via intravenous injection and the serum fluorescence concentrations were measured at different time intervals. Each value is the mean of 3 independent experiments.

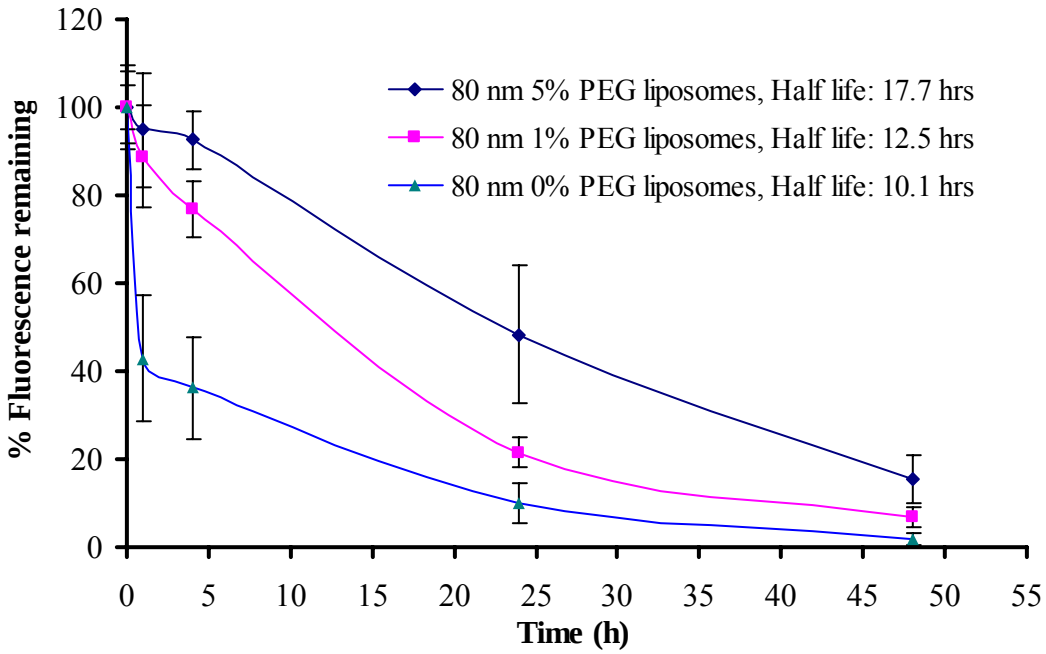

Figure 3-4. Blood clearance of liposomes made with different concentrations of PEG lipid. The Sprague Dawley rats received fluorescent labeled formulations via intravenous injection. Serum fluorescence concentrations were measured at different time intervals. Each value is the mean of 3 independent experiments.

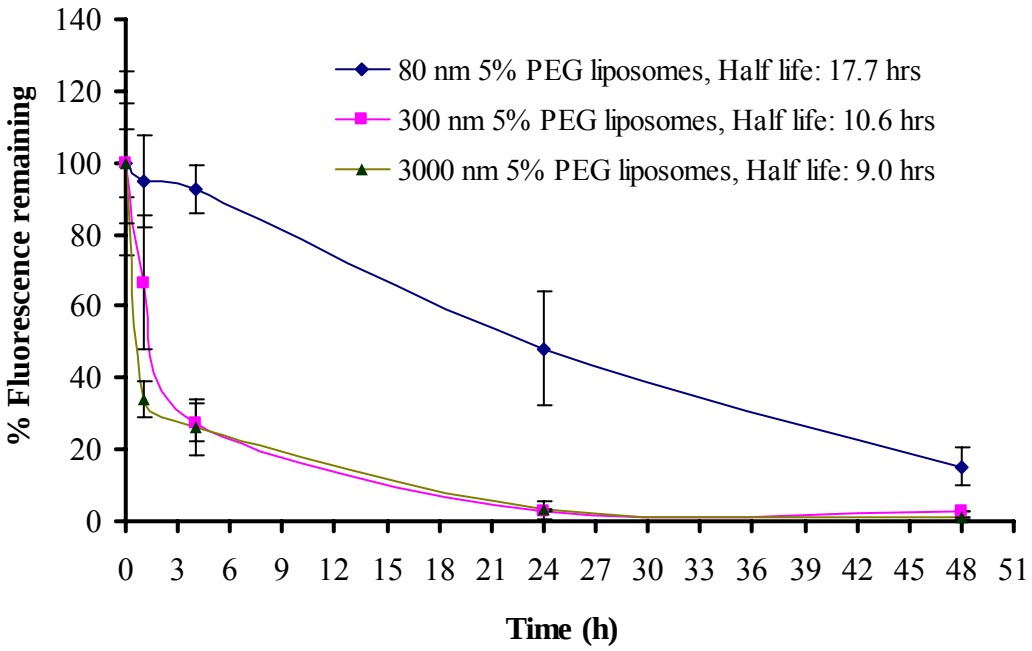

Figure 3-5. Blood clearance of different size liposomes in Sprague Dawley rats. The rats were administered intravenously fluorescent labeled formulations and the serum fluorescence concentrations were measured at different time intervals. Each value is the mean of 3 independent experiments.

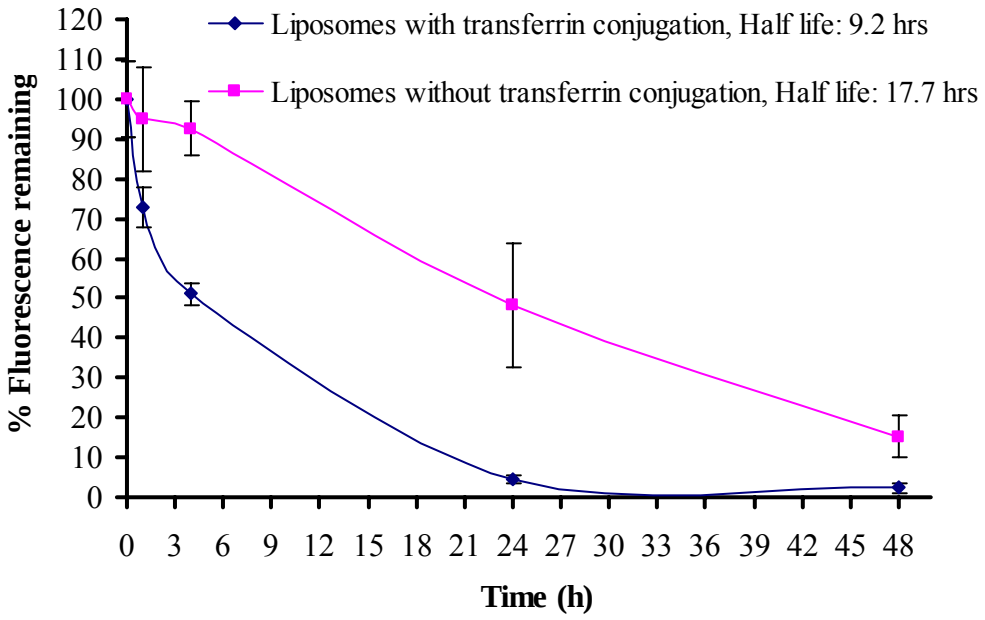

Figure 3-6. Blood clearance of non targeted and targeted liposomes. The Sprague Dawley rats received fluorescent labeled formulations via intravenous injection. Serum fluorescence concentrations were measured at different time intervals. Each value is the mean of 3 independent experiments.

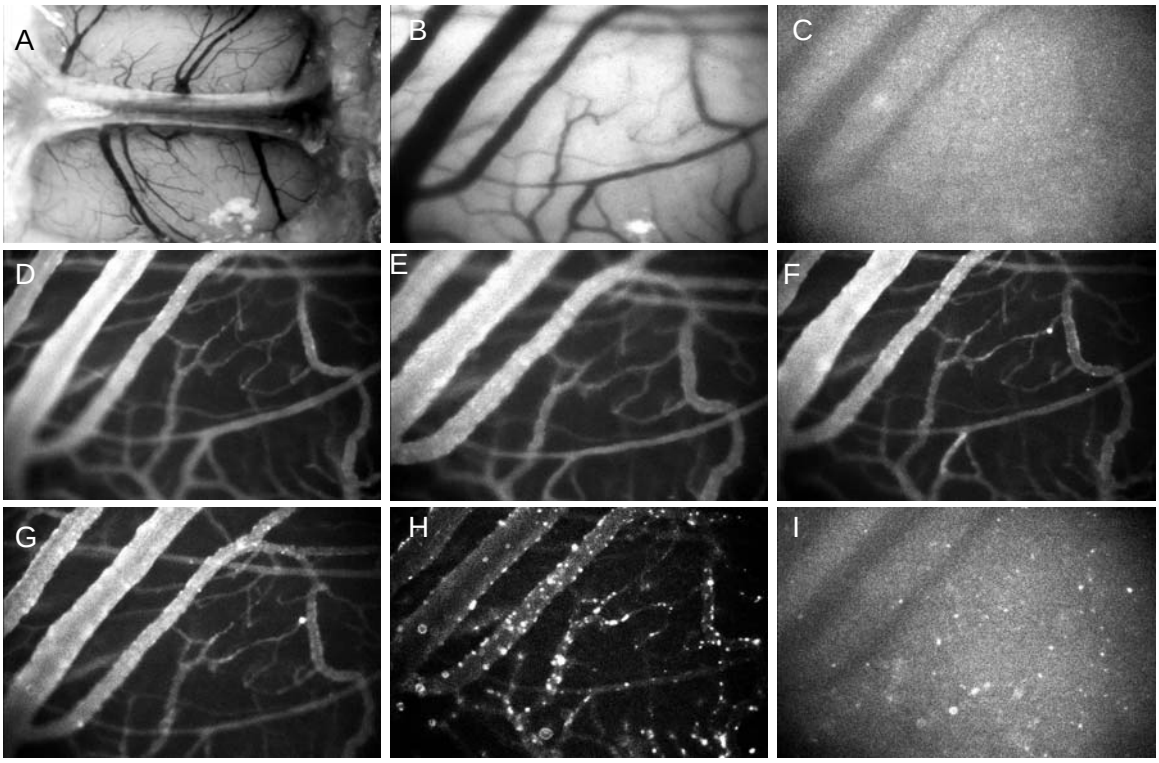

Figure 3-7. Intravital fluorescence images of brain microvasculature. Images represent A. background image with white light (1.3 X), B. background image with white light (10X), C. background image with DiI filter (555 nm Excitation – 575 nm Emission), D. 0 Tf-LCL after Tf-LCL injection, E. 1 Tf-LCL after Tf-LCL injection, F. 4 Tf-LCL after Tf-LCL injection, G. 6 Tf-LCL after Tf-LCL injection, H. 24 Tf-LCL after Tf-LCL injection, I. 48 Tf-LCL after Tf-LCL injection.

782 nm, respectively, which can prevent issues related to autofluorescence in living tissues. This facilitates to get a significant signal with very low background noise level. A charge-coupled device (CCD) based camera is used for noninvasive whole-body imaging of DIR-labeled liposome localization in live animals with tumors. This technique can potentially visualize many types of delivery systems or cells labeled with a near infrared (NIR) fluorescent tag. Tumor accumulation and the tumor-to-muscle accumulation ratio of liposomal formulation were evaluated using a non-invasive NIRF optical imaging method. The data showing that the LCL and Tf-LCL accumulate in C6 glioma flank tumors at higher concentrations when compared to solution formulation is presented in Figure 3-8. Tf-LCL accumulates in C6 glioma tumors more efficiently when compared to muscle tissue (Figure 3-9). The results obtained showed that the long circulating liposomal formulations stay in the tumor for a longer time (~ 48 Tf-LCL post injection). The tumor targeting index (Figure 3-10) was found to be 10.59 ± 1.08. Effect of liposome size on tumor targeting potential was determined in a similar C6 glioma tumor model. The results show that about 100 nm liposomes can localize in the tumors with high selectivity. On the other hand, liposomes larger than 300 nm showed very limited to no localization of liposomes in the tumor as shown in the Figure 3-11. However, higher accumulation was observed in the liver and spleen (Figure 3-11). This might be due to rapid clearance of larger liposomes by these organs. C6 GFP flank tumor sections from the tumor targeting study revealed the presence of DIR fluorescence with 100 nm long circulating liposomes and transferrin conjugated long circulating liposomes (Figure 3-12). The sterically stabilized liposomes prepared using 5% PEG (about 100 nm size) showed a pronounced increase in the blood residence time (17 Tf-LCL)

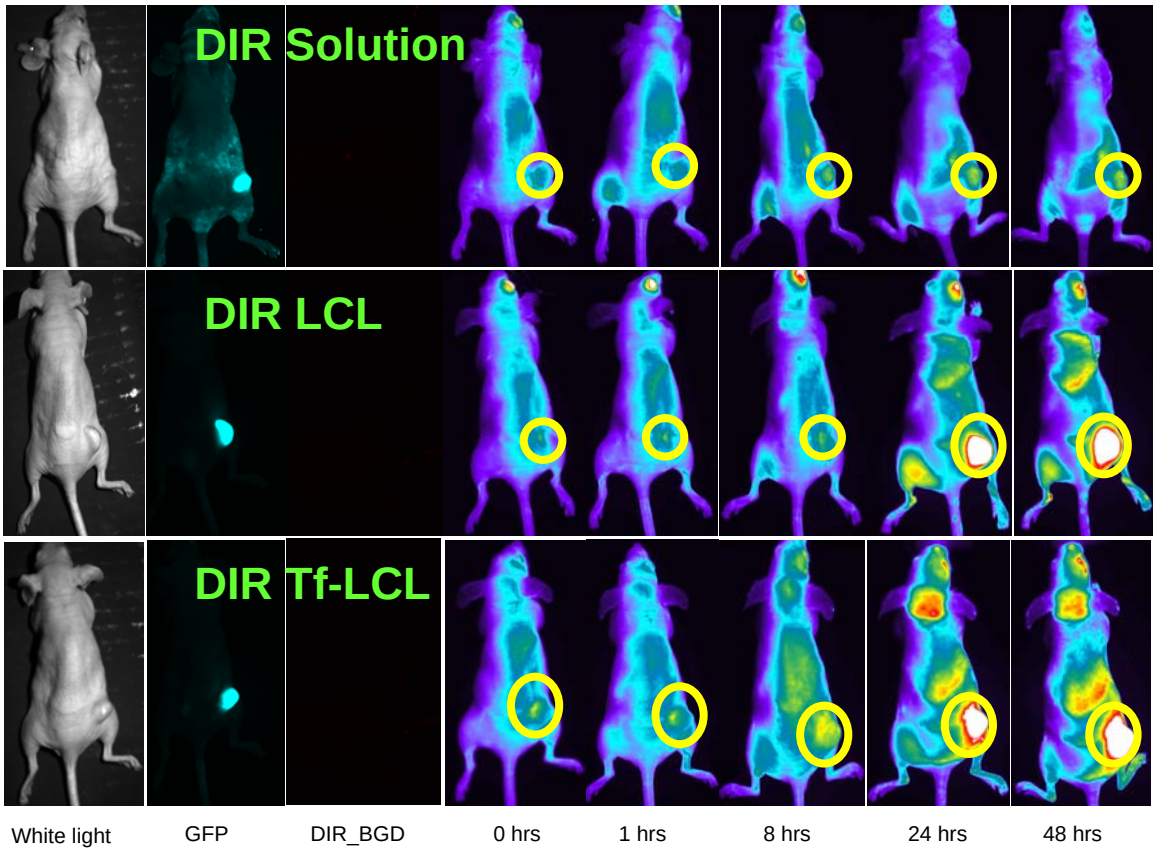

Figure 3-8. Whole body near infrared imaging of mice showing tumor localization of solution, long circulating liposomes and transferrin receptor targeted liposomes. Column 1, white light image showing location of tumor, column 2, images with GFP filter showing the C6 GFP tumor area, column 3, background images with DIR filter before injection, column 4 to 8, images were taken after injection of DIR labeled formulations at different time points.

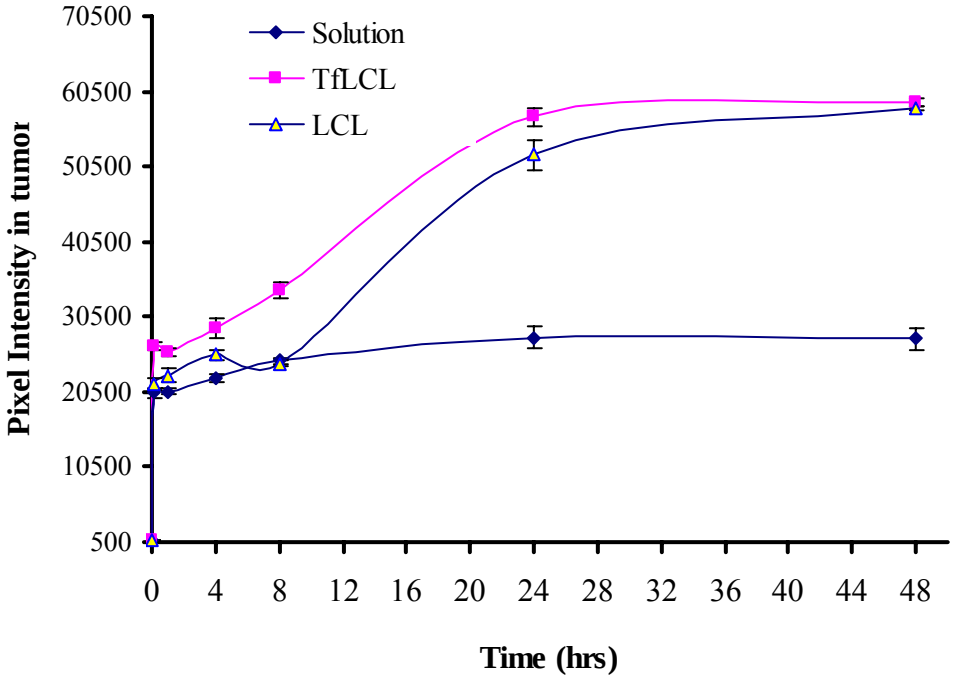

Figure 3-9. Localization of DIR labeled formulations in glioma tumors. The pixel intensity of DIR fluorescence signal of formulations in glioma tumor tissue was quantified. Transferrin conjugated liposomes showed faster and higher targeting ability to tumor tissue when compared to long circulating liposomes and solution formulations

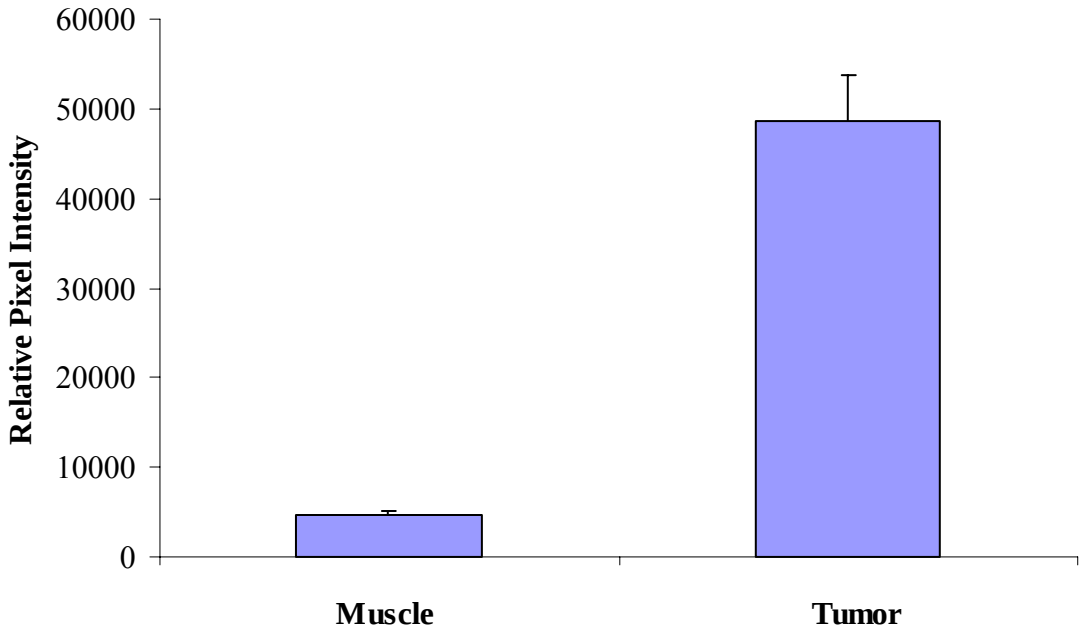

Figure 3-10. The selective accumulation of Tf-LCL in C6 GFP glioma tumors in mice. High fluorescence signals in tumor tissue were observed up to 48 Tf-LCL. The fluorescence ration between tumor and normal muscle tissue yielded up to 10 fold selectivity for the tumor in comparison with surrounding normal tissue; n = 3; Mean ± SD. (Tumor targeting index: 10.59 ± 1.08)

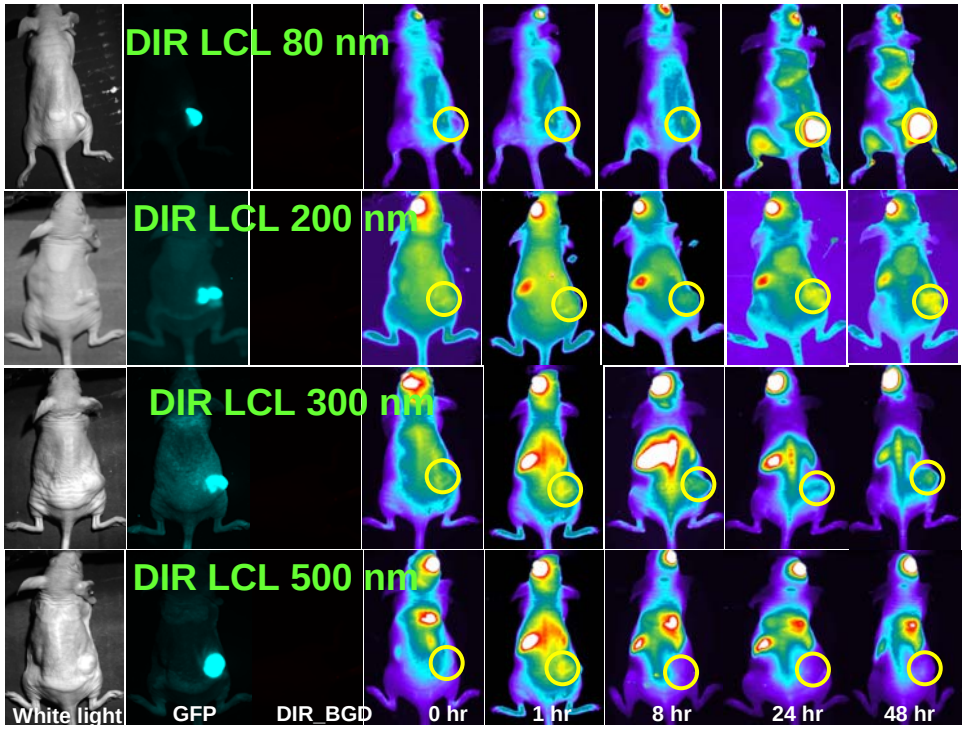

Figure 3-11. Whole body near infrared imaging of mice. Tumor localization of different size long circulating liposomes was shown. Column 1, white light image showing location of tumor, column 2, images with GFP filter showing the C6 GFP tumor area, column 3, background images with DIR filter before injection, column 4 to 8, images were taken after injection of DIR labeled formulations at different time points.

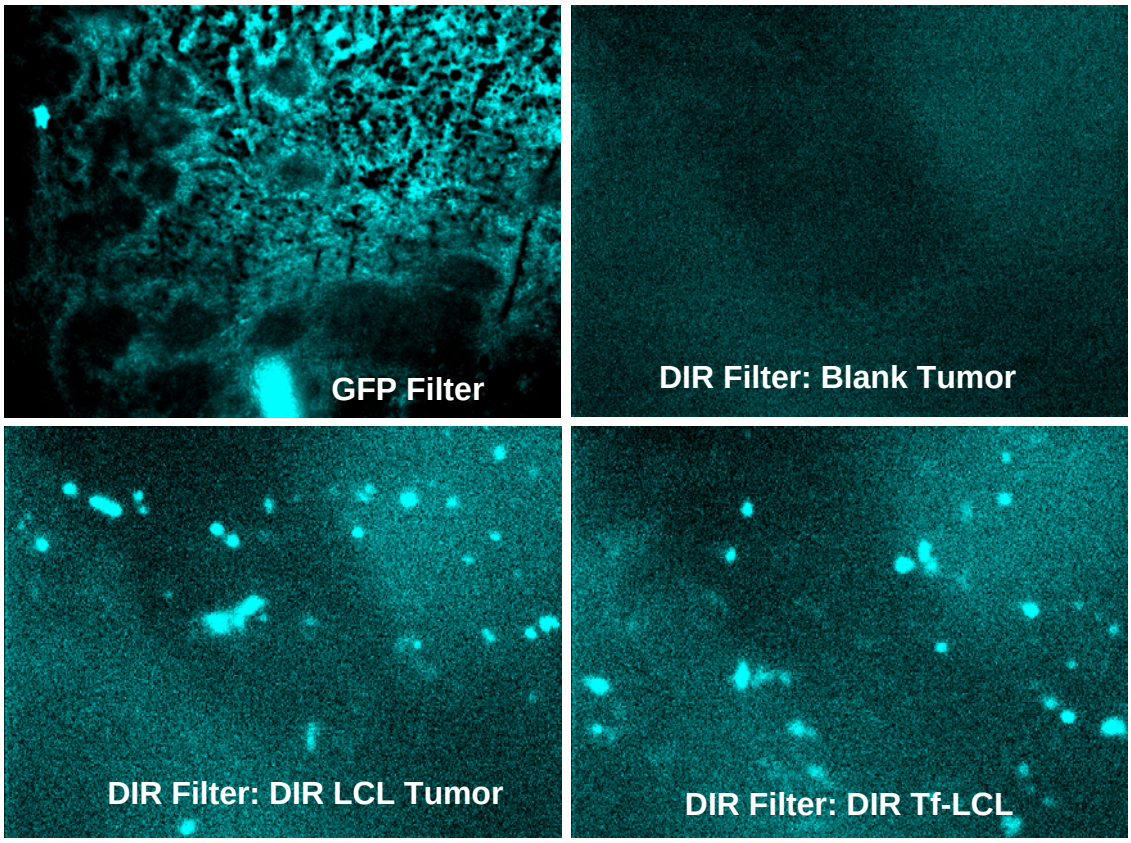

Figure 3-12. C6 GFP flank tumor sections from tumor targeting study. Tumors are showing the presence of DIR fluorescence with 100 nm long circulating liposomes and transferrin conjugated long circulating liposomes.

with a significant decrease in uptake by the RES when compared with conventional liposomes. Selective tumor localization of transferrin targeted liposomal formulations was also achieved when compared to non targeted liposomes and solution formulation as controls.

3.4 Conclusion

These findings indicate that preferential targeting to glioma tumors can be achieved with about 100 nm long circulating liposomes with transferrin conjugation. Transferrin conjugated liposomal delivery system can be a potential drug carrier for glioma tumors targeting.

Chapter 4: Efficacy of Paclitaxel Liposomal Targeted Formulations against Glioma Tumor Xenografts

4.1 Introduction

Paclitaxel is a diterpenoid pseudoalkaloid isolated from *Taxus brevifolia*, discovered at Research Triangle Institute (RTI) in 1967. Paclitaxel is approved by the FDA for the treatment of ovarian and breast cancers. Paclitaxel is the first of a new class of microtubule stabilizing agents and is considered as the most significant advance in chemotherapy for the past 15–20 years. The drug causes cell death by disrupting the normal tubule dynamics required for cell division (Sharma and Straubinger 1994; Hennenfent and Govindan 2006; Slavin, Chhabra et al. 2007). Paclitaxel is also known to induce programmed cell death (apoptosis) in cancer cells by binding to an apoptosis stopping protein called Bcl-2 (B-cell leukemia 2) and arresting its function (Henley, Isbill et al. 2007). Normal cells are also affected adversely, but cancer cells are far more susceptible to paclitaxel treatment.

Paclitaxel has anti-neoplastic activity, particularly against primary epithelial ovarian carcinoma, breast cancer, colon, head, non-small cell lung cancer, and AIDS related Kaposi's sarcoma (Rowinsky and Donehower 1993; Rowinsky, Wright et al. 1993; Markman, Francis et al. 1994; Rowinsky, Wright et al. 1994). Paclitaxel is also used for the prevention of restenosis of coronary stents (Sun and Eikelboom 2007). Tseg et. al., reported the potential use of paclitaxel efficacy against malignant brain tumors (Tseng, Bobola et al. 1999).

Paclitaxel is poorly soluble in an aqueous medium, but can be dissolved in organic solvents. Several approaches have been explored towards the development of aqueous based formulations for paclitaxel, including co-solvency, micellar solubilization, emulsification, cyclodextrins, nanoparticle and liposome formations, that do not require solubilization by Cremophor. Among these drug carrier systems, liposomes represent a mature technology with considerable potential for encapsulation of lipophilic molecules like paclitaxel. Liposomes have been used to formulate a variety of hydrophobic, poorly soluble drugs (Straubinger, Sharma et al. 1993; Sharma and Straubinger 1994; Torchilin 2005). Paclitaxel delivery to various tumor cells have has been the subject of many studies (Ho, Barbarese et al. 1997; Crosasso, Ceruti et al. 2000; Schmitt-Sody, Strieth et al. 2003; Torchilin, Lukyanov et al. 2003; Koziara, Lockman et al. 2004; Strieth, Eichhorn et al. 2004; Zhang, Anyarambhatla et al. 2005).

Tumor targeted drug delivery is a promising approach for enhancing the efficacy and therapeutic index of anticancer agents (Qian 2002; Pardridge 2003). Transferrin is a glycoprotein that transports ferric ions in the body and the Tf receptor is internalized into the cells by endocytosis through the binding of Tf. Transferrin receptor (TfR) currently shows promise as a site for receptor-mediated targeting of glioma. The density of TfR is correlated with the extent of cell growth and division (Prior, Reifenberger et al. 1990; Qian 2002; Pardridge 2003). Cancer cells ordinarily divide faster than normal cells and consequently show over expression of TfR than their surrounding tissues. The extent of TfR expression in gliomas has been shown to be linked to the severity of the tumor. The relative over expression of these transferrin receptors offers the potential for favorable targeting of glioma brain tumors (Prior, Reifenberger et al. 1990; Kurpad, Zhao et al.

1995). Transferrin has also been applied as a targeting ligand in the active targeting of anticancer agents, proteins, and genes to primary proliferating malignant cells that overexpress transferrin receptors (Pardridge 1998; Pardridge 1999; Pardridge 1999; Liao, Li et al. 2001; Li and Qian 2002; Pardridge 2002; Pardridge 2002; Qian 2002; Pardridge 2003; Soni, Jain et al. 2005; Soni, Kohli et al. 2005; Soni, Kohli et al. 2007).

Therefore, the aim of this study was to determine the efficacy of transferrin receptor targeted paclitaxel liposomal formulation (Tf-LCL) against glioma brain tumor xenografts in a flank model. In comparison with Tf-LCL, antitumoral efficacy of paclitaxel encapsulated in long circulating liposomes and paclitaxel in cremophor solubilized formulation was quantified *in vivo*. The use of non invasive NIRF imaging for visualization and quatification of tumor growth in nude mice was also demonstrated.

4.2 Materials and Methods

4.2.1 Materials

Egg phosphotidylcholine (EPC), Hydrogenated soybean phosphatidylcholine (HSPC), 1,2-distearoyl –sn-glycero-3-phosphoethanolamine-N-[PEG(2000)] conjugate (DSPE-PEG), and DSPE-PEG-maleimide were from Northern Lipids Inc., Vancouver, Canada. Cholesterol, and biotinylated Transferrin were obtained from Sigma, St. Louis, MO. These chemicals were used as received. Paclitaxel was purchased from 21CEC Pharma, East Sussex, UK. All other chemicals and solvents used were of analytical grade.

4.2.2 Preparation and characterization of liposomes

Liposomes were produced by the lipid hydration method followed by extrusion. The liposomes contained egg phosphotidylcholine (EPC), hydrogenated soy phosphatidylcholine (HSPC), cholesterol (75: 15: 5 molar ratios). Paclitaxel was encapsulated into the lipid bilayers due to its lipophilic nature. For preparation of long circulating liposomes (LCL), poly ethylene glycol-2000-grafted distearoyl phosphatidyl ethanolamine (DSPE–PEG2000) was incorporated. For preparation of Tf-LCL a part of DSPE-PEG2000 (0.01 mol%) was replaced with DSPE-PEG2000-biotin and then transferrin (Tf) was non-covalently conjugated at the distal end of DSPE-PEG2000-biotin via streptavidin-biotin bond.

4.2.3 Quantification of paclitaxel

A sensitive reverse phase HPLC method was developed and validated to quantitate paclitaxel in liposome formulations. Chromatographic system consisted of a Waters 600 controller, Waters 717 plus auto sampler and a Waters 2996 photodiode array detector. Data were acquired and processed with Waters Millennium 32 software (version 4.0). Chromatographic separation was achieved on a NovaPak® C18 reverse phase column (3.9 X 150 mm) from Waters (Milford, MA). The isocratic mobile phase consisting of acetonitrile and water (55:45, v/v) was pumped at a flow rate of 0.7 mL/min with an injection volume of 20 μL. Paclitaxel (retention time, 3.8 min) was monitored at 230 nm with a photodiode array detector. Prior to HPLC analysis, the formulation samples were treated with methanol for paclitaxel extraction. All analyses were performed in triplicate, and the mean peak area was used to determine the concentration

of paclitaxel in the samples. Drug loading was quantified with high-performance liquid chromatography (HPLC). A centrifugal ultrafiltration device (Centricon 100, MWCO 100 KD, Millipore, Bedford, MA) was used to separate free paclitaxel from the paclitaxel encapsulated in the liposomes in the finished product. Total paclitaxel concentration in the liposomes was determined using HPLC after methanol extraction. The percent paclitaxel encapsulated in the liposomes was calculated from the free and total paclitaxel in the liposomes.

4.2.4 Liposome size, morphology and zeta-potential

The size analysis of liposomes was performed by the dynamic light scattering technique using a Malvern zeta sizer nano particle size analyzer (Malvern Instruments, Malvern, UK). A 25 µL of this sample was diluted to 1 mL with water for injection for particle size determination. The diluted aqueous sample (1 mL) was added to a 2 mL cuvette and the analysis was performed in triplicate and the average particle size was calculated from the result. The transmission electron microscopic (TEM) studies were carried out using 3 mm Forman coated copper grid (400 mesh) at 60 KV using negative staining by 2% uranyl acetate at 200,000 X magnifications on a JEOL 1200EX TEM.

4.2.5 Quantification of transferrin conjugation

A sensitive gel filtration chromatographic method was developed and validated to quantitate transferrin. The gel filtration chromatographic system consisted of a Waters 600 controller, Waters 717 plus auto sampler and a Waters 2996 photodiode array detector. Data were acquired and processed with Waters Millennium 32 software (version

4.0). Gel filtration chromatographic separation was achieved on a TSK Gel G3000 SWXL (30 cm X 7.8 mm, 5 micron) column from Tosoh bioscience (South San Francisco, CA). The isocratic mobile phase consisting of 0.5 N phosphate buffered saline (pH 7.2) was pumped at a flow rate of 0.5 mL/min with an injection volume of 30 μL. Transferrin (retention time, 4.8 min) was monitored at 220 nm with a photo diode array detector. All analyses were performed in triplicate, and the mean peak area was used to determine the concentration of transferrin in the samples.

Free Tf was separated from the liposome encapsulated part using a Centricon centrifugal filter device (Centricon 100, MWCO 100 KD, Millipore, Bedford, MA). An aliquot of the liposome dispersion (100 μL) was diluted to 1 mL with hydration buffer (phosphate buffered saline pH 7.2). This sample was transferred to the centrifugal filter device. The sample was centrifuged at 5000 rpm for 30 minutes in a fixed-angle centrifuge. Free transferrin in the filtrate was then determined using high performance gel filtration chromatography (HPGFC). Subtraction of free Tf from the amount added gave the amount of liposome-conjugated Tf. Tf estimations were done in triplicate, and the values were reported as mean ± SD.

4.2.6 C6 GFP flank glioma tumor xenograft model and non-invasive imaging of tumor growth using NIRF

C6-GFP glioma cells in their exponential growth phase were harvested with EDTA/Trypsin for 5 min at 37°C. The cells were centrifuged for 5 min at 1,000 RPM. The pellets were resuspended in sterile phosphate buffered saline (PBS), at a concentration of 100,000,000/mL and placed on ice. Adult CD1 nu/nu mice (25-30g)

were used for all studies and handled in accordance with protocols approved by the Animal Care and Use Committee at the University of Tennessee Health Science Center. Mice were anesthetized with an intraperitoneal injection of ketamine/xylazine at a dosage of 8.7/1.3 mg/100 g body weight. To create the flank glioma tumor model, 4,000,000 C6-GFP glioma cells in 200 μL of phosphate buffered saline were injected into the flank using a 27 ½ G needle. Tumor growth was measured on every 3rd day with a vernier caliper, and tumor volume was measured using the formula W^2X L / 0.52. W refers to width and L is the length of the tumor. Near infrared whole body optical images of mice were taken with a CCD camera (Princeton Instruments Inc. Trenton, NJ) using GFP filter (excitation: 475 nm and emission: 510 nm). Acquired images were processed for measuring the pixel intensity of the GFP fluorescence from the tumors using the Metamorph® software (version 6.2) for determining the C6 GFP tumor area.

4.2.7 Antitumor efficacy of paclitaxel in liposomes: NIRF imaging analysis

Five days after tumor cell inoculation, animals were assigned randomly in to 4 groups (n = 4 - 5 per group). The groups included no treatment control, paclitaxel in transferrin conjugated long circulating liposomes (Tf-LCL), paclitaxel in long circulating liposomes (LCL) and paclitaxel in water containing 8.3% of cremophor EL and 8.2% ethanol. After 5 days of unrestricted tumor growth, animals were treated with 2 mg/Kg of paclitaxel on every third day (about 13 days) till the end of experiment. Injections were made using the retro orbital route of administration. For monitoring changes in tumor volume, tumor growth was measured every 3rd day with a vernier caliper, and tumor volume was measured as described in previous section. Near infrared whole body optical

imaging was also explored for monitoring the biodistribution and therapeutic effect. Optical images of mice were taken with a CCD camera (Princeton Instruments Inc. Trenton, NJ) using GFP filter to visualize the tumors. Acquired images were processed using the Metamorph® software (version 6.2) for determining the C6 GFP tumor area. On the day 18th of tumor implantation, animals were anesthetized and subjected to transcardiac perfusion first with 20 ml of normal saline and then with same amount of 4% paraformaldehyde to fix the tissue. Acquired images were processed for measuring the pixel intensity of the GFP fluorescence from the tumors using the Metamorph® software (version 6.2) for determining the C6 GFP tumor area.

Four different mouse treatment groups were observed: one group (n = 10) did not receive any treatment and served as control, another group (n = 4) was injected with Cremophor EL micellar solubilized paclitaxel at a concentration of 2 mg/Kg body weight, another group (n = 4) received 2 mg/Kg of paclitaxel in long circulating liposomes (LCL) and the last group (n = 4) received 2 mg/Kg of paclitaxel in Tf conjugated long circulating liposomes. The tumor growth delay was defined as the time required for a treated tumor to reach a specific volume (130 mm^3) minus the time for the untreated tumor to reach that same volume.

4.2.8 Statistics

The *in vivo* tumor localization and antitumor efficacy data were compared using one way analysis of variance to determine significant differences among experimental groups. All values of $P \leq 0.05$ were considered statistically significant.

4.3 Results and Discussion

4.3.1 Preparation and characterization of transferrin conjugated liposomal paclitaxel

Paclitaxel incorporation efficiency was determined by subtracting the free drug fraction from the total was found to be 98.0 ± 2%. The nontargeted liposome formulation showed average vesicle sizes of 133 ± 15 nm with unimodal distribution. The covalent coupling of Tf to the liposome surface led to a slight increase in diameter to about 141 ± 20 nm (Figures 4-1, 4-2). This slight increase in size was most probably due to the attachment of Tf to the liposome surface, which somewhat increases the hydrodynamic diameter of liposomes. The TEM images revealed that the long circulating liposomes were round and of spherical in shape. The zeta potential of Tf conjugated and non conjugated long circulating liposomes was found to be about -18 ± 3 mV. The Tf conjugation of LCL did not result in any significant change in the zeta potential of the liposomes and was about - 17 ± 4 mV.

The stability of paclitaxel liposomal formulations was monitored by changes in particle size and drug retention over a 7 day period during storage at 2 - 8ºC. The colloidal stability of liposomal formulations (size and zeta potential) was excellent with minimal or no change from the initial value. The paclitaxel retention in the liposomes was more than 97% of the label, during 7 day storage period. There were no visible changes to the physical appearance of the formulation or signs of drug precipitation from the lipid bilayers during this 7 day period. Based on free Tf concentration from a typical

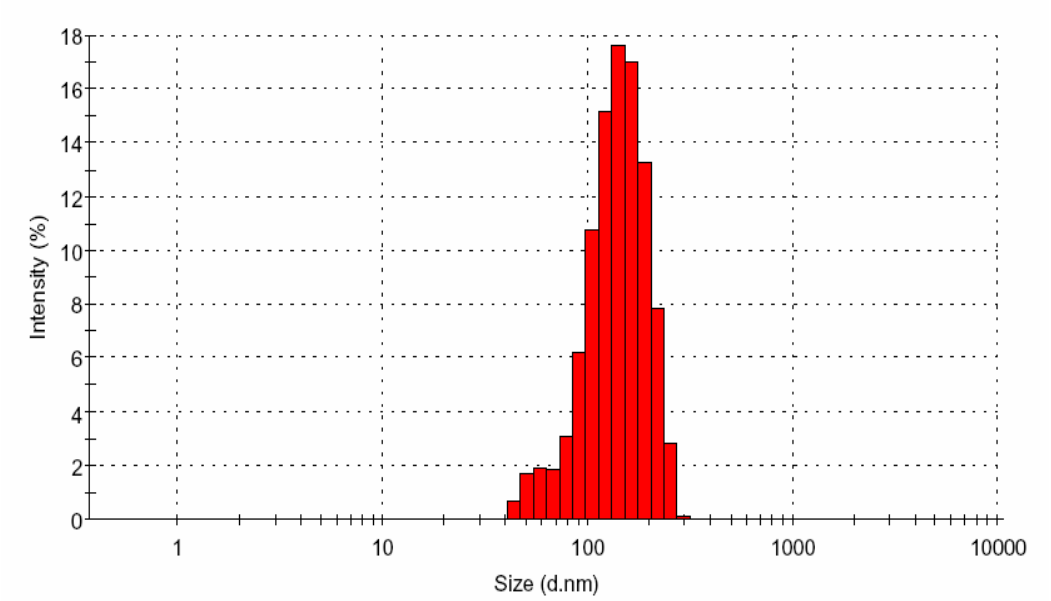

Figure 4-1. Size and size distribution of the paclitaxel long circulating liposomes. Dynamic light scattering method was used. Average diameter, 132.8 nm and PDI, 0.167.

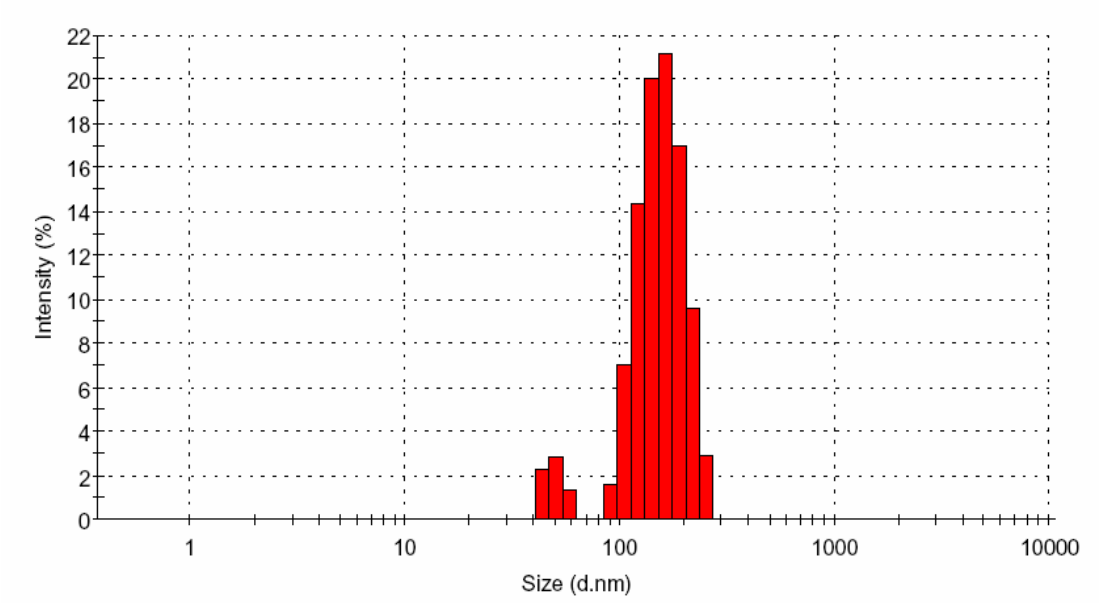

Figure 4-2. Size and size distribution of the transferrin conjugated long circulating liposomes using dynamic light scattering method. Average diameter, 141.3 nm and PDI, 0.170.

formulation, about 72% of Tf was coupled to the liposomes. It was found by this method that about 4 μg of the Tf was bound to 1μM of the total lipid; this corresponds to approximately 5 Tf molecules per 100 nm liposome.

4.3.2 NIRF imaging of tumors growth in nude mice

Flank growth of C6 GFP tumor cells was sequentially monitored in a group of 8 mice, using the total light emission over the flank tumor area as an indication of tumor burden. The C6 GFP fluorescence could be detected in mice from day 1 after inoculation of 4,000,000 cells. The tumor distribution was estimated by caliper measurements and correlated with the regions of GFP fluorescence. (Figures 4-3, 4-4 and 4-5). Relative pixel intensity of the tumor increased with time after inoculation (Figure 4-5), and the time taken for flank tumor volume to increase from 30 to 500 mm^3 (Figure 4-3) ranged from 5 to about 18 days. Overall, there was good correlation between caliper measurements of the tumors and near infrared fluorescence imaging. However, imaging is helpful in estimating the tumor area more precisely at earlier time points, as caliper measurements cannot precisely identify small tumors until approximately day 7 after tumor implantation. In contrast, caliper measurements were found to be more accurate in determining actual tumor volume, when tumors were more than 400 mm^3.

4.3.3 Anti-tumor efficacy of paclitaxel in liposomes

C6 GFP glioma tumors were induced in CD1 nu/nu nude mice by inoculation of GFP-expressing C6 glioma (C6-GFP) cells. The in vivo efficacy of paclitaxel in

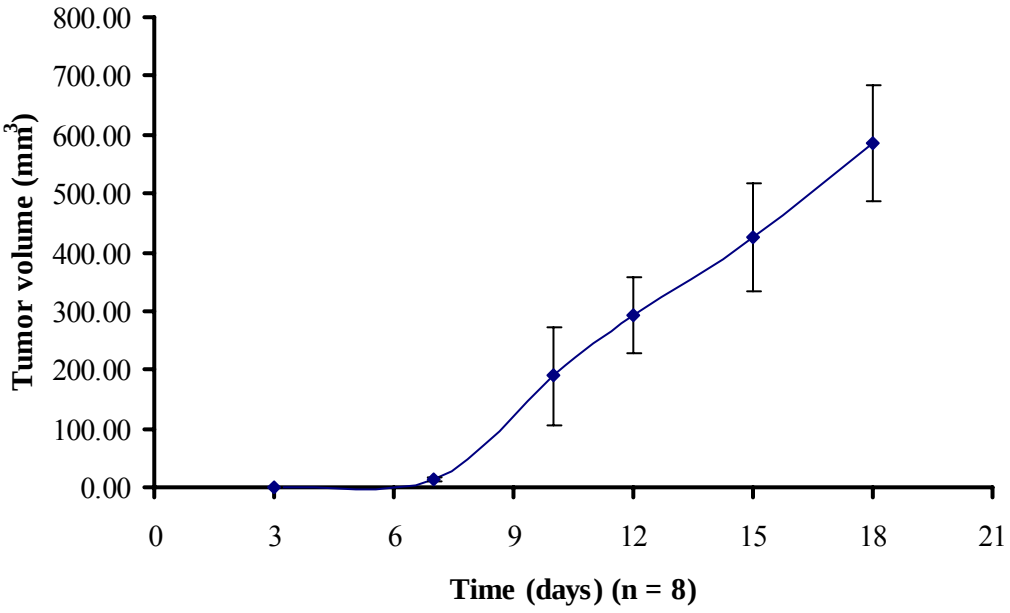

Figure 4-3. C6 GFP tumor growth curve. Tumor volume was determined after repeated caliper measurements from 2 to 18 days after tumor cell inoculation. Group mean values (± S.D.) for these mice are shown.

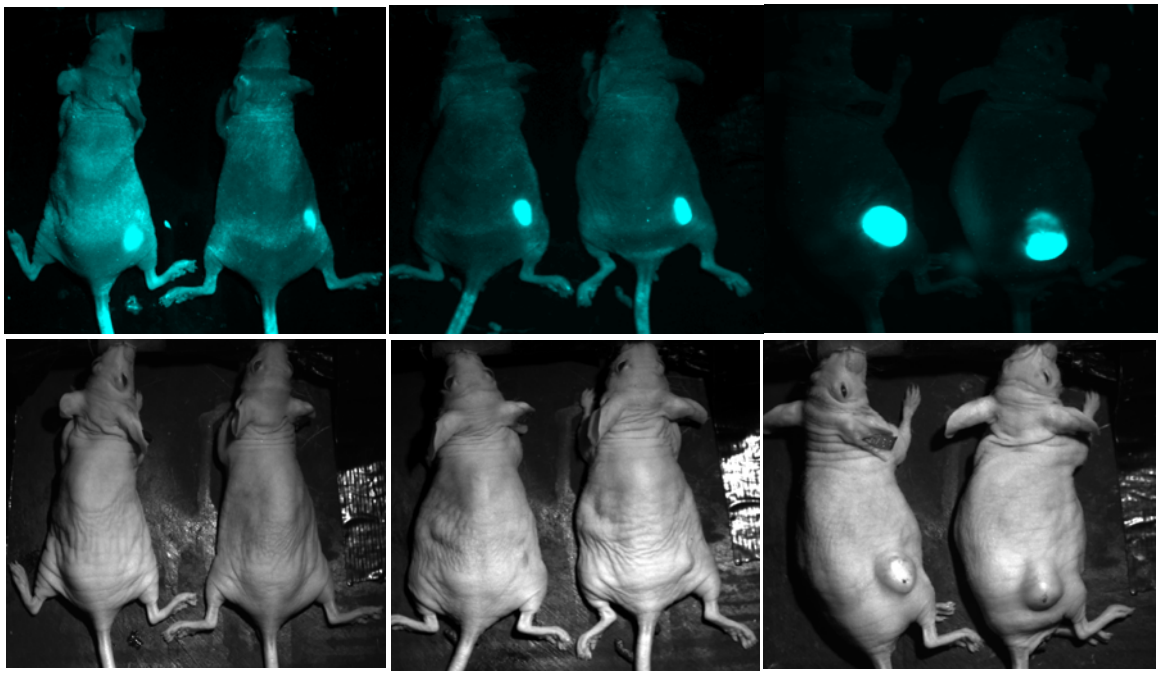

Figure 4-4. Images of nude mice showing the presence of tumor in flank region. Top row shows increase in tumor area with time using a GFP filter. Bottom row shows the respective white light images at corresponding time points.

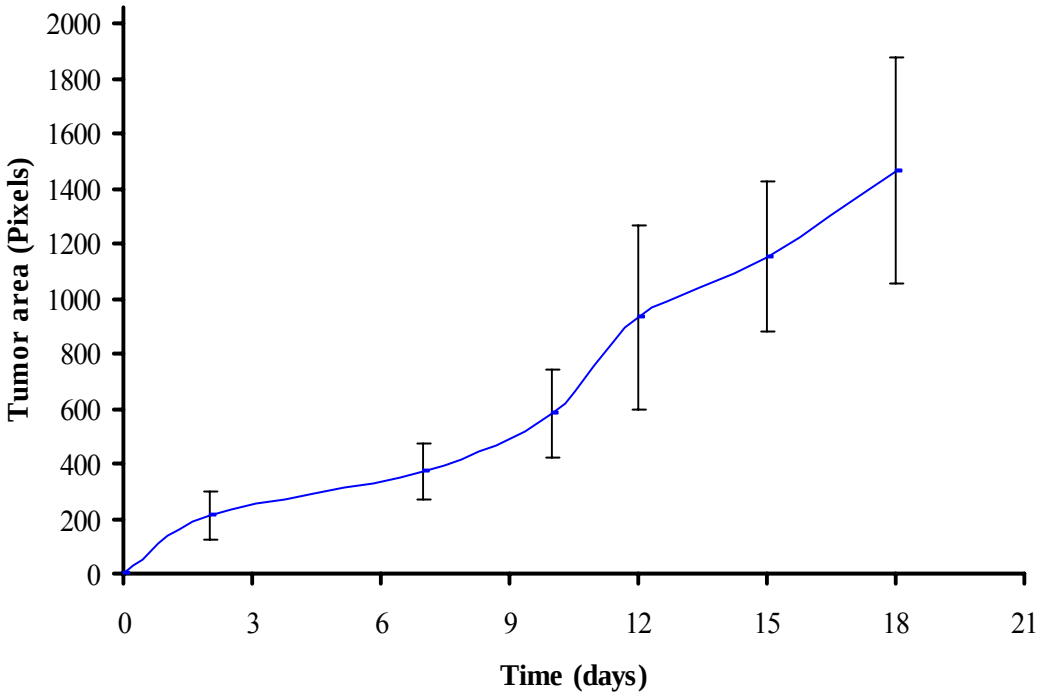

Figure 4-5. C6 GFP tumor growth curve. Tumor area was determined after repeated tumor imaging from 2 to 18 days after tumor cell inoculation. Group mean values (± S.D.) for these mice are shown.

glioma tumors was evaluated. Tumor areas were measured with Metamorph® software after taking optical images with a CCD camera with a GFP filter. As shown in Figure 4-6., paclitaxel in Tf -LCL formulation resulted in significant tumor growth delay of 7.7 days when compared to 3.3 days with LCL and 0 days with solution formulation. Clinical monitoring and daily weights were similar between groups, thus indicating that no gross deleterious effects of paclitaxel when administered systemically at the tested dose. In this study transferrin receptor targeted liposomes retained their targeting ability to glioma tumors. Treatment with these liposomal formulations significantly increased the antitumoral efficacy of the drug. Therefore, chemotherapeutic drug delivery targeted to the glioma by means of transferrin receptor targeted liposomes appears to be a promising new strategy for cancer chemotherapy.

4.4 Conclusion

These findings indicate that preferential targeting of paclitaxel in transferrin conjugated liposomes to glioma tumors results in significant tumor growth delay.

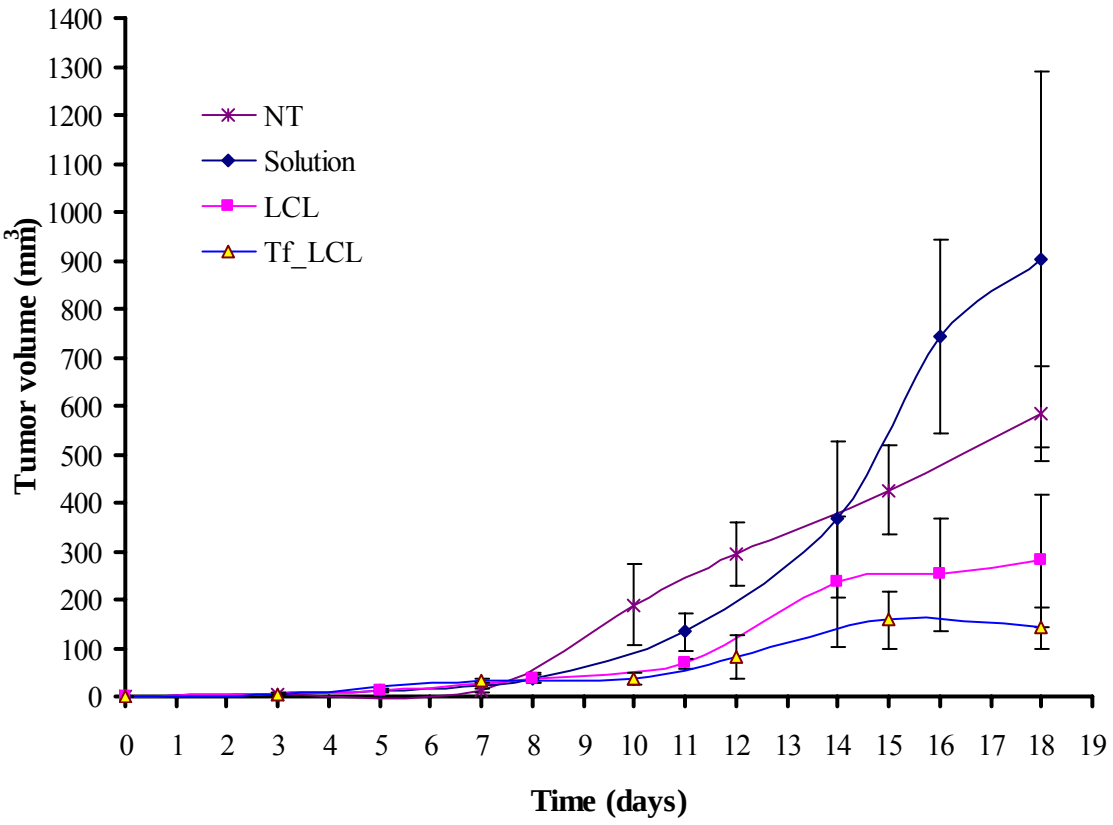

Figure 4-6. Tumor growth of subcutaneously inoculated C6 GFP tumor cells. The length and width of each tumor were measured using calipers, and mean tumor volumes were calculated for each group. Tumor growth was significantly delayed after treatment with paclitaxel encapsulated liposomes compared to solution and no treatment controls. Δ: paclitaxel in Tf-LCL, □: Paclitaxel in LCL, ◊: paclitaxel in solution, ∗: no treatment control. $P < 0.05$, Tf-LCL vs. all other groups; $n = 4 – 5$ per group; mean ± SD.

Chapter 5: Selective Intracranial Glioma Localization and Improved Efficacy of Paclitaxel in Transferrin Conjugated Liposomes

5.1 Introduction

Most malignant gliomas are incurable with the present methods of healthcare. Currently accepted therapeutic adjuvants to surgery, such as radiotherapy and chemotherapy, provide only a minor improvement in the disease course and life expectancy for patients diagnosed with malignant gliomas (Curran Jr., Scott et al. 1993; DeAngelis, Burger et al. 1998; Surawicz, Davis et al. 1998). Often, chemotherapy has failed to make any significant impact on the prognosis of disease because of significant local and systemic toxicity, problems with transport of the drug across the blood brain barrier (BBB), and a high degree of chemoresistance demonstrated by tumor cells (Grossman, Fisher et al. 1998). Newer targeted delivery systems with greater specificity for gliomas, improved safety profiles, and an enhanced ability to permeate through the BBB are actively under development as the next generation glioma therapies.

Liposomes have been investigated over decades as systemic drug delivery vehicles for the delivery and targeting of drugs to sites in the body (Torchilin 2005). Liposomes have gained increased attention, because of their structural versatility in terms of size, composition, surface charge, and their ability to incorporate most of the drugs regardless of solubility. Tumor targeting therapy has been advocated to increase the therapeutic index and decrease side effects, (Allen 2002; Scherrmann 2002; Schnyder and Huwyler 2005). The success of such a targeted liposomal drug delivery strategy for the treatment of brain tumors depends on the ability of the delivery systems to localize at

higher concentrations in the target site while avoiding the normal tissue. Brain tumor targeting using transferrin as a ligand for receptor-mediated endocytosis has attracted attention. In recent years, several studies have demonstrated that the use of the transferrin uptake pathway is highly effective for treating cancer in animal models and in humans (Pardridge 1999; Liao, Li et al. 2001; Pardridge 2002; Soni, Kohli et al. 2005; Soni, Kohli et al. 2007). Conjugation of transferrin with anticancer drugs such as doxorubicin has shown the potential to circumvent the cardiotoxicity and development of drug resistance (Lai, Fu et al. 2005; Soni, Jain et al. 2005; Soni, Kohli et al. 2007). Tseg et. al., reported the potential use of paclitaxel efficacy against malignant brain tumors (Tseng, Bobola et al. 1999).

In this study, we hypothesize that transferrin receptor up-regulation in glioma tumors can be utilized to selectively deliver paclitaxel to intracranial C6 glioma brain tumors. Paclitaxel delivery to various tumor cells have has been the subject of many studies (Ho, Barbarese et al. 1997; Crosasso, Ceruti et al. 2000; Schmitt-Sody, Strieth et al. 2003; Torchilin, Lukyanov et al. 2003; Koziara, Lockman et al. 2004; Strieth, Eichhorn et al. 2004; Zhang, Anyarambhatla et al. 2005), but the targeted liposomal delivery of paclitaxel via up-regulated transferrin receptors has not been reported.

Intracranial tumor localization of transferrin receptor targeted liposomes was demonstrated using near infrared (NIR) fluorescence imaging. We demonstrate that in xenograft intracranial glioma tumors sufficient tumor volume control can be achieved when paclitaxel is preferentially targeted to intracranial glioma tumors. This glioma tumor targeting is accomplished by incorporating the drug or fluorescent dye in a transferrin conjugated long circulating liposome delivery system.

5.2 Materials and Methods

5.2.1 Materials

Egg phosphotidylcholine (EPC), hydrogenated soybean phosphatidylcholine (HSPC), 1,2-distearoyl –sn-glycero-3-phosphoethanolamine-N-[PEG(2000)] conjugate (DSPE-PEG), and DSPE-PEG-maleimide were from Northern Lipids Inc., Vancouver, Canada. Cholesterol, and biotinylated transferrin were obtained from Sigma, St. Louis, MO and the DIR fluorescent dye was purchased from Invitrogen, Carlsbad, CA. These chemicals were used as received. Paclitaxel was purchased from 21CEC Pharma, East Sussex, UK. All other chemicals and solvents used were analytical grade.

5.2.2 Liposome preparation

Liposomes were produced by the lipid hydration method followed by extrusion. The liposomes contained egg phosphotidylcholine (EPC), hydrogenated soy phosphatidylcholine (HSPC), cholesterol (75: 15: 5 molar ratios). Paclitaxel was encapsulated in the lipid bilayers due to its lipophilic nature. For preparation of long circulating liposomes (LCL), poly (ethylene glycol-2000)-grafted distearoyl phosphatidyl ethanolamine (DSPE–PEG2000) was incorporated. For preparation of transferrin conjugated liposomes (Tf-LCL) a portion of DSPE-PEG2000 (0.01 mol%) was replaced with DSPE-PEG2000-biotin and then transferrin (Tf) was non-covalently conjugated at the distal end of DSPE-PEG2000-biotin via streptavidin-biotin bond. DIR (lipophilic fluorescent marker) was encapsulated in the liposomal bilayers.

5.2.3 Quantification of paclitaxel

A sensitive reverse phase HPLC method was developed and validated to quantitate paclitaxel in liposome formulations. Chromatographic system consisted of a Waters 600 controller, Waters 717 plus auto sampler and a Waters 2996 photodiode array detector. Data were acquired and processed with Waters Millennium 32 software (version 4.0). Chromatographic separation was achieved on a NovaPak® C18 reverse phase column (3.9 X 150 mm) from Waters (Milford, MA). The isocratic mobile phase consisting of acetonitrile and water (55:45, v/v) was pumped at a flow rate of 0.7 mL/min with an injection volume of 20 μL. Paclitaxel (retention time, 3.8 min) was monitored at 230 nm with a photo diode array detector. Prior to HPLC analysis, the formulation samples were treated with methanol for paclitaxel extraction. All analyses were performed in triplicate, and the mean peak area was used to determine the concentration of paclitaxel in the samples. Drug loading was quantified with high-performance liquid chromatography (HPLC). A centrifugal ultrafiltration device (Centricon 100, MWCO 100 KD, Millipore, Bedford, MA) was used to separate free paclitaxel from the paclitaxel encapsulated in the liposomes in the finished product. Total paclitaxel concentration in the liposomes was determined using HPLC after methanol extraction. The percent paclitaxel encapsulated into the liposomes was calculated from the free and total paclitaxel in the liposomes.

5.2.4 Liposome size, morphology and zeta-potential

The size analysis of liposomes was performed by dynamic light scattering technique using Malvern zeta sizer–nano particle size analyzer (Malvern Instruments,

Malvern, UK). A 25 µL of this sample was diluted to 1 mL with water for injection for particle size determination. The diluted aqueous sample (1 mL) was added to a 2 mL cuvette and the analysis was performed in triplicate. Average particle size was calculated from the result. The transmission electron microscopic studies were carried out using 3 mm Forman coated copper grid (400 mesh) at 60 KV using negative staining by 2% uranyl acetate at 200,000 X magnifications on a JEOL 1200EX transmission electron microscope (TEM).

5.2.5 Quantification of transferrin conjugation

A sensitive gel filtration chromatographic method was developed and validated to quantitate transferrin. The gel filtration chromatographic system consisted of a Waters 600 controller, Waters 717 plus auto sampler and a Waters 2996 photodiode array detector. Data were acquired and processed with Waters Millennium 32 software (version 4.0). Gel filtration chromatographic separation was achieved on a TSK Gel G3000 SWXL (30 cm X 7.8 mm, 5 micron) column from Tosoh bioscience (South San Francisco, CA). The isocratic mobile phase consisting of 0.5 N phosphate buffered saline (pH 7.2) was pumped at a flow rate of 0.5 mL/min with an injection volume of 30 µL. Transferrin (retention time, 4.8 min) was monitored at 220 nm with a photo diode array detector. All analyses were performed in triplicate, and the mean peak area was used to determine the concentration of transferrin in the samples.

Free Tf was separated from the liposome encapsulated part using a Centricon centrifugal filter device (Centricon 100, MWCO 100 KD, Millipore, Bedford, MA). An aliquot of the liposome dispersion (100 µL) was diluted to 1 mL with hydration buffer

(phosphate buffered saline pH 7.2). This sample was transferred to the centrifugal filter device. The sample was centrifuged at 5000 rpm for 30 minutes in a fixed-angle centrifuge. Free transferrin in the filtrate was then determined using high performance gel filtration chromatography (HPGFC). Subtraction of free Tf from the amount added gave the amount of liposome-conjugated Tf. Tf estimations were done in triplicate, and the values were reported as mean ± standard deviation.

5.2.6 Induction of C6 GFP intracranial glioma tumor xenografts

C6-GFP glioma cells in their exponential growth phase were harvested with 0.25% Trypsin with EDTA for 5 min at 37°C. The cells were centrifuged for 5 min at 1,000 RPM. The pellets were resuspended in sterile phosphate buffered saline (PBS), at a concentration of 100, 000, 000/mL and placed on ice. Adult CD1 nu/nu mice (25-30g) (Charles river, Wimington, MA) were used for all studies and handled in accordance with protocols approved by the Animal Care and Use Committee at the University of Tennessee Health Science Center. Mice were anesthetized with an intraperitoneal injection of ketamine/xylazine at a dosage of 8.7/1.3 mg/100 g body weight. To create the intracranial glioma tumor model, 500,000 C6-GFP glioma cells in 5 μL of phosphate buffered saline were injected into the brain at a depth of 3.0 mm from the surface of skull and 3.0 mm lateral from midline along the bregma suture in the right hemisphere, using a Hamilton syringe and stereotaxic frame. The scalp defect is then closed with cyanoacrylate glue.

5.2.7 NIRF imaging of tumors and tumor localization of DIR labeled liposomes in mice

Fourteen days after tumor cell inoculation, animals were injected retroorbitally with different formulations labeled with a lipophilic dye (DIR). The area and pixel intensity of the dye in the tumor was compared with the background intensity in the surrounding normal tissue using non-invasive optical imaging with a CCD camera with DIR filter at 0, 1, 8, 24 and 48 Tf-LCL after injection. 48 Tf-LCL after injection, animals were anesthetized and subjected to transcardiac perfusion first with 20 mL of normal saline and then with same amount of 4% paraformaldehyde to fix the tissue. The brains were incubated in 4% paraformaldehyde. Images of isolated brains were taken with a CCD camera (Princeton Instruments Inc., Trenton, NJ) using GFP, (excitation: 475 nm and emission: 510 nm) DIR (excitation: 750 nm and emission: 782 nm) (Omega optical, Brattleboro, VT) for visualization of tumor area and DIR dye localization in the brain tissue. Acquired images were processed for measuring the pixel intensity of the DIR fluorescence from the tumors using the Metamorph® software (version 6.2) for determining the C6 GFP tumor area. Tumor to muscle accumulation ratio of DIR dye labeled formulations was determined to calculate Tumor targeting index.

5.2.8 Antitumor efficacy of paclitaxel in liposomes

Five days after tumor cell inoculation, animals were assigned randomly into 3 groups (n = 3 - 4 per group). The groups included no treatment control, paclitaxel in transferrin conjugated long circulating liposomes (Tf-LCL) and paclitaxel in long circulating liposomes (LCL). After 5 days of unrestricted tumor growth, animals were

treated with 2 mg/Kg of paclitaxel once a day (for about 9 days) till the end of experiment. The animals were monitored visually on a daily basis and weights were measured on every 3rd day until they lost 10% of their body weight. On the 14th day of tumor implantation, animals were anesthetized and subjected to transcardiac perfusion first with 20 mL of normal saline and then with same amount of 4% paraformaldehyde to fix the tissue. The brains were incubated in 4% paraformaldehyde. Optical images of isolated brains were taken with a CCD camera (Princeton Instruments Inc., Trenton, NJ) using GFP filter. Acquired images were processed using the Metamorph® software (version 6.2) for determining the C6 GFP tumor area.

5.2.9 Statistics

The *in vivo* tumor localization and antitumor efficacy data were compared using one way analysis of variance to determine significant differences among experimental groups. All values of $p \leq 0.05$ were considered statistically significant.

5.3 Results and Discussion

5.3.1 Preparation and characterization of transferrin conjugated liposomal paclitaxel

Paclitaxel incorporation efficiency was determined by subtracting free drug fraction was found to be 98.0 ± 2%. The non conjugated liposome formulation showed average vesicle sizes of 133 ± 15 nm with a unimodal distribution. The covalent coupling

of Tf to the liposome surface led to a slight increase in diameter to about 141 ± 20 nm This slight increase in size most probably due to the attachment of Tf to the liposome surface, which somewhat increases the hydrodynamic diameter of liposomes. The TEM images revealed that the long circulating liposomes were round and of spherical in shape. The zeta potential of Tf conjugated and non conjugated long circulating liposomes was found to be about -18 ± 3 mV. The Tf conjugation of LCL did not result in any significant change in the zeta potential of the liposomes.

The stability of paclitaxel liposomal formulations was monitored by changes in particle size and drug retention over a 7 day period during storage at 4 ºC. The colloidal stability of the liposomal formulations (size and zeta potential) was found to be excellent with minimal or no change in from the initial value. The paclitaxel retention in the liposomes was more than 97% of the label, during a 7 day storage period at 2- 8 ºC. There were no visible changes to the physical appearance or signs of drug precipitation from the lipid bilayers during this 7 day period.

The total amount of the liposome attached transferrin for the typical Tf-LCL formulation was determined by using the high performance gel filtration chromatography. Tf dissolved in the mobile phase eluted at ~4.8-minute retention. Based on free Tf concentration from a typical formulation, about 72% of Tf was coupled to the liposomes. It was found that about 4 µg of the Tf was bound to 1 µM of the total lipid; this corresponds to approx. 5 Tf molecules per 100 nm liposome.

5.3.2 NIRF imaging of tumors and tumor localization of DIR labeled liposomes in mice

An enhanced permeation and retention (EPR) effect has been demonstrated for nano carriers in tumor targeting (Papisov 1998; Shan, Flowers et al. 2006). We investigated the tumor accumulation and the tumor-to-muscle accumulation ratio of liposomal formulation using a non-invasive NIR fluorescence imaging method. The data showed that the LCL and Tf-LCL selectively accumulated in C6 intracranial glioma tumors (Figure 5-1). The Tf-LCL formulation accumulated in the C6 glioma tumors more efficiently as compared to muscle tissue (Figure 5-2). The tumor targeting index for Tf-LCL was found to be 6.15 ± 1.47.

5.3.3 Anti-tumor efficacy of paclitaxel in liposomes

To study the effect of paclitaxel on C6 GFP glioma *in vivo*, tumors were induced in CD1 nu/nu nude mice by intracranial inoculation of GFP-expressing C6 glioma (C6-GFP). After 5 days of tumor cell inoculation, animals were assigned randomly to 3 groups (n = 3 - 4 per group). These groups were paclitaxel Tf-LCL, LCL, and no treatment control. Drug was administered once a day via retro orbital injection for 9 subsequent days with 2 mg/Kg in Tf-LCL or LCL formulation. The animals were then sacrificed on the 9^{th} day of treatment and the brains were isolated. Tumor areas were measured Metamorph® software after taking optical images with a CCD camera with GFP filter. As shown in Figure 5-3., paclitaxel in Tf -LCL formulation resulted in significant tumor reduction when compared to no treatment tumor control ($p = 0.038$). No

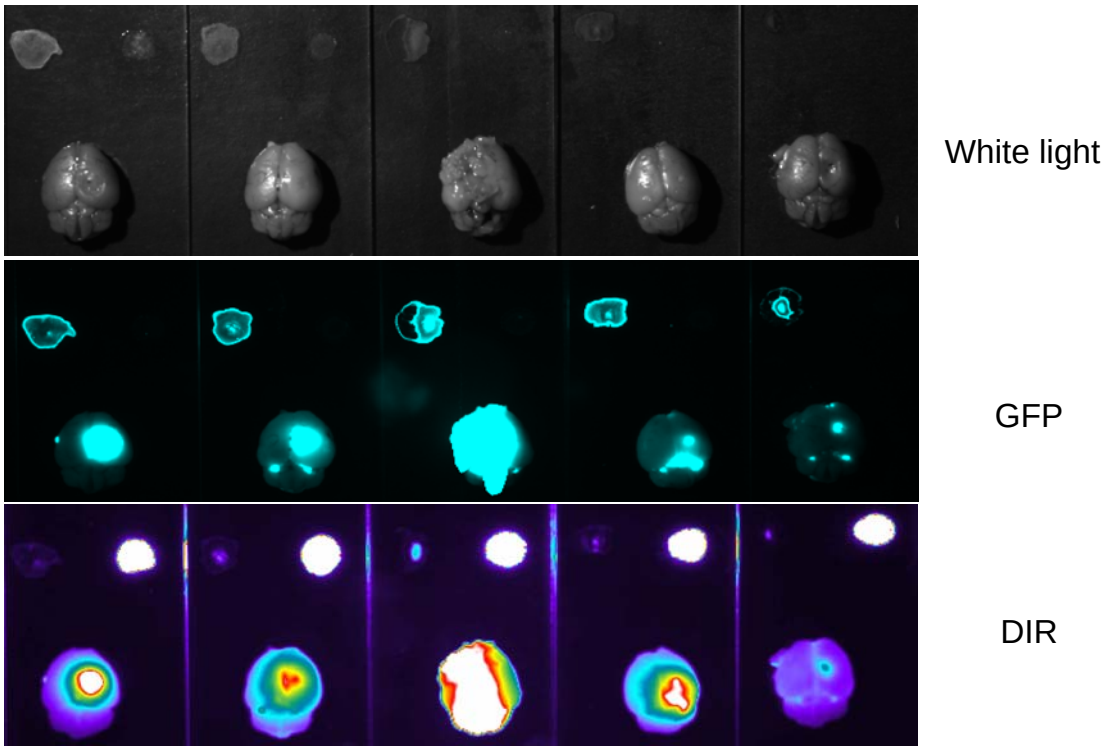

Figure 5-1. Near infrared fluorescence images of brains isolated from mice. Selective localization of Tf-LCL in intracranial GFP expressing C6 glioma brain tumors was observed. Top row images were taken with white light, second row with GFP filter and third row images were taken DIR filter.

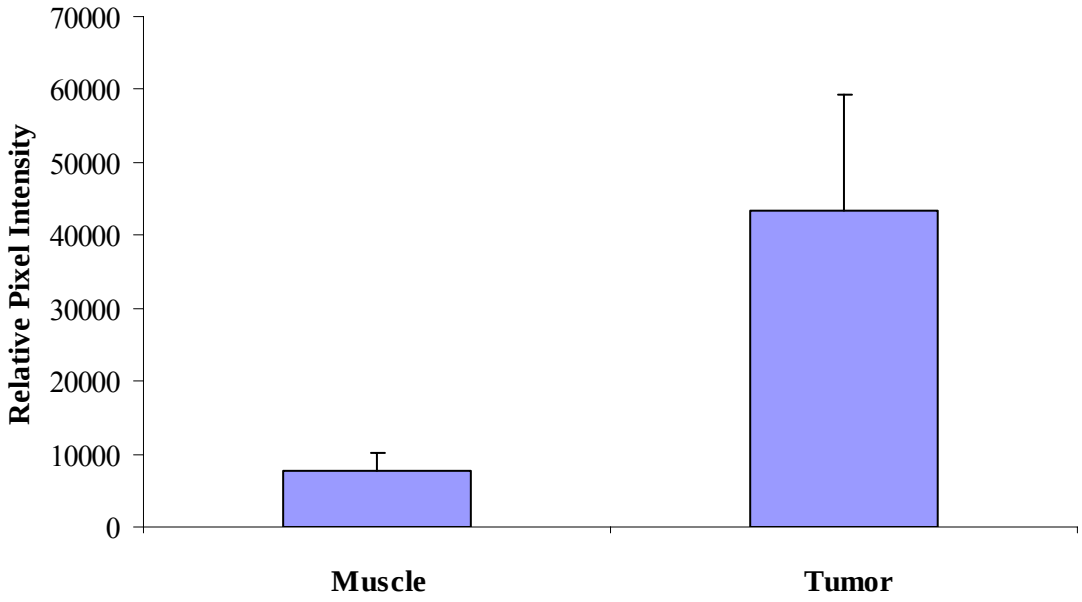

Figure 5-2. The selective accumulation of Tf-LCL in intracranial glioma tumors. High fluorescence signals in mouse intracranial tumor tissue were observed up to 24 Tf-LCL. The fluorescence ration between tumor and normal muscle tissue yielded up to 6 fold selectivity for the tumor in comparison with surrounding normal tissue; n = 3; Mean ± SD. (Tumor targeting index: 6.15 ± 3.3)

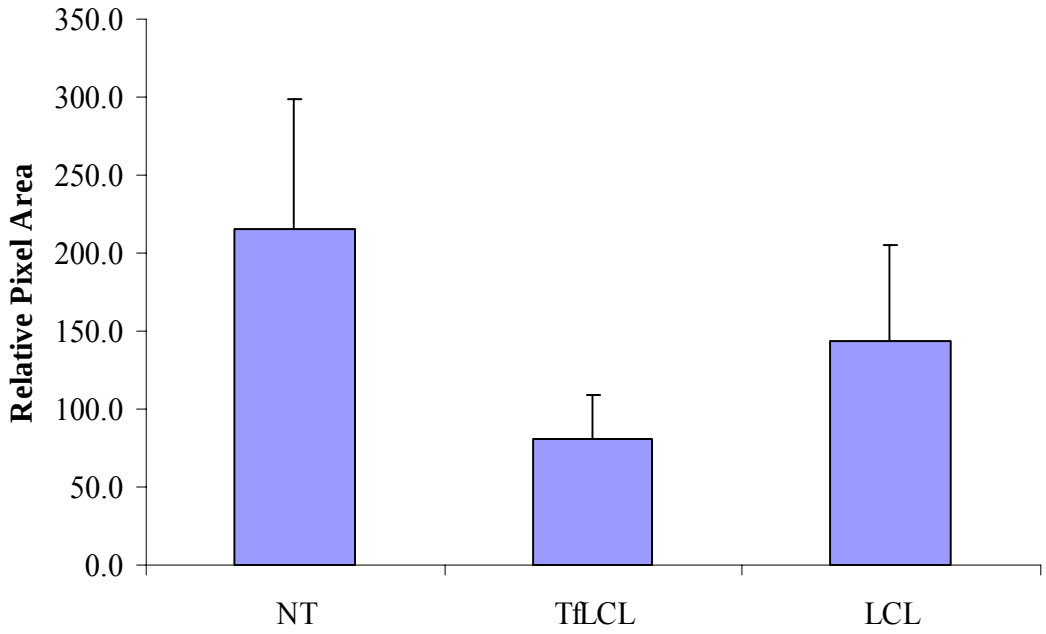

Figure 5-3. In vivo efficacy of paclitaxel against C6 intracranial glioma tumors. C6 GFP glioma cells were inoculated into the frontal lobe of the brains of nude mice (n= 3 - 5 per group). After 5 days of tumor cell incubation, groups were treated by retroorbital injection every 24 Tf-LCL for 9 subsequent days with 2 mg/kg of paclitaxel in Tf-LCL or LCL. Paclitaxel in Tf-LCL was efficacious at reducing the tumor burden ($p = 0.038$). However, no significant tumor reduction was observed with paclitaxel in LCL ($p = 0.188$)

statistical significant tumor reduction was observed with long circulating liposomes ($p = 0.188$). Figure 5-4 show representative photomicrographs of the average tumor area in animals treated with paclitaxel in Tf-LCL formulation compared with paclitaxel in LCL and no treatment control group. Clinical monitoring and daily weights were similar between groups indicating no gross deleterious effects of paclitaxel when administered systemically at the tested dose. Paclitaxel encapsulation in Tf-LCL formulation group was more active than the non-treated, and paclitaxel in long circulating liposome groups for the treatment of the intracranial glioma tumor at the 2 mg/Kg dose. Whole body NIRF imaging of mice implanted with C6-GFP intracranial glioma revealed marked selective intracranial glioma localization with Tf-LCL formulation.

5.4 Conclusion

These studies provide evidence that paclitaxel delivered in Tf-LCL accumulate effectively with relative selectivity in tumor areas, improving the overall anti-tumor efficacy in intracranial gliomas over a non targeted liposomal system.

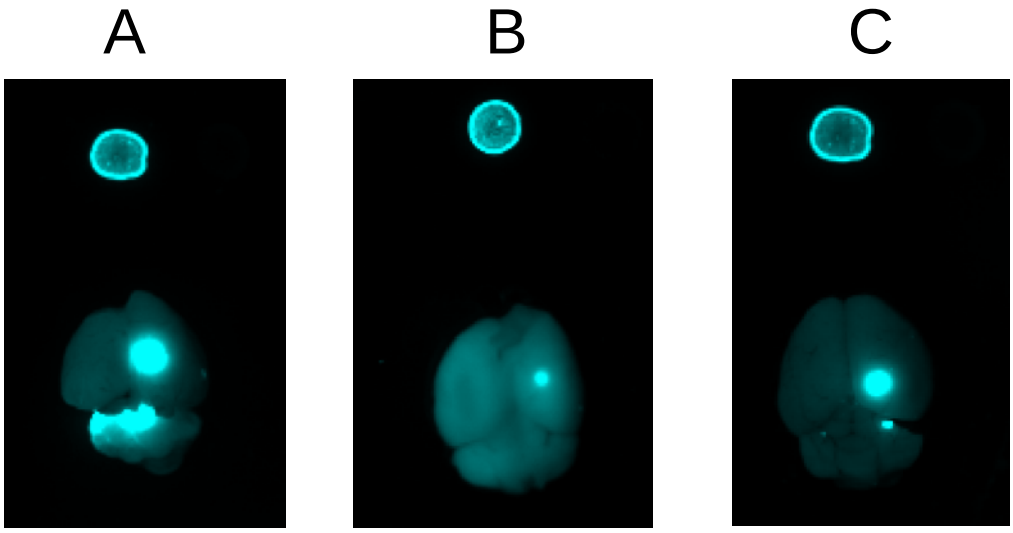

Figure 5-4. Representative images of C6 GFP intracranial glioma tumors. Animals treated with paclitaxel in Tf-LCL (panel B) as compared to the no treatment control (panel A) and paclitaxel in LCL (panel C) were shown. Top row shows reference dots for GFP filter were created with FITC solution.

Chapter 6: Development of a Lyophilized Targeted Liposome Delivery System for Paclitaxel

6.1 Introduction

The therapeutic applications of targeted liposomes are dependent on the physical integrity and stability of the lipid bilayer structure. In the liquid state, liposome formulations are subject to both) physical and chemical instability (Sharma and Sharma 1997). These physical and chemical stability parameters are critical to the *in vivo* behavior of liposomal drug delivery systems. Liposomal size distribution is a critical parameter with respect to the pharmacokinetic and pharmacodynamic behavior of drugs that are site-specifically targeted *in vivo* (Van Bommel and Crommelin 1984; Van Winden, Zhang et al. 1997). One of the practical difficulties is that liposomes are relatively unstable during storage.

Lyophilization is the method of choice for enhancement of long-term stability of liposomes (Ausborn and Nuhn 1990; Ausborn, Nuhn et al. 1992). In the process, most of the water molecules are excluded from the specimen and the aqueous suspension becomes a powder that could be stored even at ambient temperatures. Prior to use, reconstitution of the particulate system is achieved by rehydration of the dry powder (Liu 2006). Removal of water by lyophilization prevents hydrolysis of phospholipids. Other chemical and physical degradation processes are also retarded by low molecular mobility in the solid phase. Further, freeze-drying of liposome formulations, if performed successfully, results in a pharmaceutically elegant dry cake which can be reconstituted

within seconds to obtain the original dispersion (Jonkman-de Vries, Talsma et al. 1994; Wang 2000; Tang and Pikal 2004).

Lyophilization of targeted liposomes is more complex when compared to large multilamellar conventional liposomes (Van Winden, Zhang et al. 1997; Zhang, Van Winden et al. 1997). Liposome bilayer membranes may be damaged during the lyophilization cycle mainly by mechanical stress caused when high pressures vesicle membranes are exposed during ice crystal formation and chemically from increased concentrations of solute during freezing and dehydration. This can lead to massive aggregation and fusion of the vesicles as well as leakage of the entrapped compounds upon reconstitution of the lyophilized cake. In the absence of cryoprotectants, small targeted liposomes will be converted into large multi lamellar liposomes, upon lyophilization and reconstitution (Peer, Florentin et al. 2003). This change in size of the liposomes is detrimental for targeted drug delivery. Cryoprotectants have been shown to decrease vesicle fusion and leakage caused by both freeze-thaw and the freeze-drying process (Sun, Leopold et al. 1996; Crowe, Oliver et al. 1997; Crowe, Carpenter et al. 1998; Van Winden and Crommelin 1999). Sugars such as trehalose, sucrose, mannose or glucose were used as cryoprotectants at high concentrations (~ 30%) in the original liposome preparations. Among these sugars, trehalose is particularly effective in preserving the liposomes. Crowe et al. have carried out extensive investigations on possible mechanisms by which sugars protect biological membranes during freeze-drying (Crowe, Oliver et al. 1997; Crowe, Carpenter et al. 1998). Lyophilization of targeted liposome delivery systems is even more complex. Very few studies have been reported on lyophilization of targeted liposomes. The influence of functional lipids and targeting

ligands on the preservation of the targeted liposomes during freeze-drying is also not well understood (Van Winden and Crommelin 1999).

In this study we report on the development of a lyophilized targeted liposome delivery system for paclitaxel. We also provide evidence of cryoprotective ability of sucrose and trehelose during lyophilization of liposomes. The effects of these cryoprotectants on particle size and zeta potential of liposomes upon reconstitution with water for injection were investigated.

6.2 Materials and Methods

6.2.1 Materials

Egg phosphotidylcholine (EPC), hydrogenated soybean phosphatidylcholine (HSPC), and 1,2-distearoyl –sn-glycero-3-phosphoethanolamine-N-[PEG(2000)] conjugate (DSPE-PEG) were from Northern Lipids Inc., Vancouver, Canada., cholesterol, biotinylated transferrin, sucrose and trehelose were obtained from Sigma, St. Louis, MO. These chemicals were used as received. Paclitaxel was purchased from 21CEC Pharma, East Sussex, UK. All other chemicals and solvents used were of analytical grade.

6.2.2 Liposome preparation

Liposomes were produced by the lipid hydration method followed by extrusion. The liposomes contained egg phosphotidylcholine (EPC), hydrogenated soy

phosphatidylcholine (HSPC), cholesterol (75: 15: 5 molar ratios). The paclitaxel (log P is 3.96) was encapsulated in the lipid bilayers due to its lipophilic nature. For preparation of long circulating liposomes (LCL), poly (ethylene glycol-2000)-grafted distearoyl phosphatidyl ethanolamine (DSPE–PEG2000) was incorporated. For preparation of Tf-LCL a part of DSPE-PEG2000 (0.01 mol%) was replaced with DSPE-PEG2000-biotin and then transferrin (Tf) was non-covalently conjugated at the distal end of DSPE-PEG2000-biotin via streptavidin-biotin bond.

6.2.3 Lyophilization of liposomes

For cryoprotection of liposomes during lyophilization, 15% sucrose or trehelose was added to freshly prepared liposome dispersions and distributed into 5 mL freeze-dry vials (Wheaton) in 1 mL aliquots. The rubber freeze-dry closures (type V9172-FM 257, Helvoet Pharma, Alken, Belgium) were used. Vials, partially stoppered with freeze-dry closures, were loaded into the Virtis genesis freeze-dryer and frozen slowly to -45 °C at 1 °C per min. Freezing was continued for 5 Tf-LCL. At the end of the freezing step, chamber pressure was brought to 110-120 m Torr and the shelf temperature was maintained at -35 °C for 10 Tf-LCL, followed by drying at shelf temperature of -20 °C for 5 Tf-LCL and at 0 °C for 5 Tf-LCL (primary drying). The secondary drying was carried out at 50-60 m torr chamber pressure at 10 °C for 14 Tf-LCL and at 20 °C for 10 Tf-LCL. The condenser temperature ranged between -55 and -60 °C. At the end of the freeze-drying process the chamber was backfilled with nitrogen to maintain a non-reactive gaseous headspace. The vials were closed with rubber closures were unloaded from the chamber followed by crimping with aluminum seals.

6.2.4 Liposome size, morphology and zeta-potential

Lyophilized samples were reconstituted (rehydrated) to their original volume (1 mL) with sterile water for injection. A 25 µL of this sample was diluted to 1 mL with water for injection for particle size determination. The average size and polydispersity index were determined at 25 ºC by dynamic light scattering method with Malvern zetasizer nano, using the dispersion technology software version 4.10 (Malvern Ltd, Malvern, UK). Measurements were performed on three independently prepared samples for each formulation. The same sample was used for zeta potential analysis of liposomes with Malvern Zetasizer Nano, using the dispersion technology software version 4.10 (Malvern Ltd, Malvern, UK).

6.2.5 Estimation of drug entrapment in liposome formulation

A sensitive reverse phase HPLC method was developed and validated to quantitate paclitaxel in liposome formulations. Chromatographic system consisted of a Waters 600 controller, Waters 717 plus auto sampler and a Waters 2996 photodiode array detector. Data were acquired and processed with Waters Millennium 32 software (version 4.0). Chromatographic separation was achieved on a NovaPak® C18 reverse phase column (3.9 X 150 mm) from Waters (Milford, MA). The isocratic mobile phase consisting of acetonitrile and water (55:45, v/v) was pumped at a flow rate of 0.7 mL/min with an injection volume of 20 µL. Paclitaxel (retention time, 3.8 min) was monitored at 230 nm with a photo diode array detector. Prior to HPLC analysis, the formulation samples were treated with methanol for paclitaxel extraction. All analyses were performed in triplicate, and the mean peak area was used to determine the concentration

of paclitaxel in the samples. The total and free paclitaxel in the liposome formulations before and after lyophilization and reconstitution were determined using an HPLC method of analysis. The drug loading was quantified via high-performance liquid chromatography (HPLC). Briefly, a centrifugal ultrafiltration device (Centricon 100, MWCO 100 KD, Millipore, Bedford, MA) was used to separate free paclitaxel from the paclitaxel encapsulated in the liposomes. Free and total paclitaxel concentration in the liposomes was determined using HPLC after methanol extraction. Percent paclitaxel encapsulated in the liposomes was calculated from the free and total paclitaxel in the liposomes.

6.3 Results and Discussion

A formulation containing 15% (w/v) extra-liposomal sucrose or 15% (w/v) extra-liposomal trehelose were able to maintain the particle size distribution (PSD) of targeted liposomes close to initial after the lyophilization and rehydration (Figure 6-1). These formulations were also maintained drug loading after lyophilization and reconstitution. Lyoprotective effects of sucrose and trehalose are compared in Figure 6-2. Zeta potential of liposomes before lyophilization were about – 17.6 mV. The average zeta potential of liposomes with 15% sucrose or trehelose as cryoprotectant after lyophilization and reconstitution were about -20 mV (Figure 6-3)**.** As we can see from these images, both of these disaccharides were able to maintain the initial monodisperse size distribution and

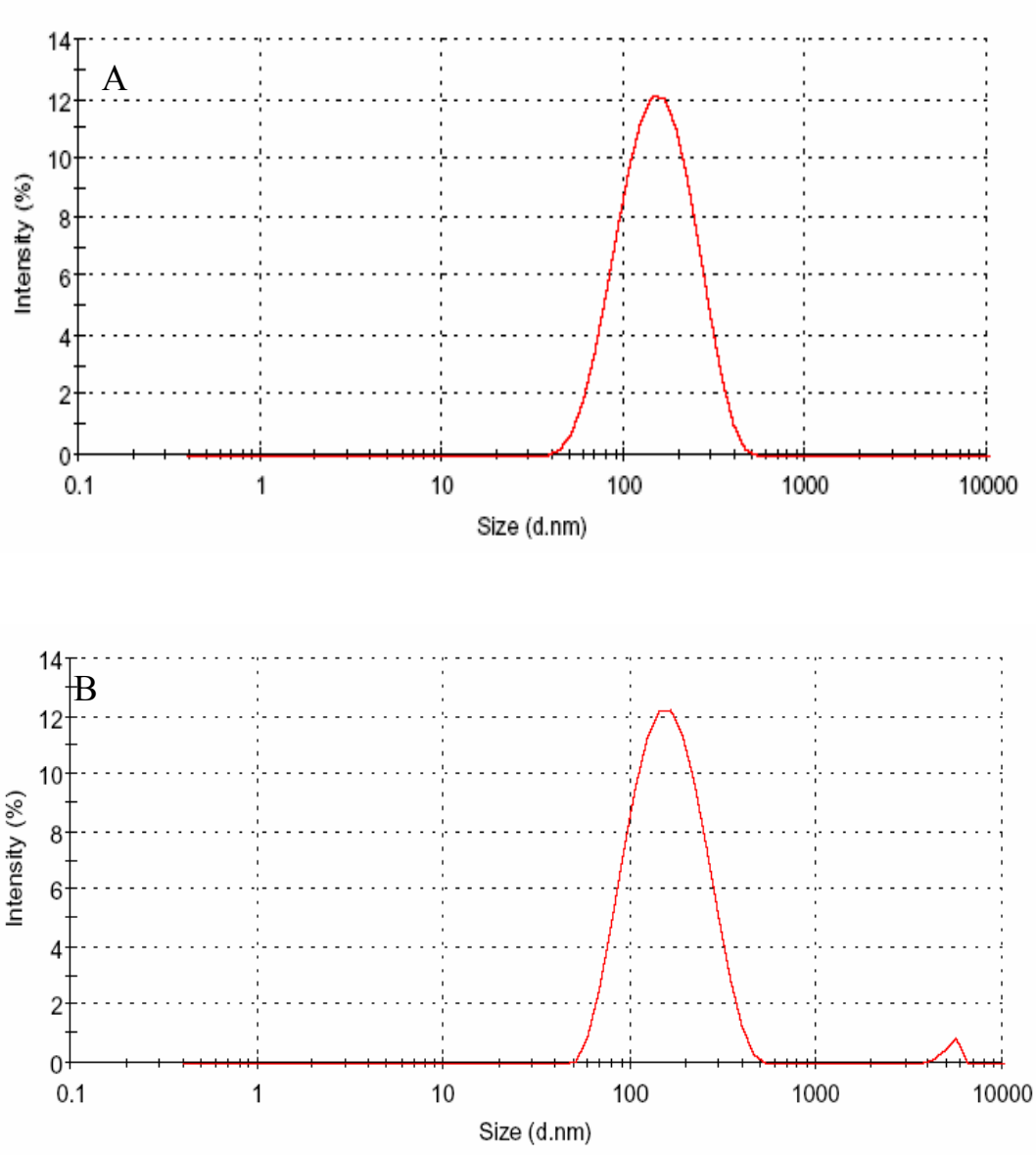

Figure 6-1. Particle size distribution (PSD) of targeted liposomes after lyophilization. (A) Original PSD before freeze-drying. Average size 137 nm, polydispersity index (PDI) 0.176. (B) PSD after freeze-drying the formulation containing 15% (w/v) extra-liposomal sucrose. Average size 150 nm, PDI: 0.215.

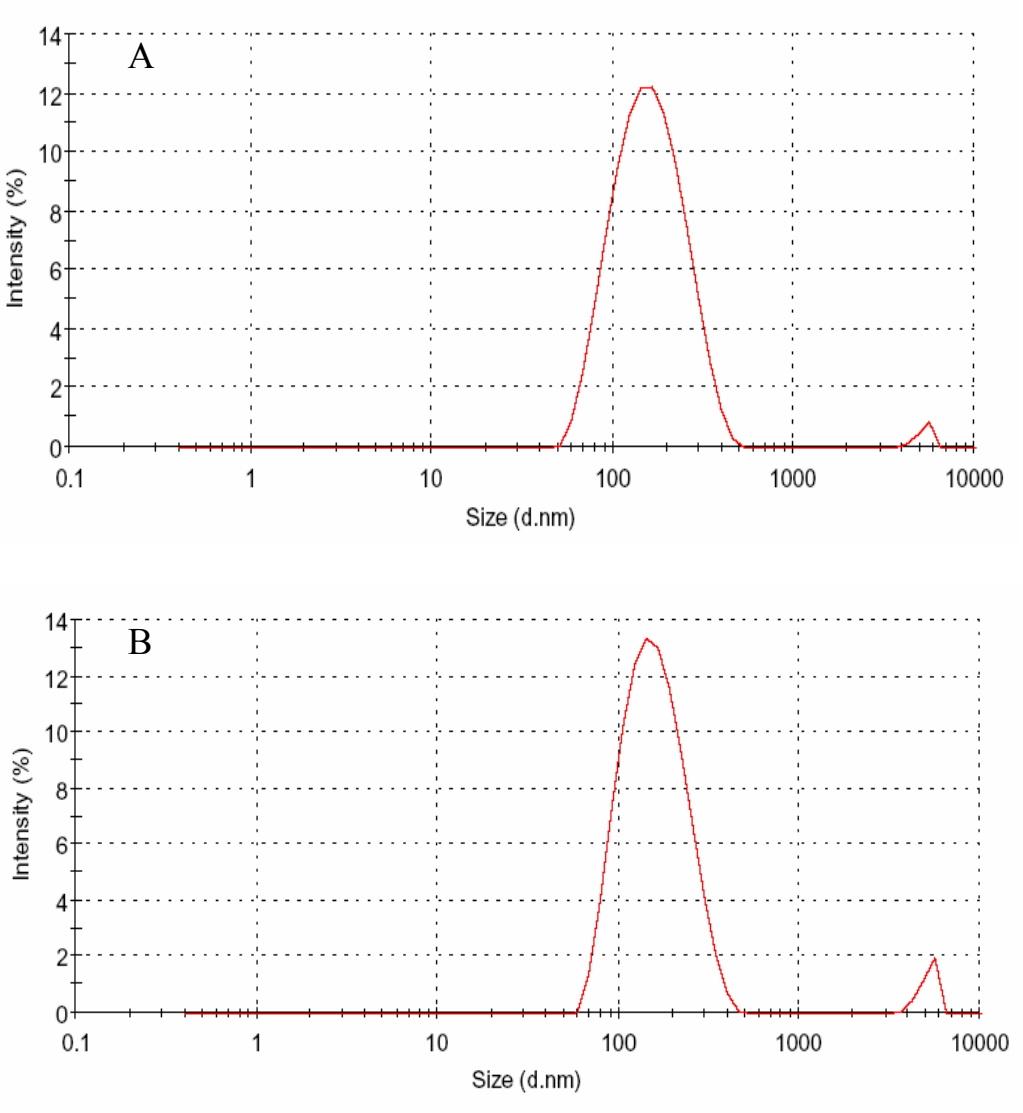

Figure 6-2. Effect of sucrose and trehalose on liposome size after lyophilization. (A) PSD after lyophilizing the formulation containing 15% (w/v) extra-liposomal sucrose. Average size 150 nm, PDI: 0.215. (B) PSD after lyophilizing the formulation containing 15% (w/v) extra-liposomal trehalose. Average size 160 nm, PDI: 0.277

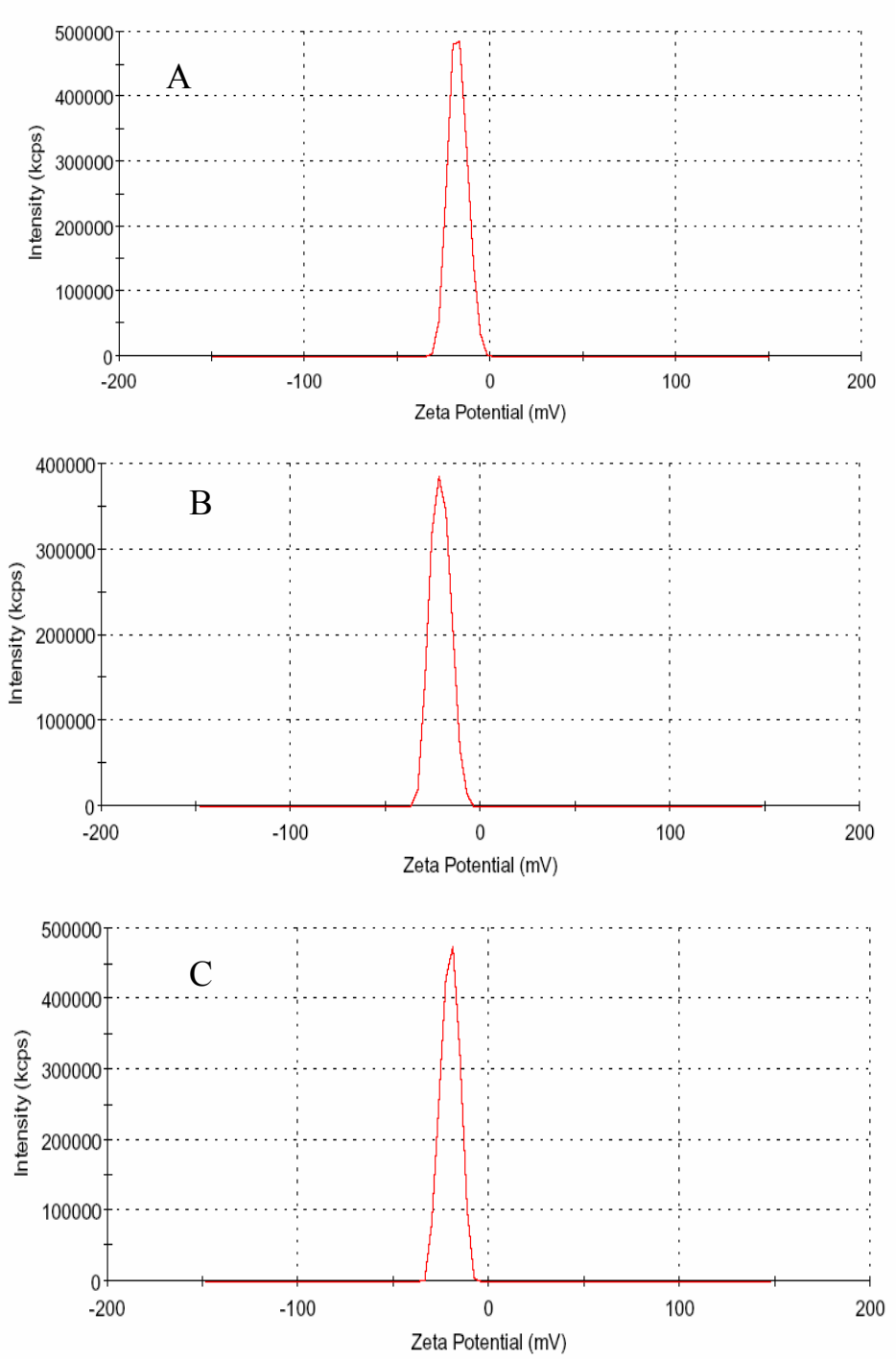

Figure 6-3. Lyoprotective effect of sucrose and trehalose. (A) Original zeta potential before freeze-drying. Average zeta potential 17.6 mV, (B) zeta potential after freeze-drying with 15% (w/v) extra-liposomal trehelose. Average zeta potential -21.3 mV (C) Zeta potential after freeze-drying with 15% (w/v) extra-liposomal sucrose. Average zeta potential -20.4 mV.

zeta potential of the targeted liposomes after freeze-drying and reconstitution. But the sucrose was slightly better on maintaining the original PSD and zeta potential of these targeted liposomes than trehalose. Average size and poly dispersity index (PDI) after freeze-drying and reconstitution for trehalose formulation were 161 nm and 0.271, respectively (Figure 6-2). Where as those numbers for the sucrose formulation were 154 nm and 0.25, respectively (Figure 6-2). The size distribution of targeted liposomes before freeze-drying (average size of 137 nm and PDI of 0.176, (Figure 6-1) was closely preserved after freeze-drying and reconstitution when sucrose was used as lyoprotectant. Similar results were reported in the literature for some other liposome systems. Sucrose was found to be more effective in maintaining size distribution of mitoxantrone liposomes after lyophilization and reconstitution (Ugwu, Zhang et al. 2005).

There was no significant change in the size and zeta potential of the liposomes after lyophilzation indicated the cryoprotection of the liposomes by the sucrose. In the absence of cryoprotectants, aggregation and fusion of liposomes is expected when lyophilized without cryoprotection. Because liposome bilayer formation itself requires presence of water, removal of this water through freeze-drying should be expected to cause irreversible damage to these structures (Winterhalter and Lasic 1993). But this is not the case with cryoprotectants. Several reports describe this process of liposome aggregation on lyophilization (Van Bommel and Crommelin 1984; Van Winden, Zhang et al. 1997; Van Winden and Crommelin 1999; Ugwu, Zhang et al. 2005; Zhang, Anyarambhatla et al. 2005). The most successful lyoprotectants were the non reducing disaccharides sucrose and trehalose (Van Bommel and Crommelin 1984; Van Winden and Crommelin 1999). Based on this information we used 15% concentration of sucrose

or trehalose in our formulation to protect the targeted liposomes during freeze-drying process.

6.4 Conclusions

A lyophilized formulation was developed to increase storage stability of the targeted liposome formulation. We report sucrose as a better lyoprotectant for this formulation and process when compared to trehelose.

Chapter 7: Summary

The main objective of this project was to develop a targeted liposome delivery system for the paclitaxel, to selectively deliver this drug to glioma brain tumors. Towards this goal, first, a targeted liposome delivery system targeting transferrin receptors highly-expressed on gliomas was designed. Then, a formulation and process for preparation of this targeted liposome delivery system was developed. The functional properties of the delivery system were evaluated both *in vitro* and *in vivo*. The delivery system was characterized and the formulation was optimized to achieve maximum *in vivo* blood circulation half life and high tumor localization. Finally, to enhance the storage stability of the delivery system, a lyophilized formulation and process were developed.

The elements of the targeted delivery system were chosen to satisfy a number of requirements such as high drug loading, stable encapsulation, good physical and chemical stability during shelf life, long circulation half-life *in vivo*, high tumor targeting potential and efficient target recognition and binding. The targeted liposome delivery system is composed of five different lipid components (Egg PC, HSPC, cholesterol, DSPE-PEG, DSPE-PEG-biotin) and a targeting ligand, transferrin. The targeting ligand transferrin was coupled to the distal ends of PEG chains. This specific way of ligand coupling to the liposome carrier was used to maximize ligand coupling to the liposome carrier as well as their interaction with the intended biological targets (transferrin receptors on glioma tumors).

The extrusion process developed for the preparation of these liposome carriers is robust. There was a great control of liposome size and size distribution in the extrusion process used. The process can be scaled up easily. A long blood circulation half-life in rats (9 Tf-LCL) for fluorescent labeled targeted formulations was achieved. The sterically stabilized liposomes prepared using 5% PEG and about 100 nm in size showed a pronounced increase in the blood residence time (17 Tf-LCL) with a significant decrease in uptake by RES when compared with conventional liposomes. The rate extent of tumor localization of the transferrin receptor targeted fluorescent liposome was found to be significantly high compared to non targeted liposomes and solution formulations.

Anti-tumor efficacy evaluation in intracranial and flank tumor models indicated that targeting paclitaxel to glioma brain tumors using this liposome delivery system is significantly more effective than free paclitaxel administered in a micellar solubilized dosage form or non targeted liposomes. This targeted delivery system also reduced the dose required for the therapeutic efficacy. Further unwanted toxic effects in other normal tissues were not observed. The significant tumor growth delay was observed. Using a multiple dosing regimen, such as repeated administration of radiation and targeted liposomes containing paclitaxel, could probably further delay the tumor growth.

Finally, a successful lyophilization formulation and process were developed to enhance the storage stability of the targeted liposome delivery system. A formulation containing 15% (w/v) extra-liposomal sucrose was able to maintain the particle size distribution and drug loading of the targeted liposomes close to initial after freeze-drying and rehydration.

In conclusion, I have developed a stable and effective targeted liposome delivery system for paclitaxel to take this drug selectively to glioma brain tumors. This targeted delivery system could potentially increase the anti-cancer activity as well as the therapeutic index of the drug compared to existing solution dosage forms.

List of References

Abbott, N. J., D. C. Chugani, et al. (1999). "Delivery of imaging agents into brain." Advanced Drug Delivery Reviews 37: 253–277.

Allen, T. M. (1997). "Liposome targeting in animal models: problems and opportunities." Journal of Liposome Research 7: 315-329.

Allen, T. M. (2002). "Ligand-targeted therapeutics in anticancer therapy." Nature Reviews Cancer 2: 750-763.

Allen, T. M. (2004). Ligand-mediated targeting: an update. Proceedings - 2004 International Conference on MEMS, NANO and Smart Systems, ICMENS 2004.

Allen, T. M. and A. Chonn (1987). "Large unilamellar liposomes with low uptake into the reticuloendothelial system." FEBS Letters 223: 42-46.

Allen, T. M., P. Sapra, et al. (2002). "Use of the post-insertion method for the formation of ligand-coupled liposomes." Cellular and Molecular Biology Letters 7: 889-894.

Ausborn, M. and P. Nuhn (1990). "Possibilities and problems concerning the stabilization of liposomes by freezing and lyophilization." PZ Wissenschaft 135: 183-188.

Ausborn, M., P. Nuhn, et al. (1992). "Stabilization of liposomes by freeze-thaw-and lyophilization techniques: problems and opportunities." European Journal of Pharmaceutics and Biopharmaceutics 38: 133-139.

Ballou, B., L. A. Ernst, et al. (2005). "Fluorescence imaging of tumors in vivo." Current Medicinal Chemistry 12: 795-805.

Barenholz, Y. (2001). "Liposome application: problems and prospects." Current Opinion in Colloid and Interface Science 6: 66-77.

Bartus, R. T., P. J. Elliott, et al. (1996). "Controlled modulation of BBB permeability using the bradykinin agonist, RMP-7." Experimental Neurology 142: 14-28.

Batchelor, T. T. and T. N. Byrne (2006). "Supportive care of brain tumor patients." Hematology/Oncology Clinics of North America 20: 1337-1361.

Begley, D. J. (1996). "The blood-brain barrier: principles for targeting peptides and drugs to the central nervous system." Journal of Pharmacy and Pharmacology 48: 136-146.

Begley, D. J. (2003). "Understanding and circumventing the blood-brain barrier." Acta Paediatrica, International Journal of Paediatrics, Supplement 92: 83-91.

Black, K. L., W. A. King, et al. (1990). "Selective opening of the blood-tumor barrier by intracarotid infusion of leukotriene C4." Journal of Neurosurgery 72: 912-916.

Bouvet, M., J. Wang, et al. (2002). "Real-time optical imaging of primary tumor growth and multiple metastatic events in a pancreatic cancer orthotopic model." Cancer Research 62: 1534-1540.

Bremer, C., V. Ntziachristos, et al. (2001). "Advances in optical imaging." Fortschritte in der optischen bildgebung radiologe 41: 131-137.

Brown, J. M. and A. J. Giaccia (1998). "The unique physiology of solid tumors: opportunities (and problems) for cancer therapy." Cancer Research 58: 1408-1416.

Cattel, L., M. Ceruti, et al. (2003). "From conventional to stealth liposomes a new frontier in cancer chemotherapy." Tumori 89: 237-249.

Ceh, B., M. Winterhalter, et al. (1997). "Stealth® liposomes: from theory to product." Advanced Drug Delivery Reviews 24: 165-177.

Chen, X., P. S. Conti, et al. (2004). "In vivo near-infrared fluorescence imaging of integrin alfa v beta 3 in brain tumor xenografts." Cancer Research 64: 8009-8014.

Chio, C.-C., T. Baba, et al. (1992). "Selective blood-tumor barrier disruption by leukotrienes." Journal of Neurosurgery 77: 407-410.

Contag, C. H., P. R. Contag, et al. (1995). "Photonic detection of bacterial pathogens in living hosts." Molecular Microbiology 18: 593-603.

Contag, C. H., S. D. Spilman, et al. (1997). "Visualizing gene expression in living mammals using a bioluminescent reporter." Photochemistry and Photobiology 66: 523-531.

Contag, P. R. (2002). "Whole-animal cellular and molecular imaging to accelerate drug development." Drug Discovery Today 7: 555-562.

Crosasso, P., M. Ceruti, et al. (2000). "Preparation, characterization and properties of sterically stabilized paclitaxel-containing liposomes." Journal of Controlled Release 63: 19-30.

Crowe, J. H. (2007). "Trehalose as a 'chemical chaperone': fact and fantasy." Advances in experimental medicine and biology 594: 143-158.

Crowe, J. H., J. F. Carpenter, et al. (1998). "The role of vitrification in anhydrobiosis." Annual Review of Physiology 60: 73-103.

Crowe, J. H. and L. M. Crowe (1988). "Factors affecting the stability of dry liposomes." Biochimica et Biophysica Acta (BBA) - Biomembranes 939: 327-334.

Crowe, J. H., L. M. Crowe, et al. (1987). "Stabilization of dry phospholipid bilayers and proteins by sugars." Biochemical Journal 242: 1-10.

Crowe, J. H., A. E. Oliver, et al. (1997). "Stabilization of dry membranes by mixtures of hydroxyethyl starch and glucose: the role of vitrification." Cryobiology 35: 20-30.

Cui, J., C. Li, et al. (2006). "Freeze-drying of liposomes using tertiary butyl alcohol/water cosolvent systems." International Journal of Pharmaceutics 312: 131-136.

Curran Jr., W. J., C. B. Scott, et al. (1993). "Recursive partitioning analysis of prognostic factors in three radiation therapy oncology group malignant glioma trials." Journal of the National Cancer Institute 85: 704-710.

Dang, W., S. Dordunoo, et al. (1999). "Polyphosphoester paclitaxel microspheres (PACLIMER(TM) DELIVERY SYSTEM): in vitro and in vivo studies." Proceedings of the Controlled Release Society: 513-514.

DeAngelis, L. M., P. C. Burger, et al. (1998). "Malignant glioma: who benefits from adjuvant chemotherapy?" Annals of Neurology 44: 691-695.

Desmettre, T., J. M. Devoisselle, et al. (2000). "Fluorescence properties and metabolic features of indocyanine green (ICG) as related to angiography." Survey of Ophthalmology 45: 15-27.

Dimeco, F., K. W. Li, et al. (2002). "Local delivery of mitoxantrone for the treatment of malignant brain tumors in rats." Journal of Neurosurgery 97: 1173-1178.

Drummond, D. C., O. Meyer, et al. (1999). "Optimizing liposomes for delivery of chemotherapeutic agents to solid tumors." Pharmacological Reviews 51: 691-743.

Edinger, M., T. J. Sweeney, et al. (1999). "Noninvasive assessment of tumor cell proliferation in animal models." Neoplasia 1: 303-310.

Edwards, R. H. (2001). "Drug delivery via the blood-brain barrier." Nature Neuroscience 4: 221-222.

El-Deiry, W. S., C. C. Sigman, et al. (2006). "Imaging and oncologic drug development." Journal of Clinical Oncology 24: 3261-3273.

Ewend, M. G., S. Elbabaa, et al. (2005). "Current treatment paradigms for the management of patients with brain metastases." Neurosurgery. 57: S66-77; discusssion S1-774.

Fine, H. A., P. Y. Wen, et al. (2003). "Phase II trial of thalidomide and carmustine for patients with recurrent high-grade gliomas." Journal of clinical oncology : official journal of the American Society of Clinical Oncology 21: 2299-2304.

Fortin, D. (2003). "Altering the properties of the blood-brain barrier: disruption and permeabilization." Progress in Drug Research 61: 125-154.

Frangioni, J. V. (2003). "In vivo near-infrared fluorescence imaging." Current Opinion in Chemical Biology 7: 626-634.

Fricker, G. and D. S. Miller (2004). "Modulation of drug transporters at the blood-brain barrier." Pharmacology 70: 169-176.

Gaber, M. W., H. Yuan, et al. (2004). "An intravital microscopy study of radiation-induced changes in permeability and leukocyte-endothelial cell interactions in the microvessels of the rat pia mater and cremaster muscle." Brain Research Protocols 13: 1-10.

Gabizon, A. and D. Papahadjopoulos (1992). "The role of surface charge and hydrophilic groups on liposome clearance in vivo." Biochimica et Biophysica Acta - Biomembranes 1103: 94-100.

Gennuso, R., M. K. Spigelman, et al. (1993). "Effect of blood-brain barrier and blood-tumor barrier modification on central nervous system liposomal uptake." Cancer Investigation 11: 118-128.

Glavas-Dodov, M., E. Fredro-Kumbaradzi, et al. (2005). "The effects of lyophilization on the stability of liposomes containing 5-FU." International Journal of Pharmaceutics 291: 79-86.

Grant, R., B. Liang, et al. (1995). "Age influences chemotherapy response in astrocytomas." Neurology 45: 929-933.

Green, N. M. (1964). "The molecular weight of avidin." Biochemical Journal 92: 16C-17C.

Green, N. M. (1990). "Avidin and streptavidin." Methods in Enzymology 184: 51-67.

Green, N. M. and M. A. Joynson (1970). "A preliminary crystallographic investigation of avidin." Biochemical Journal 118: 71-72.

Green, S. B., D. P. Byar, et al. (1983). "Comparisons of carmustine, procarbazine, and high-dose methylprednisolone as additions to surgery and radiotherapy for the treatment of malignant glioma." Cancer Treatment Reports 67: 121-132.

Grossman, S. A., J. D. Fisher, et al. (1998). "The new approaches to brain tumor therapy (NABTT) CNS consortium:
organization, objectives, and activities." Cancer Control 5: 1-3.

Gupta, B., T. S. Levchenko, et al. (2005). "Monoclonal antibody 2C5-mediated binding of liposomes to brain tumor cells in vitro and in subcutaneous tumor model in vivo." Journal of Drug Targeting 13: 337-343.

Hall, W. A. and G. T. Sherr (2006). "Convection-enhanced delivery of targeted toxins for malignant glioma." Expert Opinion on Drug Delivery 3: 371-377.

Hansen, C. B., G. Y. Kao, et al. (1995). "Attachment of antibodies to sterically stabilized liposomes: evaluation, comparison and optimization of coupling procedures." Biochimica et Biophysica Acta - Biomembranes 1239: 133-144.

Harashima, H., K. Sakata, et al. (1994). "Enhanced hepatic uptake of liposomes through complement activation depending on the size of liposomes." Pharmaceutical Research 11: 402-406.

Harasym, T. O., M. B. Bally, et al. (1998). "Clearance properties of liposomes involving conjugated proteins for targeting." Advanced Drug Delivery Reviews 32: 99-118.

Harding, J. A., C. M. Engbers, et al. (1997). "Immunogenicity and pharmacokinetic attributes of poly(ethylene glycol)-grafted immunoliposomes." Biochimica et Biophysica Acta - Biomembranes 1327: 181-192.

Henley, D., M. Isbill, et al. (2007). "Paclitaxel induced apoptosis in breast cancer cells requires cell cycle transit but not Cdc2 activity." Cancer Chemotherapy and Pharmacology 59: 235-249.

Hennenfent, K. L. and R. Govindan (2006). "Novel formulations of taxanes: a review. old wine in a new bottle?" Annals of Oncology 17: 735-749.

Ho, S.-Y., E. Barbarese, et al. (1997). "Evaluation of lipid-coated microbubbles as a delivery vehicle for Taxol in brain tumor therapy." Neurosurgery 40: 1260-1268.

Hunt, C. A. and S. Tsang (1981). "Alfa-tocopherol retards autoxidation and prolongs the shelf-life of liposomes." International Journal of Pharmaceutics 8: 101-110.

Huwyler, J., D. Wu, et al. (1996). "Brain drug delivery of small molecules using immunoliposomes." Proceedings of the National Academy of Sciences of the United States of America 93: 14164 -14169.

Huwyler, J., J. Yang, et al. (1997). "Receptor mediated delivery of daunomycin using immunoliposomes: pharmacokinetics and tissue distribution in the rat." Journal of Pharmacology and Experimental Therapeutics 282: 1541-1546.

Huynh, G. H., D. F. Deen, et al. (2006). "Barriers to carrier mediated drug and gene delivery to brain tumors." Journal of Controlled Release 110: 236-259.

Ishida, O., K. Maruyama, et al. (2001). "Liposomes bearing polyethyleneglycol-coupled transferrin with intracellular targeting property to the solid tumors in vivo." Pharmaceutical Research 18: 1042-1048.

Ishida, T., D. L. Iden, et al. (1999). "A combinatorial approach to producing sterically stabilized (Stealth) immunoliposomal drugs." FEBS Letters 460: 129-133.

Jacobs, A. H., C. Dittmar, et al. (2002). "Molecular imaging of gliomas." Molecular Imaging 1: 309-335.

Jain, A., M. K. Chourasia, et al. (2006). "Brain-specific delivery of rifampin from lactyl stearate-coupled liposomes via monocarboxylic acid transporters." American Journal of Drug Delivery 4: 43-49.

Jain, R. K. (1990). "Vascular and interstitial barriers to delivery of therapeutic agents in tumors." Cancer and Metastasis Reviews 9: 253-266.

Jain, R. K. (1994). "Barriers to drug delivery in solid tumors." Scientific American 271: 58-65.

Jain, R. K. (1998). "Delivery of molecular and cellular medicine to solid tumors." Journal of Controlled Release 53: 49-67.

Jain, R. K. (1999). "Transport of molecules, particles, and cells in solid tumors." Annual Review of Biomedical Engineering: 241-263.

Jemal, A., A. Thomas, et al. (2002). "Cancer statistics." Ca-A Cancer Journal for Clinicians 52: 23-47.

Jonkman-de Vries, J. D., H. Talsma, et al. (1994). "Pharmaceutical development of a parenteral lyophilized formulation of the novel indoloquinone antitumor agent EO9." Cancer Chemotherapy and Pharmacology 34: 416-422.

Jovanovic, N., A. Bouchard, et al. (2006). "Distinct effects of sucrose and trehalose on protein stability during supercritical fluid drying and freeze-drying." European Journal of Pharmaceutical Sciences 27: 336-345.

Kalchenko, V., S. Shivtiel, et al. (2006). "Use of lipophilic near-infrared dye in whole-body optical imaging of hematopoietic cell homing." Journal of Biomedical Optics 11: 1-2.

Kang, Y. S. and W. M. Pardridge (1994). "Use of neutral avidin improves pharmacokinetics and brain delivery of biotin bound to an avidin-monoclonal antibody conjugate." Journal of Pharmacology and Experimental Therapeutics 269: 344-350.

Kaye, S. B. (1981). "Liposomes - problems and promise as selective drug carriers." Cancer Treatment Reviews 8: 27-50.

Kirby, C., J. Clarke, et al. (1980). "Effect of the cholesterol content of small unilamellar liposomes on their stability in vivo and in vitro." Biochemical Journal 186: 591-598.

Koo, Y.-E. L., G. R. Reddy, et al. (2006). "Brain cancer diagnosis and therapy with nanoplatforms." Advanced Drug Delivery Reviews 58: 1556-1577.

Koziara, J. M., P. R. Lockman, et al. (2004). "Paclitaxel nanoparticles for the potential treatment of brain tumors." Journal of Controlled Release 99: 259-269.

Koziara, J. M., P. R. Lockman, et al. (2006). "The blood-brain barrier and brain drug delivery." Journal of Nanoscience and Nanotechnology 6: 2712-2735.

Kroll, R. A. and E. A. Neuwelt (1998). "Outwitting the blood-brain barrier for therapeutic purposes: osmotic opening and other means." Neurosurgery 42: 1083-1100.

Kurpad, S. N., X. G. Zhao, et al. (1995). "Tumor antigens in astrocytic gliomas." Glia 15: 244-256.

Lai, S. K., J. Fu, et al. (2005). Doxorubicin-loaded transferrin-targeted polymeric micelles rapidly enter cancer cells and accumulate near the cell nucleus. AIChE Annual Meeting, Conference Proceedings.

Lasic, D. D. (1994). "Sterically stabilized vesicles." Angewandte Chemie (International Edition in English) 33: 1685-1698.

Lasic, D. D. (1997). "Recent developments in medical applications of liposomes: Sterically stabilized liposomes in cancer therapy and gene delivery in vivo." Journal of Controlled Release 48: 203-222.

Lasic, D. D., F. J. Martin, et al. (1991). "Sterically stabilized liposomes: a hypothesis on the molecular origin of the extended circulation times." Biochimica et Biophysica Acta - Biomembranes 1070: 187-192.

Li, H. and Z. M. Qian (2002). "Transferrin/transferrin receptor-mediated drug delivery." Medicinal Research Reviews 22: 225-250.

Liao, G.-S., X.-B. Li, et al. (2001). "Pharmacological actions of nerve growth factor-transferrin conjugate on the central nervous system." Journal of Natural Toxins 10: 291-297.

Liu, J. (2006). "Physical characterization of pharmaceutical formulations in frozen and freeze-dried solid states: techniques and applications in freeze-drying development." Pharmaceutical Development and Technology 11: 3-28.

Lo, E. H., A. B. Singhal, et al. (2001). "Drug delivery to damaged brain." Brain Research Reviews 38: 140-148.

Lopez, K. A., A. E. Waziri, et al. (2006). "Convection-enhanced delivery in the treatment of malignant glioma." Neurological Research 28: 542-548.

Loughrey, H., M. B. Bally, et al. (1987). "A non-covalent method of attaching antibodies to liposomes." Biochimica et Biophysica Acta - Biomembranes 901: 157-160.

Madhankumar, A. B., B. Slagle-Webb, et al. (2006). "Interleukin-13 receptor-targeted nanovesicles are a potential therapy for glioblastoma multiforme." Molecular Cancer Therapeutics 5: 3162-3169.

Mamot, C., D. C. Drummond, et al. (2003). "Epidermal growth factor receptor (EGFR)-targeted immunoliposomes mediate specific and efficient drug delivery to EGFR- and EGFRvIII-overexpressing tumor cells." Cancer Research 63: 3154-3161.

Mamot, C., D. C. Drummond, et al. (2004). "Epidermal growth factor receptor (EGFR)-targeted immunoliposomes mediate specific and efficient drug delivery to EGFR- and EGFRvIII-overexpressing tumor cells." Women's Oncology Review 4: 101-103.

Mamot, C., D. C. Drummond, et al. (2005). "Epidermal growth factor receptor-targeted immunoliposomes significantly enhance the efficacy of multiple anticancer drugs in vivo." Cancer Research 65: 11631-11638.

Mamot, C., R. Ritschard, et al. (2006). "EGFR-targeted immunoliposomes derived from the monoclonal antibody EMD72000 mediate specific and efficient drug delivery to a variety of colorectal cancer cells." Journal of Drug Targeting 14: 215-223.

Markman, M., P. Francis, et al. (1994). "Intraperitoneal Taxol (paclitaxel) in the management of ovarian cancer." Annals of oncology : official journal of the European Society for Medical Oncology / ESMO 5 Suppl 6: S55-58.

Martin, F. J., W. L. Hubbell, et al. (1981). "Immunospecific targeting of liposomes to cells: a novel and efficient method for covalent attachment of Fab fragments via disulfide bonds." Biochemistry 20: 4229-4238.

Medina, O. P., Y. Zhu, et al. (2004). "Targeted liposomal drug delivery in cancer." Current Pharmaceutical Design 10: 2981-2989.

Moghimi, S. M. and J. Szebeni (2003). "Stealth liposomes and long circulating nanoparticles: critical issues in pharmacokinetics, opsonization and protein-binding properties." Progress in Lipid Research 42: 463-478.

Newton, H. B. (2006). "Advances in strategies to improve drug delivery to brain tumors." Expert Review of Neurotherapeutics 6: 1495-1509.

Ningaraj, N. S., M. Rao, et al. (2003). "Calcium-dependent potassium channels as a target protein for modulation of the blood-brain tumor barrier." Drug News and Perspectives 16: 291-298.

Ningaraj, N. S., M. Rao, et al. (2002). "Regulation of blood-brain tumor barrier permeability by calcium-activated potassium channels." Journal of Pharmacology and Experimental Therapeutics 301: 838-851.

Noble, C. O., D. B. Kirpotin, et al. (2004). "Development of ligand-targeted liposomes for cancer therapy." Expert Opinion on Therapeutic Targets 8: 335-353.

Packer, R. J., M. Krailo, et al. (2005). "A phase I study of concurrent RMP-7 and carboplatin with radiation therapy for children with newly diagnosed brainstem gliomas." Cancer 104: 1968-1974.

Papahadjopoulos, D., T. Allen, et al. (1991). "Sterically stabilized liposomes: improvements in pharmacokinetics and antitumor therapeutic efficacy." Proceedings of the National Academy of Sciences of the United States of America 88: 11460-11464.

Papisov, M. I. (1998). "Theoretical considerations of RES-avoiding liposomes: molecular mechanics and chemistry of liposome interactions." Advanced Drug Delivery Reviews 32: 119-138.

Pardridge, W. M. (1998). "CNS drug design based on principles of blood-brain barrier transport." Journal of Neurochemistry 70: 1781-1792.

Pardridge, W. M. (1999). "Non-invasive drug delivery to the human brain using endogenous blood- brain barrier transport systems." Pharmaceutical Science and Technology Today 2: 49-59.

Pardridge, W. M. (1999). "Vector-mediated drug delivery to the brain." Advanced Drug Delivery Reviews 36: 299-321.

Pardridge, W. M. (2002). "Drug and gene targeting to the brain with molecular trojan horses." Nature Reviews Drug Discovery 1: 131-139.

Pardridge, W. M. (2002). "Targeting neurotherapeutic agents through the blood-brain barrier." Archives of Neurology 59: 35-40.

Pardridge, W. M. (2003). "Blood-brain barrier drug targeting: the future of brain drug development." Molecular Interventions 3: 90-105.

Partridge, W. M. (1999). "Blood brain barrier biology and methodology." Journal of NeuroVirology 5: 556-569.

Peer, D., A. Florentin, et al. (2003). "Hyaluronan is a key component in cryoprotection and formulation of targeted unilamellar liposomes." Biochimica et Biophysica Acta - Biomembranes 1612: 76-82.

Pradilla, G., P. P. Wang, et al. (2006). "Local intracerebral administration of paclitaxel with the paclimer® delivery system: Toxicity study in a canine model." Journal of Neuro-Oncology 76: 131-138.

Prior, R., G. Reifenberger, et al. (1990). "Transferrin receptor expression in tumours of the human nervous system: Relation to tumour type, grading and tumour growth fraction." Virchows Archiv - A Pathological Anatomy and Histopathology 416: 491-496.

Qian, Z. M. (2002). "Targeted drug delivery via the transferrin receptor-mediated endocytosis pathway." Pharmacological Reviews 54: 561-587.

Raghavan, R., M. L. Brady, et al. (2006). "Convection-enhanced delivery of therapeutics for brain disease, and its optimization." Neurosurgical focus 20: 1-7.

Rao, J., A. Dragulescu-Andrasi, et al. (2007). "Fluorescence imaging in vivo: recent advances." Current Opinion in Biotechnology 18: 17-25.

Richards, G. M., D. Khuntia, et al. (2007). "Therapeutic management of metastatic brain tumors." Critical Reviews in Oncology/Hematology 61: 70-78.

Rowinsky, E. K. and R. C. Donehower (1993). "The clinical pharmacology of paclitaxel (TAXOL®)." Seminars in Oncology 20: 16-25.

Rowinsky, E. K., M. Wright, et al. (1994). "Clinical pharmacology and metabolism of Taxol (paclitaxel): update 1993." Annals of oncology : Official journal of the European Society for Medical Oncology / ESMO 5 Suppl 6: S7-16.

Rowinsky, E. K., M. Wright, et al. (1993). "Taxol: Pharmacology, metabolism and clinical implications." Cancer Surveys 17: 283-304.

Sakahara, H. and T. Saga (1999). "Avidin-biotin system for delivery of diagnostic agents." Advanced Drug Delivery Reviews 37: 89-101.

Schackert, G., D. Fan, et al. (1989). "Arrest and retention of multilamellar liposomes in the brain of normal mice or mice bearing experimental brain metastases." Selective Cancer Therapeutics 5: 73-79.

Scherrmann, J.-M. (2002). "Drug delivery to brain via the blood-brain barrier." Vascular Pharmacology 38: 349-354.

Schmidt-Wolf, I. G. H., R. S. Negrin, et al. (1991). "Use of a SCID mouse/human lymphoma model to evaluate cytokine-induced killer cells with potent antitumor cell activity." Journal of Experimental Medicine 174: 139-149.

Schmitt-Sody, M., S. Strieth, et al. (2003). "Neovascular targeting therapy: paclitaxel encapsulated in cationic liposomes improves antitumoral efficacy." Clinical Cancer Research 9: 2335-2341.

Schnyder, A. and J. Huwyler (2005). "Drug transport to brain with targeted liposomes." NeuroRx 2: 99-107.

Schnyder, A., S. Krahenbuhl, et al. (2005). "Targeting of daunomycin using biotinylated immunoliposomes: pharmacokinetics, tissue distribution and in vitro pharmacological effects." Journal of Drug Targeting 13: 325-335.

Schnyder, A., S. Krahenbuhl, et al. (2004). "Targeting of skeletal muscle in vitro using biotinylated immunoliposomes." Biochemical Journal 377: 61-67.

Seymour, L. W. (1992). "Passive tumor targeting of soluble macromolecules and drug conjugates." Critical Reviews in Therapeutic Drug Carrier Systems 9: 135-187.

Shah, K. and R. Weissleder (2005). "Molecular optical imaging: Applications leading to the development of present day therapeutics." NeuroRx 2: 215-225.

Shan, S., C. Flowers, et al. (2006). "Preferential extravasation and accumulation of liposomal vincristine in tumor comparing to normal tissue enhances antitumor activity." Cancer Chemotherapy and Pharmacology 58: 245-255.

Sharma, A. and U. S. Sharma (1997). "Liposomes in drug delivery: progress and limitations." International Journal of Pharmaceutics 154: 123-140.

Sharma, A. and R. M. Straubinger (1994). "Novel taxol formulations: preparation and characterization of taxol-containing liposomes." Pharmaceutical Research 11: 889-896.

Shi, N. and W. M. Pardridge (2000). "Noninvasive gene targeting to the brain." Proceedings of the National Academy of Sciences of the United States of America 97: 7567-7572.

Silvander, M. (2002). "Steric stabilization of liposomes - a review." Progress in Colloid and Polymer Science 120: 35-40.

Slavin, L., A. Chhabra, et al. (2007). "Drug-eluting stents: preventing restenosis." Cardiology in Review 15: 1-12.

Soni, V., S. K. Jain, et al. (2005). "Potential of transferrin and transferrin conjugates of liposomes in drug delivery and targeting." American Journal of Drug Delivery 3: 155-170.

Soni, V., D. V. Kohli, et al. (2005). "Transferrin coupled liposomes as drug delivery carriers for brain targeting of 5-florouracil." Journal of Drug Targeting 13: 245-250.

Soni, V., D. V. Kohli, et al. (2007). "Transferrin coupled liposomes for enhanced brain delivery of doxorubicin." Vascular Disease Prevention 4: 31-38.

Sparreboom, A., L. van Zuylen, et al. (1999). "Cremophor EL-mediated alteration of paclitaxel distribution in human blood: clinical pharmacokinetic implications." Cancer Research 59: 1454-1457.

Straubinger, R. M., A. Sharma, et al. (1993). "Novel Taxol formulations: Taxol-containing liposomes." Journal of the National Cancer Institute. Monographs: 69-78.

Strieth, S., M. E. Eichhorn, et al. (2004). "Neovascular targeting chemotherapy: encapsulation of paclitaxel in cationic liposomes impairs functional tumor microvasculature." International Journal of Cancer 110: 117-124.

Sun, J. C. J. and J. W. Eikelboom (2007). "Treatment of restenosis with a paclitaxel-coated balloon catheter." New England Journal of Medicine 356: 1071.

Sun, W. Q., A. C. Leopold, et al. (1996). "Stability of dry liposomes in sugar glasses." Biophysical Journal 70: 1769-1776.

Surawicz, T. S., F. Davis, et al. (1998). "Brain tumor survival: results from the National Cancer Data Base." Journal of Neuro-Oncology 40: 151-160.

Sweeney, T. J., V. Mailander, et al. (1999). "Visualizing the kinetics of tumor-cell clearance in living animals." Proceedings of the National Academy of Sciences of the United States of America 96: 12044-12049.

Tae, K. A., J. K. Hui, et al. (2002). "Characteristics of BCNU-loaded PLGA wafers." Polymer 26: 691-700.

Tang, X. and M. J. Pikal (2004). "Design of freeze-drying processes for pharmaceuticals: practical advice." Pharmaceutical Research 21: 191-200.

Tarr, B. D. and S. H. Yalkowsky (1987). "A new parenteral vehicle for the adminstration of some poorly water soluble anti-cancer drugs." Journal of Parenteral Science and Technology 41: 31-33.

Temsamani, J., A. R. Rees, et al. (2001). "Vector-mediated drug delivery to the brain." Expert Opinion on Biological Therapy 1: 773-782.

Terasaki, T. and A. Tsuji (1994). "Drug delivery to the brain utilizing blood-brain barrier transport systems." Journal of Controlled Release 29: 163-169.

Tirosh, O., Y. Barenholz, et al. (1998). "Hydration of polyethylene glycol-grafted liposomes." Biophysical Journal 74: 1371-1379.

Torchilin, V. P. (2004). "Targeted polymeric micelles for delivery of poorly soluble drugs." Cellular and Molecular Life Sciences 61: 2549-2559.

Torchilin, V. P. (2005). "Fluorescence microscopy to follow the targeting of liposomes and micelles to cells and their intracellular fate." Advanced Drug Delivery Reviews 57: 95-109.

Torchilin, V. P. (2005). "Recent advances with liposomes as pharmaceutical carriers." Nature Reviews Drug Discovery 4: 145-160.

Torchilin, V. P., A. N. Lukyanov, et al. (2003). "Immunomicelles: targeted pharmaceutical carriers for poorly soluble drugs." Proceedings of the National Academy of Sciences of the United States of America 100: 6039-6044.

Tseng, S. H., M. S. Bobola, et al. (1999). "Characterization of paclitaxel (Taxol®) sensitivity in human glioma- and medulloblastoma-derived cell lines." Neuro-Oncology 1: 101-108.

Tsuji, A. and I. Tamai (1999). "Carrier-mediated or specialized transport of drugs across the blood-brain barrier." Advanced Drug Delivery Reviews 36: 277-290.

Ugwu, S., A. Zhang, et al. (2005). "Preparation, characterization, and stability of liposome-based formulations of mitoxantrone." Drug Development and Industrial Pharmacy 31: 223-229.

Van Bommel, E. M. G. and D. J. A. Crommelin (1984). "Stability of doxorubicin-liposomes on storage: as an aqueous dispersion, frozen or freeze-dried." International Journal of Pharmaceutics 22: 299-310.

Van Winden, E. C. A. and D. J. A. Crommelin (1999). "Short term stability of freeze-dried, lyoprotected liposomes." Journal of Controlled Release 58: 69-86.

Van Winden, E. C. A., W. Zhang, et al. (1997). "Effect of freezing rate on the stability of liposomes during freeze-drying and rehydration." Pharmaceutical Research 14: 1151-1160.

Wang, W. (2000). "Lyophilization and development of solid protein pharmaceuticals." International Journal of Pharmaceutics 203: 1-60.

Widera, A., F. Norouziyan, et al. (2003). "Mechanisms of TfR-mediated transcytosis and sorting in epithelial cells and applications toward drug delivery." Advanced Drug Delivery Reviews 55: 1439-1466.

Woodle, M. C. and D. D. Lasic (1992). "Sterically stabilized liposomes." Biochimica et Biophysica Acta - Reviews on Biomembranes 1113: 171-199.

Wu, D. (1997). "Drug targeting of a peptide radiopharmaceutical through the primate blood-brain barrier in vivo with a monoclonal antibody to the human insulin receptor." Journal of Clinical Investigation 100: 1804-1811.

Wu, G., R. F. Barth, et al. (2006). "Targeted delivery of methotrexate to epidermal growth factor receptor-positive brain tumors by means of cetuximab (IMC-C225) dendrimer bioconjugates." Molecular Cancer Therapeutics 5: 52-59.

Wu, J., Q. Liu, et al. (2006). "A folate receptor-targeted liposomal formulation for paclitaxel." International Journal of Pharmaceutics 316: 148-153.

Yuan, F., M. Dellian, et al. (1995). "Vascular permeability in a human tumor xenograft: Molecular size dependence and cutoff size." Cancer Research 55: 3752-3756.

Zhang, J. A., G. Anyarambhatla, et al. (2005). "Development and characterization of a novel cremophor® EL free liposome-based paclitaxel (LEP-ETU) formulation." European Journal of Pharmaceutics and Biopharmaceutics 59: 177-187.

Zhang, W., E. C. A. Van Winden, et al. (1997). "Enhanced permeability of freeze-dried liposomalbilayers upon rehydration." Cryobiology 35: 277-289.

Vita

Murali Krishna Divi was born in Andhra Pradesh, India on June 4th, 1976. He received his Bachelor of Pharmacy degree from the Kakatiya University, Warangal, India, in 1998 and Master of Science (Pharmaceutics) from the National Institute of Pharmaceutical Education and Research, SAS Nagar, India, in 2000 with first class honors. He joined the University of Tennessee Health Science Center, Memphis, in August 2003.

Before joining the graduate program, Mr. Divi has worked as formulation development scientist in Dr. Reddy's Laboratories, a New York stock exchange listed Indian pharmaceutical company, for about 2 years. He is the recipient of Parenteral Drug Association's 2005 and 2006 Annual Graduate Research Symposium Awards. He is a member of the American Association of Pharmaceutical Scientists, Parenteral Drug Association and Controlled Release Society. So far he has 2 patents and published couple of research articles in international journals and contributed several scientific abstracts.